



BRNO UNIVERSITY OF TECHNOLOGY

VYSOKÉ UČENÍ TECHNICKÉ V BRNĚ

FACULTY OF MECHANICAL ENGINEERING

FAKULTA STROJNÍHO INŽENÝRSTVÍ

INSTITUTE OF SOLID MECHANICS, MECHATRONICS AND BIOMECHANICS

ÚSTAV MECHANIKY TĚLES, MECHATRONIKY A BIOMECHANIKY

CREATION OF AN APPLICATION FOR POST-PROCESSING RESULTS OF STRUCTURAL ANALYSES IN THE SPACE INDUSTRY

VYTVOŘENÍ APLIKACE PRO ZPRACOVÁNÍ VÝSLEDKŮ STRUKTURÁLNÍCH ANALÝZ V KOSMICKÉM
PRŮMYSLU

MASTER'S THESIS

DIPLOMOVÁ PRÁCE

AUTHOR

Bc. Petr Šprta

AUTOR PRÁCE

SUPERVISOR

Ing. Petr Lošák, Ph.D.

VEDOUCÍ PRÁCE

BRNO 2023

Master's Thesis Assignment

Institute: Institute of Solid Mechanics, Mechatronics and Biomechanics
Student: **Bc. Petr Šprta**
Degree programme: Engineering Mechanics and Biomechanics
Branch: Engineering Mechanics
Supervisor: **Ing. Petr Lošák, Ph.D.**
Academic year: 2022/23

As provided for by the Act No. 111/98 Coll. on higher education institutions and the BUT Study and Examination Regulations, the director of the Institute hereby assigns the following topic of Master's Thesis:

Creation of an application for post-processing results of structural analyses in the space industry

Brief Description:

Specific requirements are placed on the calculations in the space industry. Generally, many load cases are analysed there from which the maximal stresses on particular elements are needed. Commonly, a linear theory is applied for structural analyses which allows the use of superposition of constituent loads which, if used during post-processing, can simplify the calculation and assessment process, and thus save a considerable amount of time. The aim of this master's thesis is the creation of such an application, including a graphical user interface, allowing the combination and evaluation of outputs from structural analyses performed in the software Nastran. This master's thesis is created in cooperation with the company SAB Aerospace.

Master's Thesis goals:

1. To describe specifications of the design process and structural calculations in the space industry
2. To program application for post-processing, evaluation, and preparation for visualisation of results from software Nastran
3. To verify the functionality of created application through an illustrative task

Recommended bibliography:

TURNER, R.: Python Programming, nelly B.L. International Consulting LTD, 2020.

ECSS-E-HB-32-26A: Spacecraft mechanical loads analysis handbook, 2013

MSC Nastran: Quick Reference Guide

SARAFIN, T.: , ed. Spacecraft Structures and Mechanisms: From Concept to Launch. Torrance, California: Microcosm, 1995. ISBN 978-1881883036.

Deadline for submission Master's Thesis is given by the Schedule of the Academic year 2022/23

In Brno,

L. S.

prof. Ing. Jindřich Petruška, CSc.
Director of the Institute

doc. Ing. Jiří Hlinka, Ph.D.
FME dean

ABSTRAKT

Cílem této práce je vytvoření softwarové aplikace pro dodatečné zpracování výsledků strukturálních analýz prováděných metodou konečných prvků v programu Nastran. Náplň a téma této práce vyplývá z požadavků kladených na vývoj konstrukcí v kosmickém průmyslu, kde je pro zaručení bezpečnosti zapotřebí ověřit chování struktury při mnoha zatěžovacích stavech v různých zatěžovacích podmínkách. Díky využívání lineárních statických analýz je možné využít superpozice napětí v rámci dodatečného zpracování výsledků a tím ušetřit cenný výpočetní čas a zvýšit celkovou efektivitu pevnostních výpočtů a vyhodnocování jejich výsledků. Všechny tyto aspekty by měly být zahrnuty při vývoji aplikace, jejímž cílem je načtení výsledků dílčích analýz z programu Nastran, jejich superpozice a vyhodnocení, zapsání výsledků do programu Excel a příprava textových souborů pro vizualizaci v programu HyperView. V úvodní části práce jsou popsány specifika pevnostních výpočtů v kosmickém průmyslu ze kterých vyplývá motivace a požadavky pro vývoj aplikace. V následujících částech je popsán vývoj aplikace a na závěr je její funkčnost ověřena na reálné pevnostní analýze konstrukce vyvíjené v rámci programu Evropské kosmické agentury. Práce byla vytvořena ve spolupráci s firmou SAB Aerospace.

KLÍČOVÁ SLOVA

strukturální analýza, zpracování výsledků, zatěžovací stav, metoda konečných prvků

ABSTRACT

The objective of this work is to create a software application for post-processing the results of structural analyses conducted using the finite element method in the Nastran software. The contents and topic of this work stem from the requirements imposed on the development of structures in the space industry, where ensuring safety involves verifying the behaviour of structures under many load cases during various loading environments. By employing linear static analyses, the superposition of stresses can be utilized during the post-processing of results, thereby saving valuable computational time and enhancing the overall efficiency of strength calculations and result evaluation. All these aspects should be incorporated in the development of the application, which aims to import analysis results from Nastran, perform superposition and evaluation, export the results to Excel, and prepare text files for visualization in the software HyperView. The introductory part of the work describes the specific characteristics of strength calculations in the space industry, which serve as motivation and requirements for the application's development. The subsequent sections detail the application's development process, and finally, its functionality is verified through a real structural analysis of a structure being developed within the programme of the European Space Agency. This work was conducted in collaboration with the company SAB Aerospace.

KEYWORDS

structural analysis, post-processing, load case, Finite Element Method

BIBLIOGRAPHIC CITATION

ŠPRTA, P. *Creation of an application for post-processing results of structural analyses in the space industry*. Brno, 2023. Master's Thesis. Brno University of Technology, Faculty of Mechanical Engineering, Institute of Solid Mechanics, Mechatronics and Biomechanics. 122 p. Supervised by Petr Lošák, Ph.D.

DECLARATION

I declare that I have written this master's thesis *Creation of an application for post-processing results of structural analyses in the space industry* on my own according to the instructions of my master's thesis supervisor Petr Lošák, Ph.D., and using the sources listed in references.

Petr Šprta

This master thesis was developed in cooperation with SAB Aerospace.



ACKNOWLEDGEMENT

I would like to express my gratitude to my supervisor Petr Lošák, Ph.D. for the professional guidance, patience, and insightful suggestions to this master's project. Further thanks go to the company SAB Aerospace for allowing me to elaborate this master's thesis within my internship during which I gained invaluable experience. Special thanks belong to the structural team, namely to Václav Stavárek, Zdeněk Petřela, and Petr Horák for their incentive suggestions and remarks. Another big thanks belong to my parents and the whole family for great support during the whole period of my study. Helena deserves biggest thanks for her incredible patience.

CONTENTS

Introduction	12
1 Description of the problem situation	13
2 Space activities in Europe	14
2.1 The European Space Agency	14
2.1.1 Beginnings of ESA	14
2.1.2 ESA's purpose and activities	14
2.1.3 ESA members and funding.....	15
2.1.4 The European Cooperation for Space Standardization (ECSS)	16
2.2 Participation of the Czech Republic on ESA projects	17
2.2.1 The Czech Republic in ESA.....	17
2.2.2 SAB Aerospace CZ	17
3 General procedures in the development of spacecraft structures.....	19
3.1 Introduction into the space structures design.....	19
3.1.1 The requirements for the spacecraft structures.....	20
3.1.2 Space structures categorisation.....	21
3.1.3 Main considerations for the space structures design	22
3.1.4 Design process.....	24
3.2 Materials	25
3.2.1 Metal alloys	25
3.2.2 Composite materials	27
3.2.3 Sandwich structures	28
3.3 The loading environments	29
3.3.1 Launch	30
3.3.2 Static loads.....	30
3.3.3 Dynamic loads	31
3.3.4 Derivation of the QSL from the dynamic loads	33
3.4 Structural analysis.....	35
3.4.1 Types of analyses	35
3.4.2 FEA software and workflow.....	36
3.4.3 FE model pre-processing.....	38
3.4.4 Material models	43
3.4.5 Mass distribution in FE models	45
3.4.6 Properties	45
3.4.7 Representation of CFRP parts	46
3.4.8 Mesh quality checks	47
3.4.9 Export of the model	48
3.4.10 Solution and Post-processing	49
3.5 Strength evaluation	50
3.5.1 Metallic parts	50
3.5.2 Composite components	51
4 Development of the software	57
4.1 Requirements and possible approaches	57
4.1.1 Introduction	57

4.1.2	Possible approaches	57
4.1.3	Choice of approach	57
4.1.4	Requirements on the new software application	58
4.2	Choice and description of the programming language.....	59
4.2.1	Choice of the programming language	59
4.2.2	Python	59
4.2.3	Frequently used data structures	61
4.3	Reading and sorting of the input data.....	62
4.3.1	Reading data from the BDF file	63
4.3.2	Reading of the PCH file	67
4.4	Organisation and assignment of the read data.....	69
4.4.1	Organisation and assignment of the corresponding information	69
4.4.2	Organisation and used data structures.....	71
4.5	Combination function.....	72
4.5.1	Combination of the composite stresses	73
4.6	Evaluation and tabular outputs	73
4.6.1	Structure of the tabular output data.....	74
4.7	Display of the evaluated data in the HyperView.....	75
4.7.1	Altair ASCII file.....	75
4.7.2	Visualisation of isotropic shell envelopes results	75
4.7.3	Visualisation of the load case results for isotropic shell components.....	77
4.7.4	Visualisation of envelopes for shell elements with PCOMP property.....	77
4.7.5	Visualisation of load case results for composite shell elements	78
4.7.6	Visualisation of results for isotropic solid elements	79
4.8	Graphical user interface of the new tool	79
5	Validation of the functionality of the tool	83
5.1	Description of the FE model	83
5.2	Validation of the standard shell elements.....	83
5.2.1	Visualisation of individual load cases.....	83
5.2.2	Visualisation of envelope.....	86
5.3	Validation of the evaluation of iso-skin composite shell elements	87
5.3.1	Quasi-isotropic CFRP skins	87
5.3.2	Metallic skins	89
5.3.3	Core strength evaluation	91
5.3.4	Core local instabilities evaluation	92
5.4	Validation of the orthotropic composite shell elements.....	94
5.4.1	Visualisation of the load cases	94
5.4.2	Visualisation of the envelope.....	95
5.4.3	Evaluation of ILSS.....	96
5.5	Solid elements	97
5.5.1	Visualisation of load cases	97
5.5.2	Visualisation of envelopes	98

Conclusion	100
List of abbreviations.....	105
List of symbols and physical constants	107
List of appendices	109

INTRODUCTION

Since the release of the first spacecraft, Sputnik 1, in 1957, thousands of spacecrafts have been launched into Earth's orbit and outer space. Since then, technology has undergone significant advancements in all areas, enabling space programs to be designed, tested, and launched more quickly and at lower costs. One technology advancement that has greatly influenced design and development, not only in the space industry but also in other fields, is the Finite Element Method. This tool allows structural engineers to efficiently design and evaluate the mechanical behaviour of structures, surpassing the capabilities of purely analytical methods. Over the past few decades, it has become the primary tool for structural engineers in the space industry.

Despite the successful utilization of this method and the availability of numerous commercial software that facilitate its implementation, there are still significant challenges associated with the method and the efficient design of spacecraft structures. These challenges arise from the stringent requirements imposed on space structures and their design, particularly due to the extreme loading conditions and the demand for lightweight design.

This thesis focuses on the development of an application with the primary goal of enhancing the efficiency of calculations performed using the Finite Element Method. By doing so, it aims to streamline the overall process of structural design development.

The first chapter provides a detailed description of the problem that needs to be addressed, while the second chapter delves into the background of the space industry in Europe which stands behind the demand for this project. The third chapter focuses on describing the general procedures used in the development of spacecraft structures. The detailed description of the requirements for the new software together with the description of its development are described in the fourth chapter. The final chapter focuses on validating the functionality of the tool using a real-life example.

1 DESCRIPTION OF THE PROBLEM SITUATION

Throughout its operational life, a spacecraft encounters various loading environments. Each phase, from transport and integration to launch and in-orbit loads, places substantial demands on the structure. To ensure the design can withstand all potentially hazardous operations, a large number of load cases are typically verified, derived from launcher manuals and space program requirements. Structural design is commonly performed using commercial finite element packages, with the extensive number of load cases imposing high demands on computational time and results evaluation.

Considering that linear static analysis is employed for the vast majority of these analyses, there is an opportunity to bypass calculating such a large number of analyses in the solver by using linear superposition of results calculated for specified subcases instead. Since commercial packages offer limited functionality for addressing these issues, many companies in the space industry invest in developing custom software tools to simplify the process of solution and post-processing of large datasets.

The principal purpose of this thesis is to develop an application that performs linear superposition of results from a commercial finite element solver, evaluates the results, writes the evaluated data into Excel tables, and prepares the evaluated data for visualization in commercial post-processing software. To ensure user-friendliness, the software application should be operated using a graphical user interface. Requirements for the software and source code include not only reliability, speed, and user-friendliness, but also code readability and modularity of the software architecture, as further changes and development of the software can be expected in the future.

The motivation for this project is to replace the current software tool, which has significant drawbacks, and consequently save a substantial amount of time and effort for all structural departments within the company.

2 SPACE ACTIVITIES IN EUROPE

This brief chapter has been included at the beginning of this thesis because the development of this master's thesis project is driven by the European space programme, its projects, and engineering procedures.

2.1 THE EUROPEAN SPACE AGENCY

The European Space Agency (ESA) is an international organization that coordinates European space activities. ESA is currently composed of 22 member states, and its headquarters are located in Paris. [1]

2.1.1 BEGINNINGS OF ESA

The origins of the ESA date back to the early 1960s when several European countries formed the European Launcher Development Organisation (ELDO) to build heavy launchers. This was followed by the establishment of the European Space Research Organisation (ESRO) in pursuit of scientific satellite programs. In 1975, a convention was signed at the political level to merge ESRO and ELDO, creating the European Space Agency and expanding its mandate to include operational space application systems, such as telecommunications satellites. The Convention from 1975 came into effect in 1980. [2]



Fig. 1: Current logo of the ESA

2.1.2 ESA'S PURPOSE AND ACTIVITIES

PURPOSE

In basic terms, the ESA is responsible for designing and executing the European space program, with a focus on peaceful scientific and research activities in space. The agency coordinates and centralizes the efforts of its member states to gather information about the Earth, Solar System, and Universe, providing raw data for research in various scientific fields. In supporting science, the ESA also promotes and supports the development of European industries, as projects for space applications often require innovative and original solutions. The ESA's importance extends beyond Europe, as it maintains close cooperation with space organizations such as NASA and JAXA. [1][3]

ACTIVITIES

The ESA leads or participates in a large number of projects. Namely the ESA contributes to the maintenance and modernization of International Space Station (Columbus, Automated Transfer Vehicle), develops its own launchers (Vega, Ariane), develops, or operates a variety of scientific satellites observing the Earth and the Universe (Copernicus, Plato), helps to provide telecommunication and GPS data (Galileo), etc. The complete list of all ESA projects can be found in the source [4]. [4]

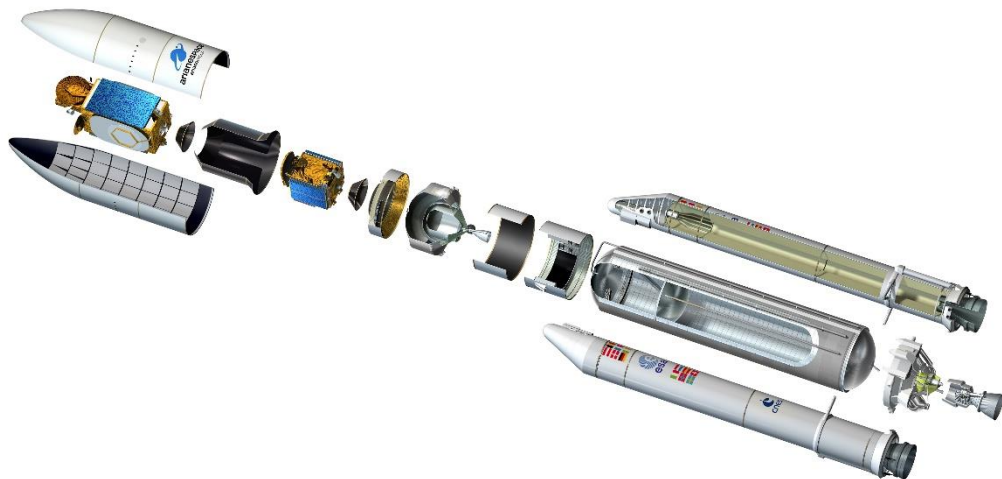


Fig. 2: Exploded view of the European launch vehicle Ariane 5 [5]

2.1.3 ESA MEMBERS AND FUNDING

MEMBER STATES

The ESA currently has 22 Member States and 9 Cooperating States, which are shown in the following picture:



Fig. 3: Map of the Member States (dark blue) and the Cooperating States (light blue) [6]

FUNDING AND PROJECT ALLOCATION

Each member state contributes to ESA based on their Gross National Product (GNP), and companies from each country are allowed to participate in ESA contracts up to the level of the country's contribution. Every project has a prime contractor responsible for project management. For large projects, prime contractors are usually major players in the European

space industry, such as Ariane Group, OHB, Avio, or Thales Alenia Space, with headquarters in the countries making the highest contributions to ESA. Subcontracting companies are often from smaller countries with lower contributions. SAB Aerospace is one such company in the ESA's supply chain, with whom this master's project was carried out. [7]

2.1.4 THE EUROPEAN COOPERATION FOR SPACE STANDARDIZATION (ECSS)

The European Cooperation for Space Standardization (ECSS) is an initiative that was established under the ESA in 1994. Its main goal is to set a single, user-friendly set of standards for all European space activities in order to unify processes and procedures, reduce life-cycle costs, and improve the quality, integrity, and compatibility of parts of European space projects. This was achieved through the creation of normative documents in various branches, as shown in the following figure. The ECSS standards are available to the public and can be downloaded from the source [8]. [8][9]

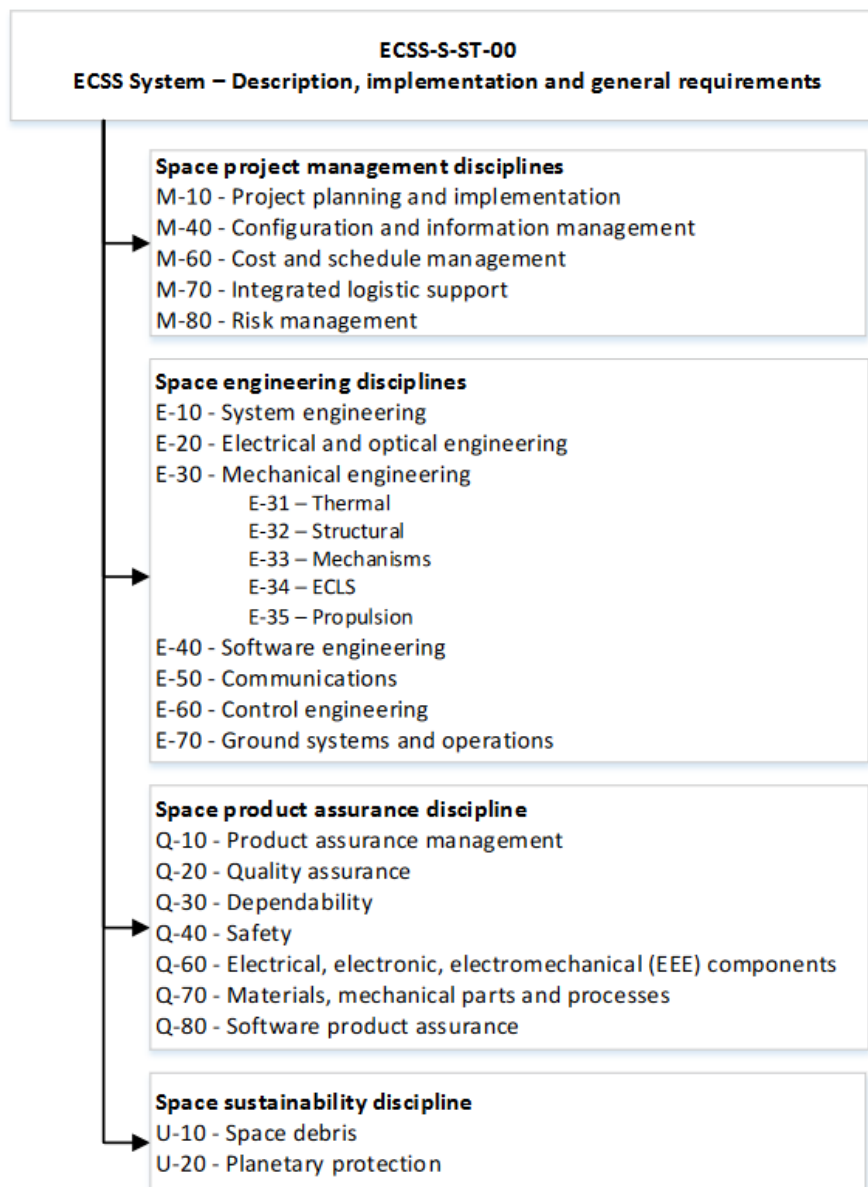


Fig. 4: Scheme of the ECSS documents [10]

2.2 PARTICIPATION OF THE CZECH REPUBLIC ON ESA PROJECTS

2.2.1 THE CZECH REPUBLIC IN ESA

The Czech Republic first showed its intention to participate on ESA projects in 1990s and officially entered the ESA in 2008. All space activities in the Czech Republic come under the purview of the Ministry of Transport, which established the Coordination Council for Space Activities comprising representatives of other ministries, organisations, universities, etc. [11][12]

Participation of the Czech Republic on ESA activities (up to 2020) [11]:

- Approximately 50 companies directly cooperated with the ESA; dozens of other companies participated in the ESA projects indirectly
- Over 20 Czech research institutes and universities were involved in research projects
- Over 350 projects were successfully finished

The participation of Czech industry and research institutions in ESA projects is expected to increase even further in the current decade.

2.2.2 SAB AEROSPACE CZ

The Czech branch of SAB Aerospace, an Italian company, was established in 2014 and is currently the largest purely space-focused company in the country. Its primary focus is on designing and integrating mechanical structures for spacecrafts, launchers, and mechanical ground support equipment (MGSE). SAB Aerospace is an ESA-approved and registered supplier and has also passed audits for collaboration with major players in the European space industry, including Thales Alenia Space and Ariane Group. To carry out space structure integration, the company built an ISO 8 cleanroom at its headquarters in Brno. [13][14]



Fig. 5: Current logo of the company SAB Aerospace

PROJECTS

The company projects comprise about 15 % of the budget the Czech Republic contributes to ESA. Among others, the most important projects in which the company participates are [13][14]:

- **PLATO** – PLANetary Transits and Oscillations of stars is a scientific mission that will search for exoplanets. The responsibility of SAB is the development and integration of the structure of the service module (SVM)
- **VEGA and VEGA-C Dispenser (SSMS)** – the top part of the two European launcher's which enables the deployment of multiple satellites on orbit
- **ROSE-L** – radar satellite for the ESA Copernicus Earth observation programme. The task of SAB is to develop and integrate the structure and thermal control system
- **SLAVIA** – scientific project whose purpose is the exploration of natural resources in space. SAB Aerospace is prime contractor of the whole project.
- **Biomission 2019** – development of hardware for scientific experiments on the ISS
- **Ariane 6 Sequencer** – development of a sequencer that will be responsible for releasing multiple satellites on board the Ariane 6 launcher



Fig. 6: Integration of satellites on Vega Dispenser in Europe's Spaceport in Kourou, French Guiana [15]



Fig. 7: PLATO SVM test model integration in company's cleanroom in Brno (published with permission of SAB Aerospace)

3 GENERAL PROCEDURES IN THE DEVELOPMENT OF SPACECRAFT STRUCTURES

3.1 INTRODUCTION INTO THE SPACE STRUCTURES DESIGN

In general terminology, spacecraft is a designation for the space segment of a space mission, such as a satellite that operates outside of the atmosphere of the Earth. As per [16], spacecraft usually consists of two parts:

- Payload – responsible for performing the assigned task, such as radio communications in a communication satellite
- Service modules – contains support systems, such as attitude control, propulsion, power supply, etc.

The size of the spacecraft can vary from subtle satellites (so-called CubeSats, for example 1U CubeSat's dimensions are 10 cm x 10 cm x 10 cm) to large spacecrafts weighing up to tens of tons. Since mass and dimensions are critical parameters for mechanical behaviour, different approaches are used for the development of small satellites compared to medium or large spacecrafts. [17]

Namely, small satellites do not typically respond to low-frequency excitations due to their low mass and high rigidity. As a result, many analyses and tests that are necessary for large spacecrafts do not apply to them. Environmental testing is relied upon instead of structural analyses to meet the requirements of small and fine structures that are difficult to model and simulate. In contrast, large structures require a greater emphasis on structural analyses to avoid complicated testing, since it is challenging to test them in a real environment where many different loads may affect them simultaneously. Furthermore, larger structures are more predictable and easier to control product variations, making them more suitable for computational modelling. However, even large space structures must undergo testing. [17]

The main objective of this master's thesis is the development of software primarily used for designing medium and large space structures. Therefore, this chapter will focus on procedures related to them. However, many of the following procedures also apply to the development of small space structures.

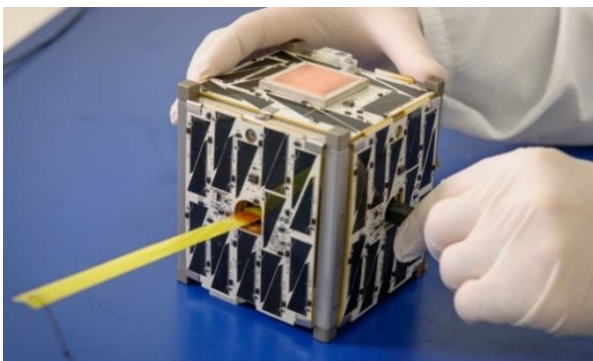


Fig. 8: 1U CubeSat (weight approx. 1.3 kg) [18]

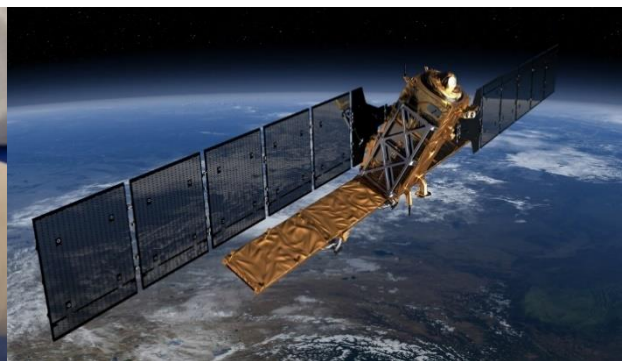


Fig. 9: Sentinel-1A (weight circa 2300 kg) [19]

3.1.1 THE REQUIREMENTS FOR THE SPACECRAFT STRUCTURES

Both calculations and testing are essential engineering tools used to ensure that the spacecraft structure will not fail in any way. Failure is not only limited to "breaking," and because there are various requirements for spacecraft structures, they can be categorized as follows [17]:

- The successful functioning of a spacecraft largely depends on the secure positioning of its key components, such as cameras and sensors, in their designated locations. Furthermore, the entire setup must fit within the payload envelope of the carrier while still providing easy access for component installation and servicing.
- To ensure that the sensitive parts of a spacecraft, particularly the electronics, are protected and deployed during the various potentially damaging environments throughout the spacecraft's lifespan, the structure must be sufficiently rigid yet light enough for the chosen launcher
- The vibration spectrum of the structure must not coincide with the launcher's control system which has to be able to recognise the motion of the spacecraft itself from the motion caused by the structural vibrations.
- The components themselves must withstand the ground, launch, and on-orbit conditions without experiencing excessive deformations, ruptures, or collapses. Moreover, they are often designed to aid in the regulation of temperatures.

In particular, based on [17], the structural requirements can be categorized as follows:

Required characteristic	Definition	Reason
Strength	The ability of the structure to withstand the load without rupturing or permanent deformation	To prevent fatal failures due to static, quasi-static or dynamic loading
Fatigue life	The number of loading cycles up to the rupture caused by material fatigue	To avoid rupture as a result of material fatigue – often neglected due to short duration of the critical loading environments
Structural response	Duration and amplitude of structural vibrations as a result of excitation	Avoiding damage to critical components
Natural frequency	The frequency at which a system oscillates when not subjected to any driving or damping force	To avoid excessive loads
Stiffness	The extent to which an object resists deformation in response to applied force	To secure positional stability of the components or allocated to the parts of bigger structure to achieve a certain natural frequency limit of the whole assembly as well as to monitor potential couplings between subsystems
Damping	The ability to dissipate vibrational energy	To mitigate impact of vibrations
Mass properties	Maximum weight, CoG, moments of inertia	Required to achieve certain natural frequency and/or imposed by load capacity of the launcher
Dynamic envelope	The space within which the spacecraft has to stay when deformed under the loading.	To avoid collisions between launcher's fairing or different parts of the spacecraft

Mechanical interface	The geometrical compatibility of the parts of the structures that are to be attached to each other (position of holes, flatness, etc.).	To ensure that the structure can be assembled easily without introducing additional loads and deformations
Positional stability and pointing	The property ensuring that the key devices stay in the predefined orientation. Thermal distortions and shift of the mechanical joints are usually key issues.	Important requirement for the sensitive measurement and optical devices requiring fixed position and orientation

Tab. 1: Structural requirements [17]

3.1.2 SPACE STRUCTURES CATEGORISATION

In a space mission, various types of structures are typically required, ranging from large brackets that connect the thrusters to the launch vehicle body to delicate mechanisms. All solid parts can be considered structures since they are all subjected to external or internal loads during acceleration caused by the launcher. [17]

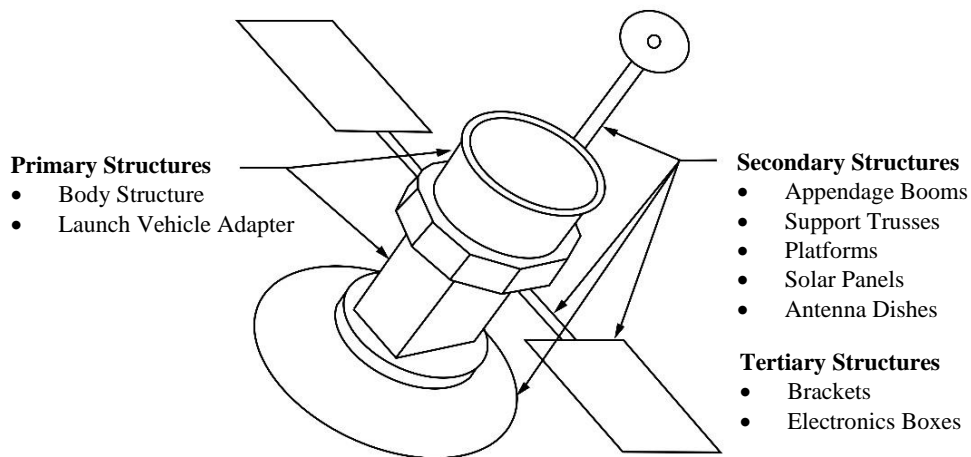


Fig. 10: Categorisation of spacecraft structures [17]

Usually, space structures are divided into the following categories [17]:

- 1) **Primary structure** is the skeleton of the spacecraft. It is the main path through which loads are transferred from the launcher to the spacecraft components. Typically, it consists of central massive tube or cone, launch vehicle adapter (LVA), struts, sandwich panels, etc.
- 2) **Secondary structure** is a category which usually contain structural components that are attached to the primary structure for supporting payloads or equipment. Trusses, brackets, and support panels are some of the typical types of secondary structures
- 3) **Tertiary structure** is a category into which usually belong small brackets and other subtle parts

The division into these categories does not mean that any of these are more important than the others. This categorization is used because these particular groups are usually sensitive to different types of loading, and therefore different types of analyses and tests are required. [17]

The main purpose of the design of the primary structure is sufficiently high first eigenfrequency which means high stiffness and low mass according to the well-known formula:

$$\omega_0 = \sqrt{\frac{k}{m}} \quad (1)$$

where ω_0 is the first eigenfrequency of an undamped dynamic system with 1 degree of freedom (DOF), k is stiffness and m is mass. Another key requirement for primary structure is ability to withstand large static and quasi-static loads during the launch.

In addition to the requirements mentioned earlier, secondary structures are often subjected to random vibrations and sometimes acoustic loads. High-frequency vibrations pose the most significant threat to tertiary structures. Stiffness and positional stability are critical requirements for both secondary and tertiary structures. For all three categories, low mass is a key consideration, usually not exceeding 15% of the spacecraft's total mass. [17]

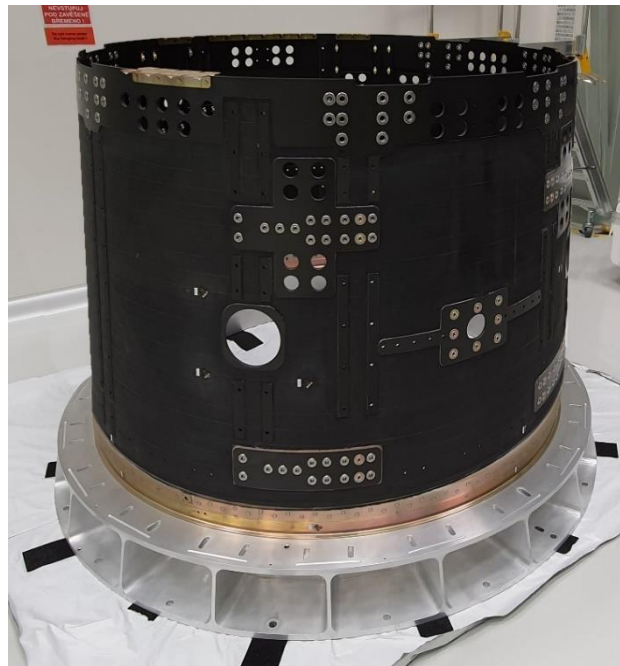


Fig. 11: Central tube – integral part of primary structure of the PLATO SVM (published with the permission of SAB Aerospace)

3.1.3 MAIN CONSIDERATIONS FOR THE SPACE STRUCTURES DESIGN

Budget is a crucial factor that needs to be considered at the outset of any space program. To design a cost-effective spacecraft, it is important to take into account the subsequent development activities. By doing so, the development team can identify important characteristics and simplify further procedures significantly. It is worth noting that since each spacecraft is essentially a prototype, procedures and requirements may differ significantly from project to project. Therefore, key development requirements should not be firmly established until the conceptual design and important trade studies have been conducted and the cost, as well as the criteria for compliance, have been defined. [17]

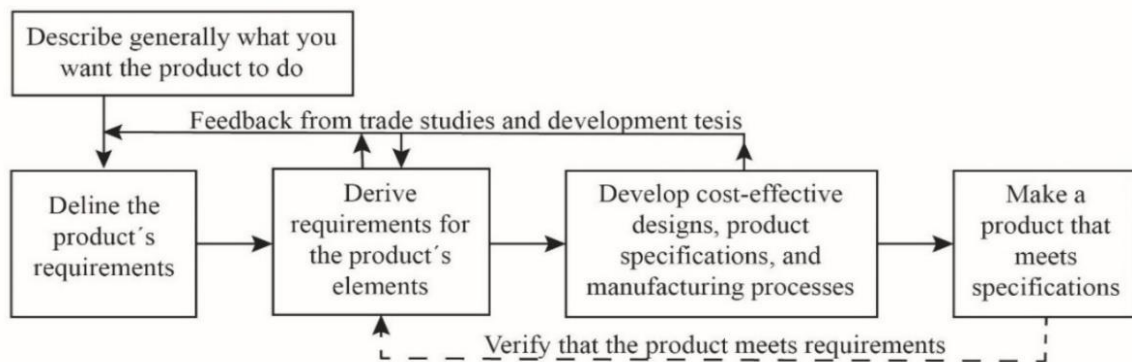


Fig. 12: The process of development [17]

Once the requirements are established, the aim is to fulfill them at the lowest possible cost. This budgeting process is crucial, but it does not necessarily mean cutting costs in every aspect of the development process. For instance, economizing on analyses may lead to critical issues and a significant increase in costs during the manufacturing and testing stages. Moreover, the design should be managed from the beginning to be as resilient as possible to inevitable variations, such as manufacturing processes or environmental uncertainties. [17]

Other key considerations during the development of space structures are briefly mentioned in the following points [17]:

- **Usually, it is not possible to make repairs after the launch**, which means that it is essential to make the design in a way that the general functioning is not influenced by single failures.
- **It is necessary to accept some possibility of failure** even though the development team takes all the steps to avoid it. Otherwise, the structure would be too heavy or extremely expensive. However, it is crucial to implement measures such as redundancy to mitigate the criticality of the potential failure and ensure that it does not compromise the mission objectives.
- **Spacecrafts are frequently sensitive to permanent deformations**, however small they are, otherwise the functioning of the sensors or antennas might be jeopardised.
- **Structural failure can occur for a variety of reasons**. Damage to the critical component might be caused, for example, by vibrations in the truck during the transport, no matter how carefully the structure has been verified for launch or on-orbit environments.
- **It is necessary to develop and maintain proper documentation** of the whole design process. Often, during the iterative design loop there are met the same problems over again, and documentation can help to address them immediately. Proper documentation is the key to successful design development.
- **While design boundaries may be flexible in the space industry, it is still necessary to deliver a high-quality product**. Unlike commercial industries that are strictly regulated by government design codes, ECSS guidelines are often used as a reference rather than a binding requirement.

3.1.4 DESIGN PROCESS

According to [15], the development of the spacecraft structures consists of the following five phases:

- 1) Spacecraft configuration definition
- 2) Conceptual design
- 3) Analyses
- 4) Production
- 5) Testing

At first glance, it may seem that the development process is linear. However, in reality, each phase is closely interconnected, and the entire process has an iterative nature. Once the iterative process of establishing design requirements through preliminary design is complete and the requirements are well-defined, the next iterative process begins to meet those requirements. This is because the loads acting on the spacecraft are influenced not only by external conditions but also by its own structural and thermal properties. Therefore, the properties of the structure directly affect the loads that drive the design process. This loop, called the loads cycle, involves the repetitive prediction and evaluation of structural loads. [17][20]

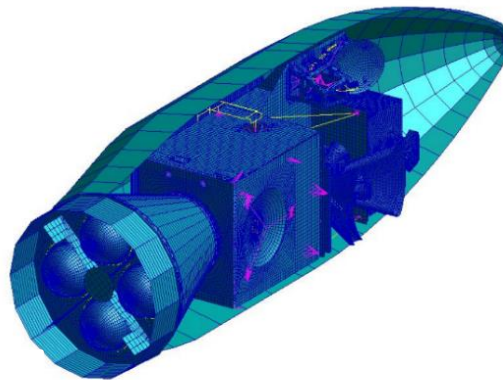


Fig. 13: FE model for coupled Load Analysis of a spacecraft on the launcher Vega [21]

During spacecraft development, several load cycles are typically performed. The first load cycle is usually based on the loads and load factors specified by the launcher user guide. In the subsequent cycles, load analysis should be performed whenever significant changes are made to the structure. The Coupled Load Analysis (CLA) plays an essential role in the load cycle. Since the dynamic behaviour of the launcher and spacecraft mutually affect each other, CLA is carried out to investigate the dynamic interaction between them. This involves incorporating the finite element model of both the launcher and payload (spacecraft). The CLA is usually performed up to 100 Hz, and the loads obtained from it primarily drive the design of the primary structure. The secondary and tertiary structures are more sensitive to excitations from acoustic and high-frequency vibrations, and thus, their design is driven by loads from other analyses. [21]

In the design phase, it is crucial to consider all the predetermined requirements and collaborate across all fields of expertise from the early stages. When engineering departments work in isolation, they tend to focus more on the requirements within their area of expertise, which can lead to complications for other departments. The following scheme visualizes the iterative loops and mutual connections within the various aspects of the design. [17]

Throughout the development process, several design reviews are typically conducted, with the most crucial ones being the Preliminary Design Review (PDR) and Critical Design Review (CDR). PDR is typically conducted before the production of the test model (model used for testing), while CDR is usually held before the production of the flight model (final product). [17]

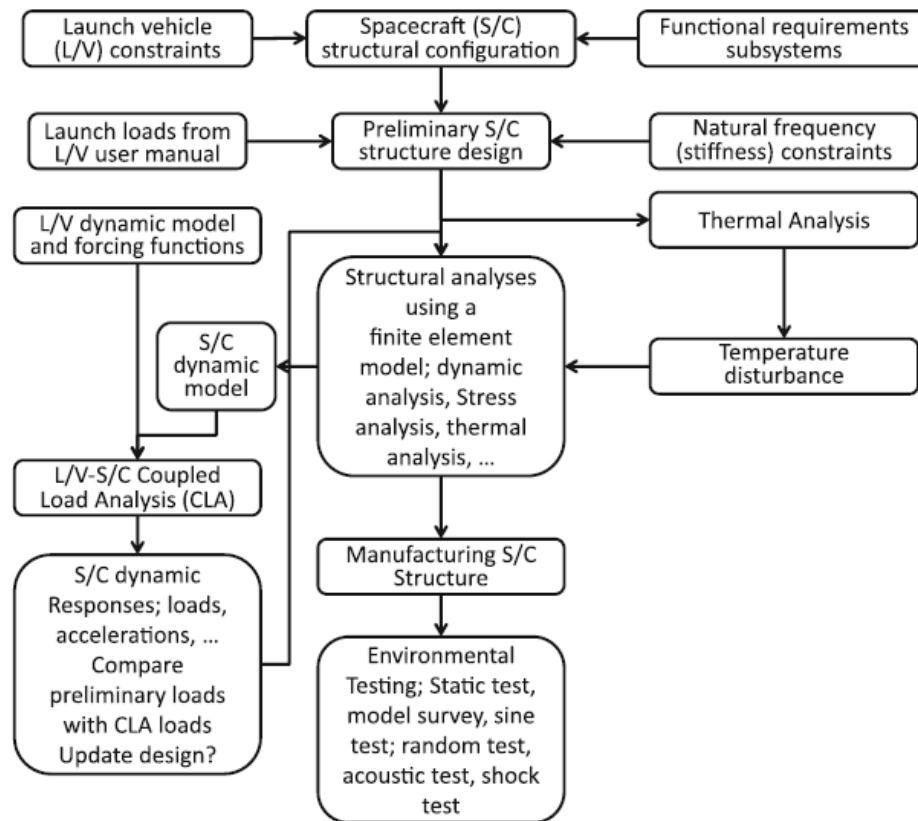


Fig. 14: Design process of the spacecraft structure [23]

3.2 MATERIALS

Due to the stringent requirements for space structures, where high stiffness and low mass are crucial, numerous advanced materials are employed. The commonly used materials include metallic alloys and composites, which will be briefly described below.

3.2.1 METAL ALLOYS

ALUMINIUM ALLOYS

Due to their high strength, low density, and easy availability, aluminium alloys are among the most widely used materials. They are used for almost all structural elements, including sandwich skins, brackets, struts, or casings. For critical structural components, aluminium alloys are typically used after heat treatment, which significantly increases their strength. Another advantage is that most of them can be welded. The comparison of properties of the most commonly used aluminium alloys is presented in the following table. [17]

Material	2014-T6	2219-T8511	6061-T6	7075-T6
σ_y [MPa]	410	300	240	440
σ_u [MPa]	460	400	290	430
Corrosion resistance	Fair to poor	Good	Good	Fair to poor
Weldability	Fair	Good	Good	Poor
Machinability	Very good	Very good	Very good	Good

Tab. 2: Basic characteristics of mostly used aluminium alloys [17] (edited)

TITANIUM ALLOYS

Titanium alloys are widely used in the space industry due to their high strength-to-weight ratio. Even though the density of titanium is approximately half that of steel, the ultimate tensile strength of high-strength alloys can go up to almost 1400 MPa. Additionally, they exhibit excellent corrosion resistance. However, they have poor machinability and weldability. The two most commonly used titanium alloys in the industry are Ti-6Al-4V and Ti-5Al-2.5Sn. [17]

MAGNESIUM ALLOYS

Magnesium alloys have a strength-to-weight ratio similar to that of aluminium alloys, but their density and strength are lower. Due to their low density, they are often used for parts that may buckle if there is enough space to make the component sufficiently thick. Although they are easily weldable, there are serious drawbacks such as poor corrosion resistance, low ductility, and low wear resistance, which limits their use. Another disadvantage is that, although their machinability is good, the chips produced during the manufacturing process can easily ignite, making the process more complicated. [17]

BERYLLIUM ALLOYS

Beryllium has a very high E/ρ ratio, which means it has a very high specific stiffness. This makes it highly sought after for high-stiffness applications, such as supports for optical equipment and sensitive measurement devices. Beryllium is also beneficial for these applications due to its low coefficient of thermal expansion and high thermal conductivity. However, beryllium also has disadvantages such as low ductility and fracture toughness. It is also toxic and expensive. [17]

STEELS

Due to their high density, steels are usually only used in space applications for fasteners and mechanisms parts. Stainless steel is the most commonly used type of steel for spacecraft structures due to its corrosion resistance and high strength. Specifically, the 300-series austenitic stainless steels are the most frequently used. [17]

Material	ρ (kg/m ³)	σ_u (MPa)	E (MPa)	σ_u/ρ ($\times 10^3$)	E/ ρ
Magnesium alloys	1800	230	42000	128	23
Titanium alloys	4500	920	115000	204	25
Aluminium alloys	2800	400	72000	143	26
Steel alloys	7800	1050	205000	135	26
HR carbon fiber/epoxy (unidirectional)	1560	1400	130000	897	83
HM carbon fiber/epoxy (unidirectional)	1660	1100	250000	663	150

Tab. 3: Basic characteristics of mostly used materials [23] (edited)

3.2.2 COMPOSITE MATERIALS

In general, composites are materials that combine two or more components to take advantage of the strengths of both. The most commonly used composites are laminates produced by assembling many layers of fibres in combination with a matrix material. Sandwich structures are another example of composite materials. [24]

CARBON FIBRE REINFORCED POLYMER (CFRP)

Although there are many materials used for the fibres of the laminates such as glass, aramid, etc., the most frequently used are carbon fibres. For the matrix, polymers (epoxies) are mostly used. The combination of these materials is then called carbon fibre reinforced polymer, which is currently the most widely used composite material for space purposes. [24]

The carbon fibres are sometimes divided into two categories as is also in the Tab. 3. High-modulus (HM) fibres indicate high Young's modulus, while the high-resistance (HR) fibres indicate higher strength. The laminas are tape-like plies of unidirectional fibres or layers of woven cloth. The laminate usually consists of plies laid in various orientations with respect to the axis of the laminate to achieve the desired properties with respect to the type and direction of the load. Mostly, the laminas (especially unidirectional) are laid evenly and symmetrically to achieve as much as possible isotropic properties in the plane of lamina, as it is depicted in the following image. [17][24]

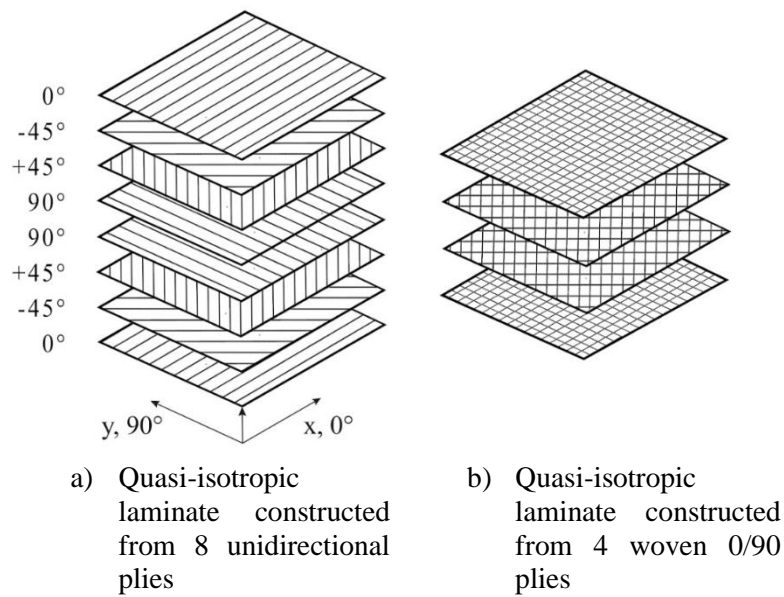


Fig. 15: Examples of quasi-isotropic laminates which have nearly isotropic properties for in-plane loading [17] (edited)

Although CFRPs are known and used for a very high strength-to-weight ratio, they also have significant drawbacks such as delamination, poor out-of-plane strength, joints, complicated manufacturing, etc. Despite this, CFRP is used for many applications, such as monolithic cleats and supporting rods, sandwich panel skins, etc. [17]

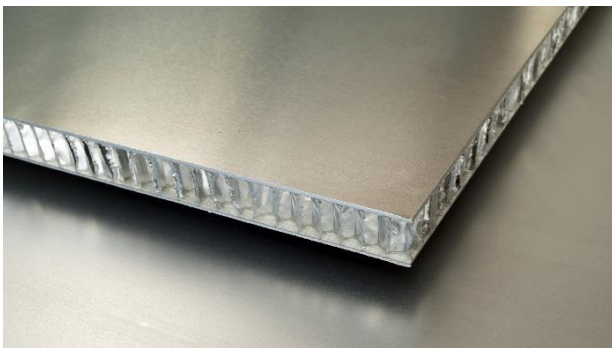


Fig. 16: Sandwich panel with aluminium skins [25]

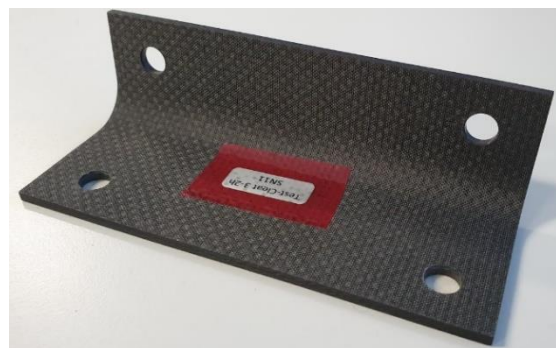
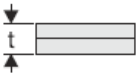
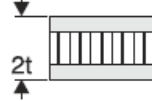
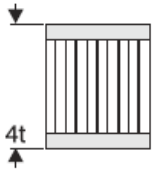


Fig. 17: Monolithic CFRP cleat for the structure of the PLATO SVM (published with permission of SAB Aerospace)

3.2.3 SANDWICH STRUCTURES

Sandwich composites are layered structures consisting of a lightweight core and two thin face sheets. Face sheets are typically from CFRP laminate, but they can also be from the aluminium sheets. Such aluminium skinned sandwich structures are used because of the significantly better heat conductivity and are used as a radiators. The most typical material for cores is aluminium honeycomb, but special foams can also be used for specific purposes. From a structural point of view, the structure resembles the 'I' cross-section beam where the skins (such as the flanges) carry the tension and compression loading and the core (such as the web) carries the shear forces. The huge contribution of the core to the mechanical properties can be seen from the relative comparison in the Tab. 4. Another benefit is also good vibration and acoustic damping. [16][24]

If the skin (metal or CFRP skin) of the sandwich panel needs to be locally reinforced, so-called doublers are used. Doubler is an extra skin which helps to carry the load or is added for better thermal properties. Core can also be locally reinforced using so-called core splices. [26]

	Separate sheet	Core thickness t	Core thickness $3t$
			
Relative stiffness	1	7	37
Relative strength	1	35	9.25
Relative weight	1	1.03	1.06

Tab. 4: Contribution of the core in the panel [27]

3.3 THE LOADING ENVIRONMENTS

In order to establish the necessary structural requirements, analyse and test the structural behaviour, it is crucial to have a clear understanding of the different environments in which the spacecraft structure will operate throughout its entire life cycle, from ground operations to on-orbit events. In fact, each operation places a certain type of structural load, which can be characterized as follows [17]:

- Static, external loads – weight of the payload, acceleration from the thrust
- Static, self-contained – bolt pretension, thermoelastic load due to thermal expansion
- Dynamic, external loads – vibrations due to launcher thrust, acoustic pressure waves, shock loads
- Dynamic, self-contained loads – the dynamic response on excitation after the source is removed

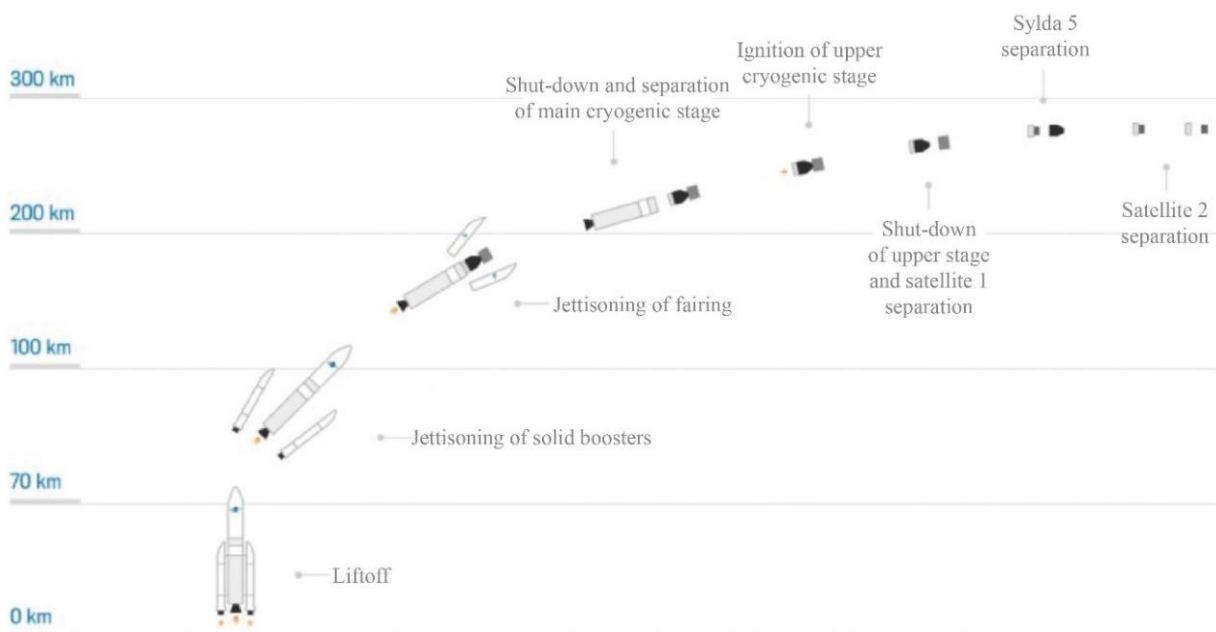


Fig. 18: The flight phases of the European launcher Ariane 6 [28]

Among all the potential hazards that a spacecraft may encounter during its lifecycle, the launch phase is undoubtedly the most perilous.

3.3.1 LAUNCH

The launch process commences when the first stage booster engines ignite and ends with the deployment of the spacecraft onto the final orbit. During the first few minutes of launch, the spacecraft is exposed to several potentially damaging events. These events include significant static axial loading generated by the thrust acceleration, lateral accelerations caused by wind gusts or steering, and strong mechanical vibrations. Additionally, the immense noise caused by the thrust results in considerable acoustic excitations, especially at lift-off due to the reflection of the sound wave from the ground. Aerodynamic noise is also a significant loading event, mainly near Mach 1 speed. The high-speed of the rocket causes aerodynamic heating, which leads to friction between the fairing and the air within the atmosphere, imposing additional structural loading as a result of the heat expansion of the structure. Furthermore, shock loads are produced during stage ignitions, shutdowns, separation, and fairing jettison. In addition, the pressure changes from sea-level atmospheric pressure to vacuum in space during the initial phase of the launch. It is important to consider all these factors during the development of the spacecraft structure. The most critical load environments are described in detail in the following sections. [29]

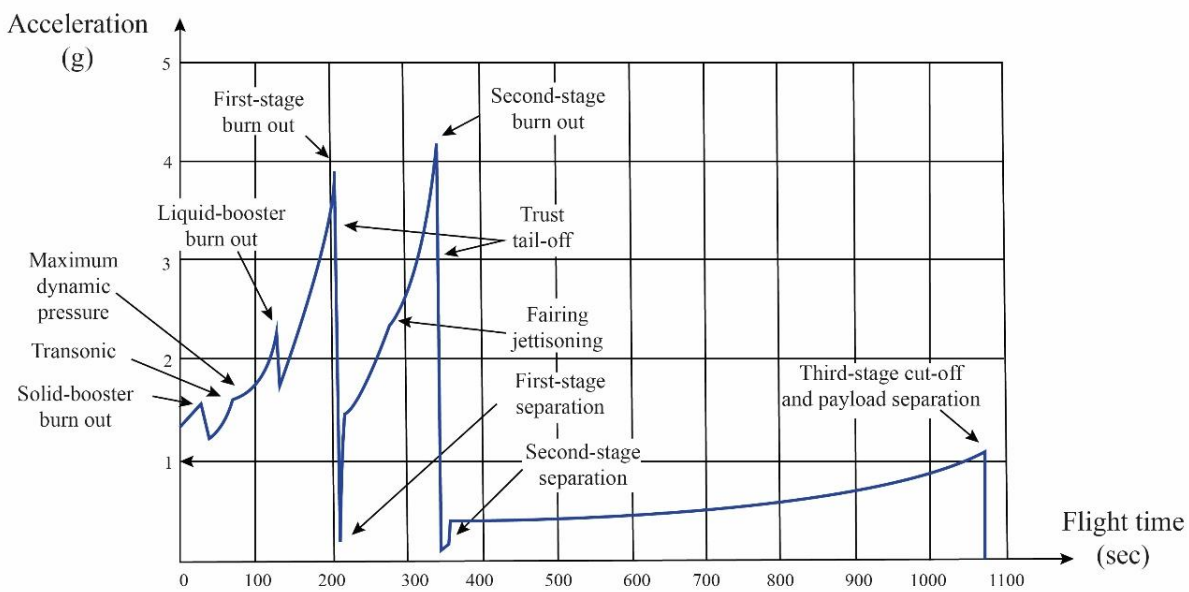


Fig. 19: The course of axial acceleration of Ariane launch vehicle [17]

3.3.2 STATIC LOADS

Steady-state static loads are primarily generated by the engine thrust, crosswind loads, and manoeuvres. The image above shows an example of the longitudinal acceleration during the flight of the Ariane rocket. The maximum values occur before the burnout of the rocket stages because during the burning of the stages, the mass decreases while the thrust remains constant. Steady-state accelerations in the lateral direction, caused by wind gusts or steering, are usually much lower. [16]

Static loads, also known as quasi-static loads, are typically characterized using a load factor, which is a dimensionless multiple of g that represents the inertia force acting on the structure. It is important to note the sign convention, where the sign of the load factor is opposite to that of the acceleration. [20]

Usually, the dynamic loads are also transferred to equivalent static loads, which is described in more detail in subchapter 3.3.4.

	Acoustics	Random Vibration	Sine Vibration	Shock
Lift-off	X	X		
Aerodynamics/Buffer	X	X		
Separation (stage, fairing, spacecraft)				X
Motor bum /Combustion/ POGO		X	X	

Tab. 5: Launch vehicle loading environments [30]

3.3.3 DYNAMIC LOADS

SINE VIBRATION

Sinusoidal vibrations in low frequency domain up to 100 Hz occur as a consequence of the dynamic coupling between spacecraft and launcher and are elicited by the loads during [16][20]:

- Lift-off – the fast increase of thrust introduces a shock load which causes vibration in low frequency domain
- Combustion of the engines – the propulsion of the propellants causes sinusoidal vibrations both in the longitudinal and lateral directions. This phenomenon is often referred to as POGO (Propulsion Generated Oscillations)

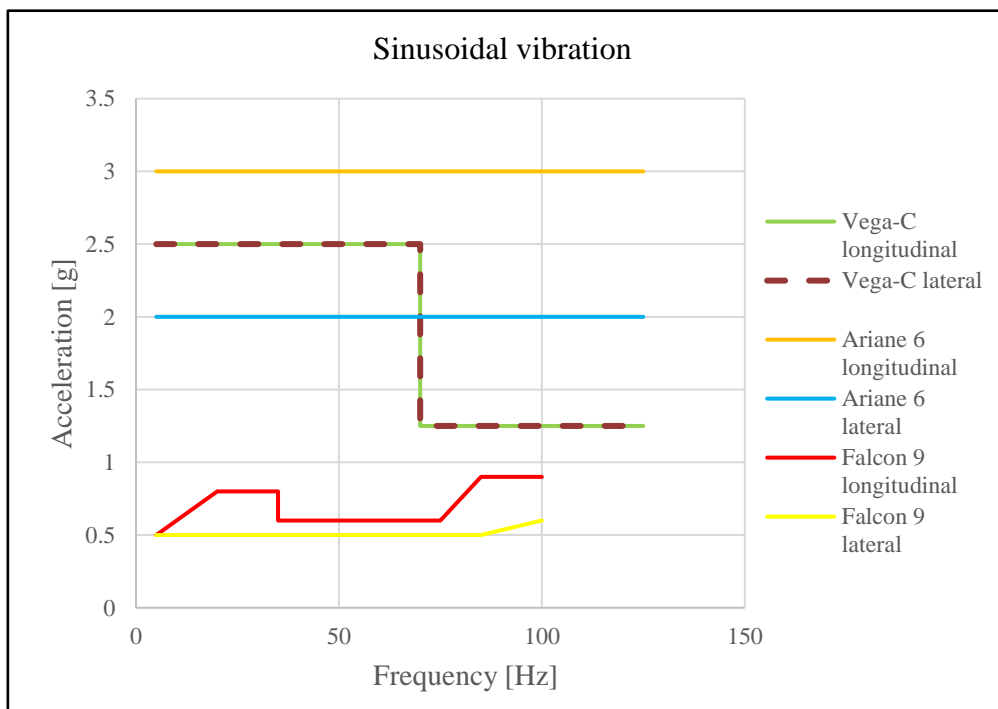


Fig. 20: Sinusoidal vibrations of some currently available launchers

Due to the low frequencies, the sine oscillations are usually driving the design of the primary structure. It is usually specified in g given in the frequency bands up to 100 Hz for longitudinal and lateral directions. [20]

ACOUSTIC LOADS AND RANDOM VIBRATIONS

Although the acoustic load is not the only source of random vibrations, these two environments are strongly associated and often referred to as vibroacoustics. Acoustic loads are most severe during lift-off (due to sound waves reflecting off the ground) and in the transonic flight phase (around Mach 1 speed) and are usually described in terms of sound pressure level (SPL), which is measured in decibels (dB) and varies with frequency. Lightweight structures with a large area, such as solar panels, are particularly vulnerable to acoustic loading. [16]

Random vibrations are induced at the spacecraft by acoustic loads and are usually also transmitted via LVA. Random vibrations are characterized by power spectral density (PSD), which is usually expressed in g^2/Hz . Essentially, PSD can be understood as an intensity of vibrations at the different frequencies. Random vibrations are usually the driving load environment for the design of electronics and electro-mechanical parts of the structure. [17]

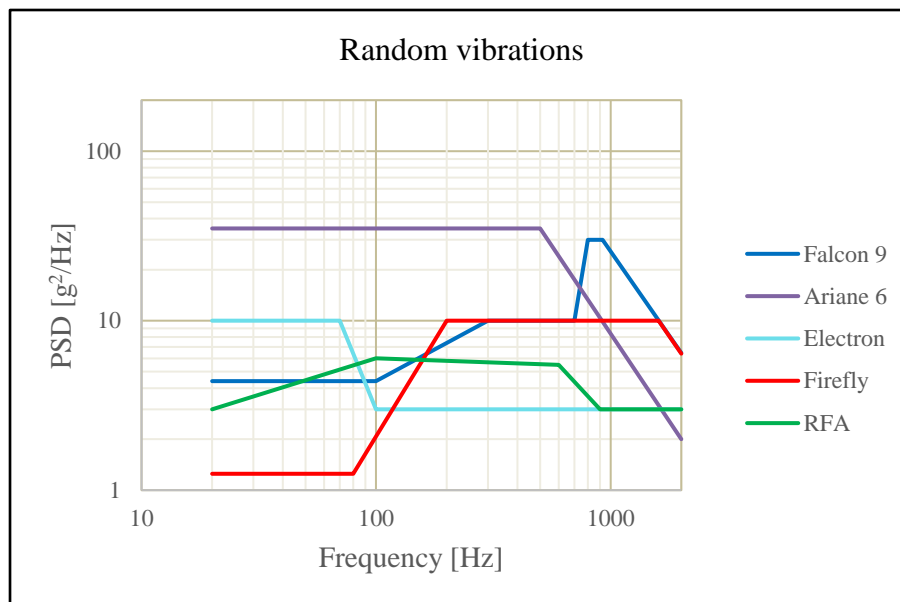


Fig. 21: Random vibration levels of some currently available launchers

SHOCK LOADS

During the mission, the spacecraft is subjected to very short duration loads (approx. 0.5 ms) caused by the engine ignition and cut-off, separation of the launcher stages, fairing jettisoning, and separation of the spacecraft from the last stage. These events are not typically associated with the natural frequencies of the structure due to their short duration. While shock loads may not often impact large structures, they can cause damage to electronics, mechanisms, valves, and other components. Shock loads have vibration frequencies ranging from 100-10000 Hz and are usually specified in the shock response spectrum (SRS). [17][31]

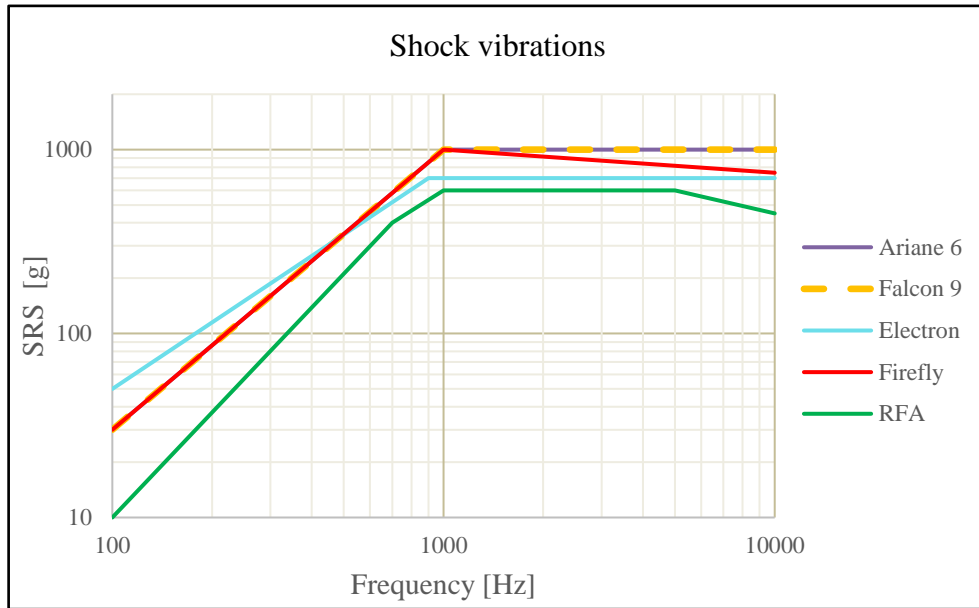


Fig. 22: Shock vibration levels of some currently available launchers

3.3.4 DERIVATION OF THE QSL FROM THE DYNAMIC LOADS

To simplify the process of evaluating the strength of the structure, quasi-static loads (QSL) are used, which are equivalent static loads resulting from the dynamic response of the structure. This is achieved through frequency response analysis, which determines the dynamic response of the structure to different frequencies of excitation. The maximum acceleration in g is then used as a load factor for linear static analysis. QSLs represent the most dangerous combinations of static and dynamic accelerations that the spacecraft can encounter at any stage of the mission. The launcher’s user manual specifies a set of load factors that are used for the preliminary design of the structure. These load factors are updated from the results of the combined load analysis (CLA) in later phases of the project, but the process is complex and varies depending on the project. This methodology is depicted in the following image.

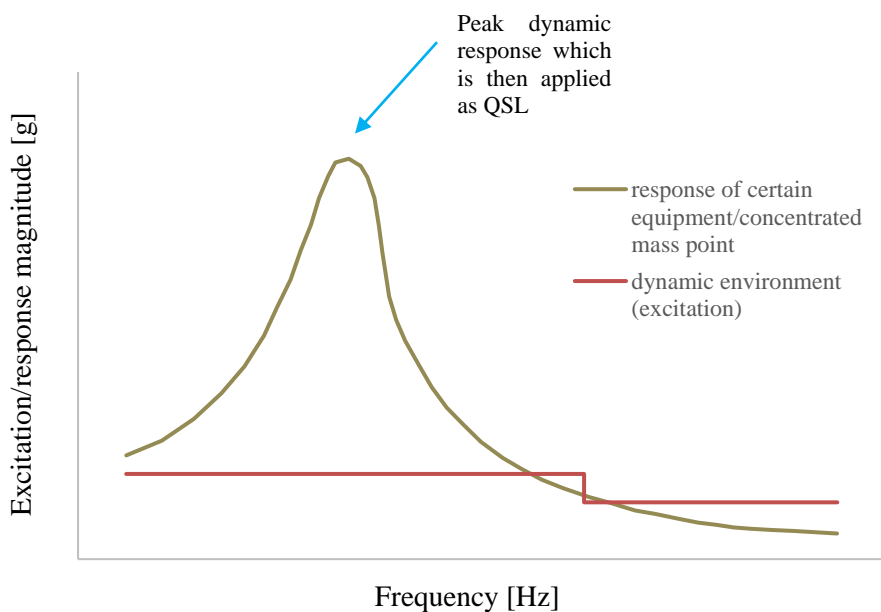


Fig. 23: Derivation of QSL based on dynamic excitation

LOAD CASES AND SUBCASES

Because QSL load factors are derived based on dynamic analyses and may be specified for different parts of the structure separately, to find how the structure behaves when the individual load factors are applied in different directions for different parts of the structure, it is necessary to make many combinations of them. These combinations are called load cases, and they consist of subcases. It is a common practice in some companies to define subcases as a unitary loads which are then multiplied by different scaling values (the maximum value of the multiplier is the load factor) to cover as many loading combinations/force directions as possible. At each project there are usually several sets of QSL defined by the prime contractor as tables with load cases consisting of different subcases. The number of subcases and load cases varies greatly depending on the project and the cause of the load. For example, launcher QSL (L-QSL) are usually represented by 3 subcases which are 1 g accelerations in the x,y,z axes. These subcases are multiplied by various scaling values and combined into many load cases because the resulting force during the launch can be applied in an arbitrary direction.

Acceleration (g)	Longitudinal		Lateral	Additional line load (N/mm)
Critical flight events	Static	Dynamic	Static + Dynamic	
Lift-off	- 1.8	± 1.5	± 2	26
Aerodynamic phase	- 2.7	± 0.5	± 2	23
Pressure oscillations /SRB end of flight	- 4.4	± 1.6	± 1	37
SRB jettisoning*	- 0.7	± 3.2	± 0.9	0

Tab. 6: QSL load factors for a design of a spacecraft to be launched on Ariane 5 [20]

The example of a derivation of an illustrative load case is shown below using the L-QSL of the Ariane 5 rocket at the lift-off introduced in the table above.

Subcase 1 = 1 g in the x direction (longitudinal)

Subcase 2 = 1 g in the y direction (lateral-1)

Subcase 3 = 1 g in the z direction (lateral-2)

Load case 1 =

$$\begin{aligned}
 & \text{Subcase 1} \times -3.3 \text{ (static + dynamic)} \\
 & \quad + \\
 & \text{Subcase 2} \times 2 \\
 & \quad + \\
 & \text{Subcase 3} \times -2
 \end{aligned}$$

In the table of load cases this load case would be written in the following manner:

	1L	2L	3L
1	-3.3	2	-2

Tab. 7: Illustrative first load case of the table with QSL

If we substitute a component of element stress (for example for shell element one of σ_x , σ_y , τ_{xy}) instead of the subcase in the above equation, the product of multiplication and summation would represent the overall value of that stress component for the given load case. However, it is crucial to note that linear superposition of stress components is only valid for linear static analysis with a linear material model. Furthermore, it is important to mention that the values of principal stresses or von Mises stress cannot be combined using this approach since they are not subject to linear superposition. Only individual stress components can be combined in this way. This method is shown and applied directly to particular element stresses in the last chapter where the functionality of the developed software is verified.

The table with the first ten load cases from the real set of 96 load cases of L-QSL specified by the prime contractor for the design of PLATO SVM is shown in Tab. 8. Except from the launcher QSL, for every project, many other sets of QSL are specified, among which are usually also:

- Payload QSL – load factors specify acceleration of payload (cameras, antennas, ...) of the spacecraft
- Equipment QSL – load factors specify acceleration of the equipment units (boxes with electronics, reaction wheels, ...)
- Transport QSL – specifies the QSL during transport
- Hoisting QSL – specifies the QSL during manipulation such as hoisting by crane

These load cases are usually analysed separately because they typically require different boundary conditions. The stresses for each load case can be obtained either by calculation directly in Nastran or by superposition of the element stresses that were previously obtained by linear static analysis for each subcase separately. These approaches, along with the post-processing techniques that follow these procedures, will be discussed in more detail below in the section 4.1.

3.4 STRUCTURAL ANALYSIS

3.4.1 TYPES OF ANALYSES

After initial sizing, to meet the requirements specified in section 3.1.1 and thus, to predict the structural response on loading environments specified in section 3.3 and also to plan appropriate testing procedures the following structural analyses are usually performed [17][23]:

- Modal analysis – to calculate natural frequencies and modes of vibration of the structure in the frequency domain
- Transient analysis – to obtain the dynamic response in the time domain to any time-dependent loads
- Frequency response (harmonic) analysis – to simulate response to sinusoidal excitations
- Static analysis – to calculate stresses, internal loads, displacements, and stiffness of the structural parts
- Acoustic analysis – to predict the response to acoustic excitation and to infer random spectra for random analysis
- Random response analysis – to calculate the behaviour under the random vibrations loading specified by power spectral density (PSD)

- Fatigue and crack growth analysis – to predict behaviour under the cycle loading (often not considered during launch due to short period of loading but often calculated for in-orbit cyclic thermal loading)
- Thermo-elastic analysis – to determine distortions and stresses imposed by the thermal expansion and contraction loading
- Buckling analysis – to predict the behaviour of structures prone to abrupt changes in shape configuration under the loading
- Fracture Mechanics analysis – to predict behaviour of the structure with the defect (often not performed because the structures are properly checked by CT to detect defects)

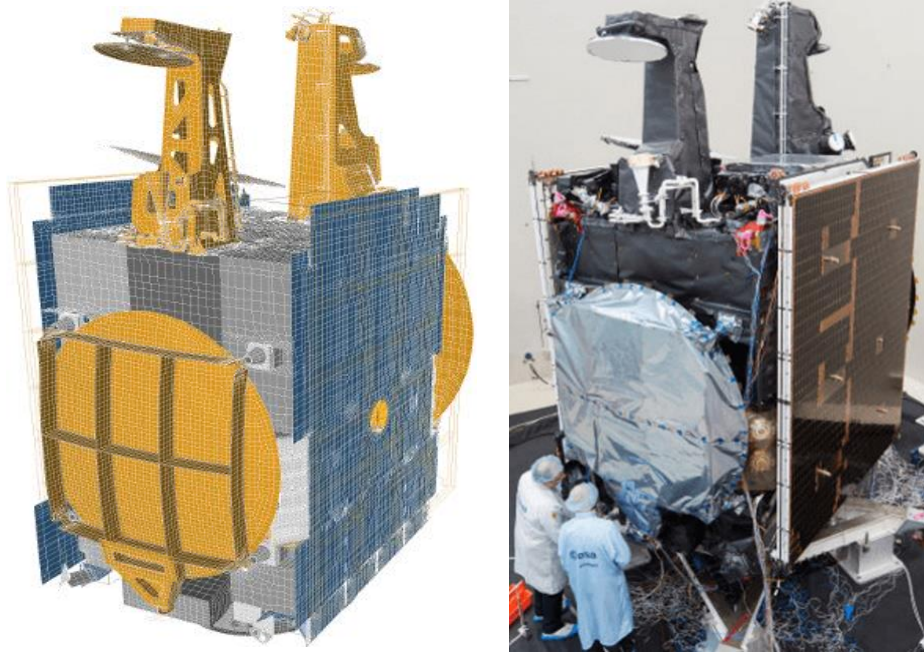


Fig. 24: SGeo/Hispasat 36W-1 satellite FE model and real structure [32]

Although the analytical methods of structural mechanics can be used for some of these analyses, finite element analysis (FEA) is currently the most commonly used tool by space structural engineers.

3.4.2 FEA SOFTWARE AND WORKFLOW

NASTRAN

Although there are many commercial FEA solvers, Nastran is arguably the most used solver in the field of mechanical behaviour analysis of space structures. This is partly given by the historical background since Nastran was initially created for NASA (**N**ASA **S**tructure **A**nalysis) by The MacNeal-Schwendler Corporation (MSC) in the late 1960s as a consequence of growing need for a software that would simplify the process of structures development. Since then, the Nastran source code has been integrated into many commercial packages distributed by various companies. [33][34]

Throughout the years many capabilities have been added including transient, nonlinear, explicit and other advanced solver options and features that might be applied to static, dynamic, and thermal analyses. The type of analysis is specified by the solution sequence (SOL) number. The complete overview of software's capabilities can be found in MSC Nastran Quick Reference Guide. [35]

NASTRAN FILES

To run MSC Nastran successfully, the FE model must be fully defined. This can be achieved through the bulk data file (.bdf) and/or the data file (.dat). While either of these can contain all the necessary information, it is common to separate the input, with the BDF file containing information about the FE model (such as nodes, elements, and properties) and the DAT file containing analysis settings (including SOL, loads, constraints, and file paths). Both files are in ASCII format. [36]

Although there are more output files containing different types of information related to the performed analysis, for the user are mostly important [36]:

- **.f06** – the main output file containing potential error, warning, and diagnostic messages, can contain printed outputs such as calculated displacements, stresses, etc., it is in ASCII format
- **.pch** – punch file, in this file are outputs specified by the user in input files, it can be used as a main file for printing results (stress, element forces, etc.), it is in ASCII format
- **.op2** – output database for post-processing of the results, is used for direct loading into the post-processing software and for visualisation of both the FE model and the requested results, it is in binary format

It was decided to use the PCH file as the main output file for the new post-processing tool. This is because the stresses in ASCII format can be easily checked and worked with, making the process more straightforward. It is important to note that, due to the development of the post-processing software, there are two possible ways in which the requested stress results can be written into the PCH output file. In both cases, the stress data are grouped by the element type.

- **SORT1** – in this format the data are organised in a way that the parent category is a subcase, to which elements with corresponding results are assigned
- **SORT2** – in this format the superior class is element to which are assigned stresses from all the subcases

```

$title =
$SUBTITLE= 1 G X
$LABEL =
$ELEMENT STRESSES
$REAL OUTPUT
$SUBCASE ID =          1
$ELEMENT TYPE =       33 QUAD4      VONM
10000001              -2.500000E-03   -3.890612E+03   -1.635137E+03
-CONT-                -4.905692E+03   -5.147321E+01   2.270773E+03
-CONT-                -7.796522E+03    9.145835E+03    2.500000E-03
-CONT-                -4.571477E+03   -1.707530E+03   -5.092004E+03
-CONT-                -5.285353E+01    2.150020E+03   -8.429027E+03
-CONT-                9.684712E+03
10000002              -2.500000E-03   -4.775520E-12   1.786765E-12
-CONT-                -4.540435E+03   -4.500000E+01   4.540435E+03
-CONT-                -4.540435E+03   7.864265E+03    2.500000E-03
-CONT-                -9.901628E-12    4.336809E-13   -3.829553E+03
-CONT-                -4.500000E+01    3.829553E+03   -3.829553E+03
-CONT-                6.632981E+03
10000003              -2.500000E-03    3.890612E+03    1.635137E+03
-CONT-                -4.905692E+03   -3.852679E+01   7.796522E+03
-CONT-                -2.270773E+03    9.145835E+03    2.500000E-03
-CONT-                4.571477E+03    1.707530E+03   -5.092004E+03
-CONT-                -3.714647E+01    8.429027E+03   -2.150020E+03
-CONT-                9.684712E+03

```

Name of the subcase

Element stress results

Fig. 25: Organisation of the data using SORT1 format

FEA WORKFLOW

The process of preparing the finite element (FE) model for the solver is called pre-processing. Typically, computer-aided design (CAD) is used as input, and the FE mesh is created using appropriate elements. Pre-processing also involves setting up material models and their properties, defining boundary conditions such as constraints and loads, and other relevant data. After the model is created, its reliability is checked using established procedures before solving. Once the solver completes the solution, post-processing is performed to evaluate and visualize the solver's output results.

Commercial software is commonly used for both pre-processing and post-processing tasks. Some software packages combine both tasks in a single graphical user interface, such as Patran or Femap. Others split these functions into two separate programs, such as HyperMesh for pre-processing and HyperView for post-processing. The typical workflow of FEA can be illustrated through the following chart:

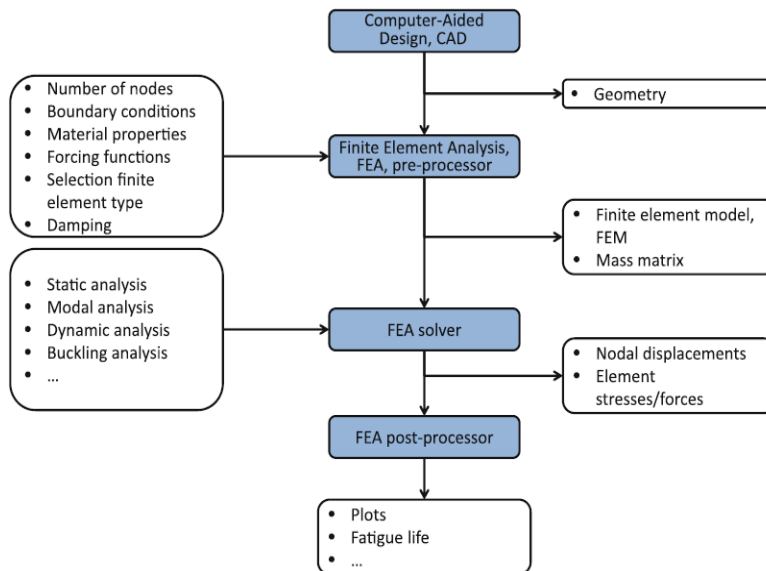


Fig. 26: Flowchart of structural FEA [23]

3.4.3 FE MODEL PRE-PROCESSING

The process of creating an FE model usually begins with importing CAD geometry, which can be in various formats such as STEP, IGES, etc. After importing, it is important to check the quality of the model and fix any potential issues such as redundant or unstitched surfaces. Before meshing, it is often necessary to perform geometry clean-up, which involves removing holes, radii, and other features that correspond to the chosen modelling philosophy and element types to be used. [37]

The FE model is typically composed of diverse types of elements, each with distinct properties to represent different parts of the structure. The selection of an appropriate modelling approach is crucial to obtaining accurate results, and understanding how to represent the actual structure while minimizing the number of elements to save computational time is a critical skill for each structural engineer.

1D ELEMENTS

1D elements are typically used for structural parts that have one dimension significantly larger than the others. This means they are useful for representing long, thin parts of a structure, such as tie-down members, beams, supports, and so on. The main advantage of this type of element is that it can replace a much larger number of shell or solid elements, thereby saving a significant amount of computational time. [37]

In Nastran, there are several 1D elements with numerous optional specifications. However, the most commonly used 1D elements and their essential properties can be listed as follows. All of the following 1D elements have two nodes (grid points) [38]:

- CROD
 - The simplest one, has only axial (tension-compression) and torsional stiffness
 - Properties must be constant along the length of the element
 - 2 DOFs in one node - U_x, R_x (1,4)
- CBAR
 - It also has shear and bending stiffness
 - The shear centre of the cross section must coincide with the neutral axis
 - 6 DOFs in one node – $U_x, U_y, U_z, R_x, R_y, R_z$ (1,2,3,4,5,6)
- CBEAM
 - It has all kinds of stiffness as well as the CBAR element
 - The shear centre can be specified outside the neutral axis
 - The properties can change along the element (e.g., variable cross section)
 - Used when effect of cross-sectional warping on torsional stiffness is critical
 - 6 DOFs in one node

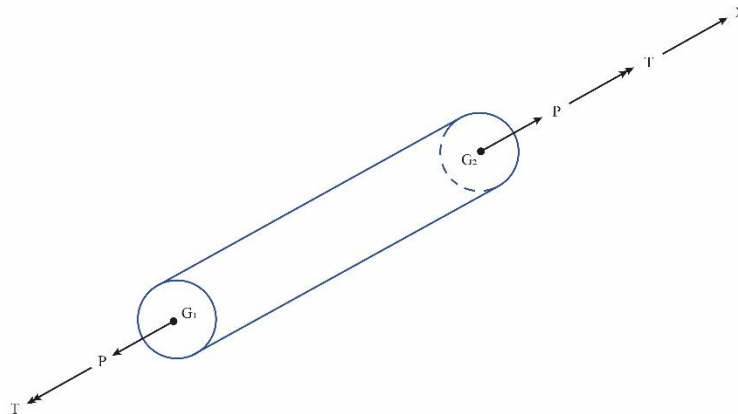


Fig. 27: CROD element internal forces and moments

The format of the bulk data entry in the 8-character fields of BDF file for CROD is shown in the following picture, EID – Element identification number, PID – Property identification number of a PROD entry, G1 and G2 – grid point identification numbers of connection points.

1	2	3	4	5	6	7	8	9	10
CROD	EID	PID	G1	G2					

Fig. 28: Bulk data entry for CROD elements

The elements mentioned above must be assigned corresponding properties that define their characteristics, which are described in detail below.

2D ELEMENTS

2D elements are mainly used to represent structural parts where one of the dimensions is significantly smaller than the others. Since space structures are typically composed of lightweight, thin-walled components, 2D elements are a primary constituent of spacecraft FE models. The mesh is usually created on the mid-surface of the original thin-walled structure. An exception is in the case of adjacent components, such as flanges, where the 2D mesh is created on the interface of these two adjacent components to model the bolts. This will be explained in more detail in the section dedicated to spring elements.

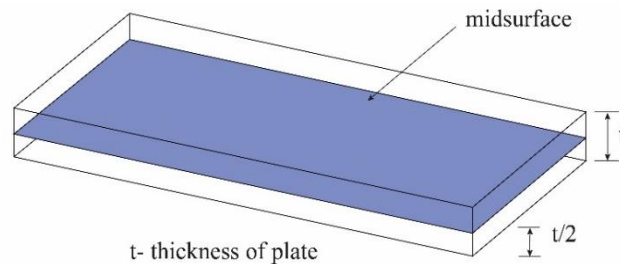


Fig. 29: Representation of the mid-surface [37]

Although Nastran offers several 2D elements with various properties, the most commonly used ones are the linear shell elements CQUAD4 and CTRIA3, both with all six DOFs in each node. Occasionally, their quadratic versions with midnodes on the edges (CQUAD8, CTRIA6) are also used. Due to their greater accuracy, quadrilateral elements are generally preferred over triangular elements. [38]

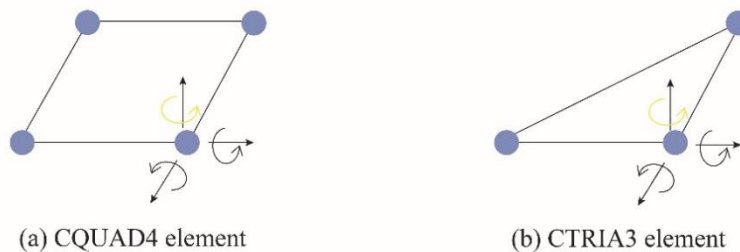


Fig. 30: Shell elements

An important aspect of the formulation of these shell elements is that they do not inherently provide the sixth DOF, R_z (rotation about the normal to the surface of the element). Therefore, it must be added artificially to avoid potential singularities by specifying the `PARAM,K6ROT,x` parameter in the analysis settings. The value of x can range from 1.0 to 100.0, and ECSS recommends comparing values within this range and monitoring whether the changes significantly affect the results. It should be noted that this additional stiffness is only an artificial extension of the element's capabilities to avoid singularities and should not be relied upon when a CROD element is attached to the shell element and the bending stiffness should depend on the R_z DOF. [38]

The stress element output is by default written for the centroid of the element. But by command `STRESS(CORNER)=ALL` also results for the corner nodes on all elements can be requested. The CQUAD4 and CTRIA3 elements can be assigned the PSHELL or PCOMP property which are both described below. [38]

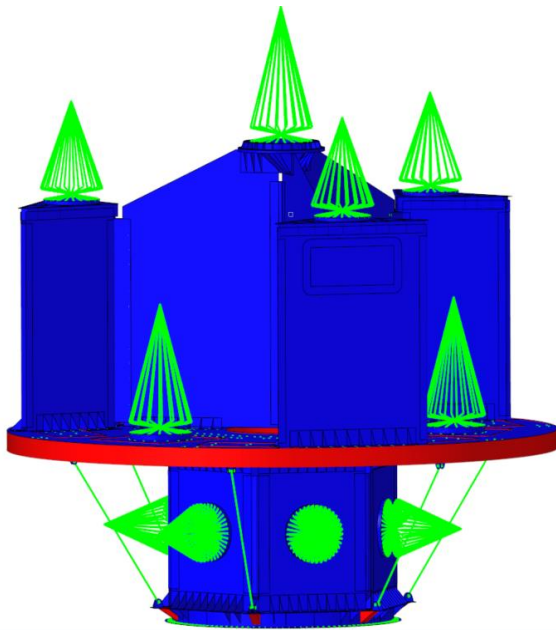


Fig. 31: FE model of SSMS Dispenser

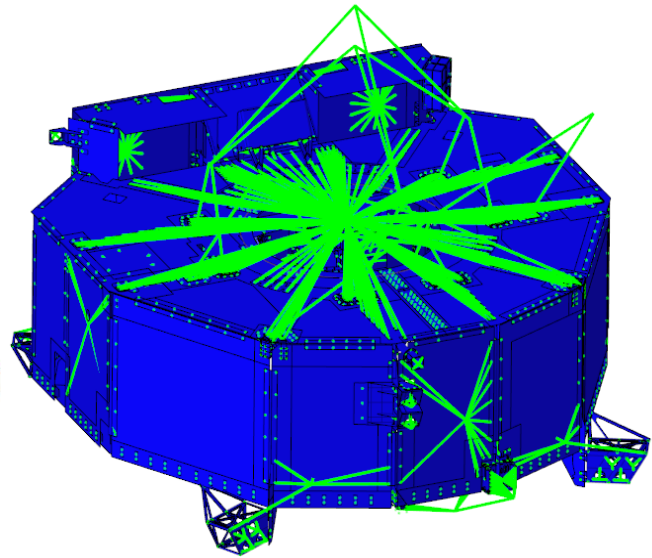


Fig. 32: FE model of PLATO SVM

3D ELEMENTS

3D elements are commonly used to represent parts of larger volumes with all three dimensions being comparable in size. Although these element types are not frequently used in the modelling of space structures, they are occasionally employed for specific purposes. For example, in the SSMS Dispenser FE model, solids were used to represent the thick ribs at the bottom of the hexagonal module and the core of the main deck composite panel. In the FE model of PLATO SVM, 3D elements were used in one project phase to represent small brackets, which are used in the last chapter for validating the post-processing of solid elements. The pictures above show the element types used for the FE models of the following space structures: 1D elements in green, 2D elements in blue, and 3D elements in red.

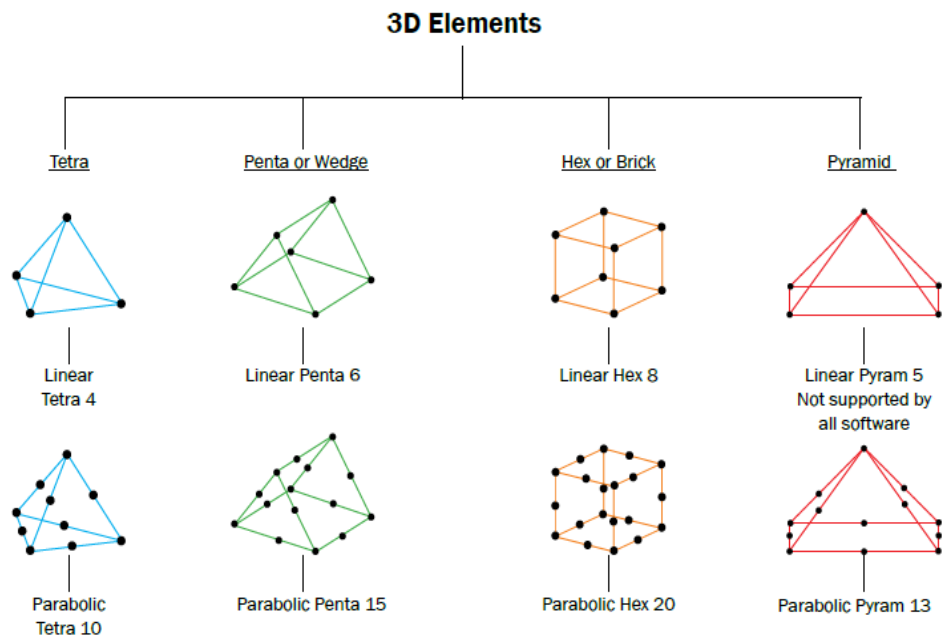


Fig. 33: Types of 3D elements [37]

The available types of 3D elements are shown in the picture above. These elements have only 3 translational DOFs per node, which makes direct connection to bar or shell elements with rotational DOFs difficult. The K6ROT parameter does not apply to solid elements, so other methods such as RBE3 elements or solid-to-shell element connectors (RSSCON) must be used. By default, stress results for solid elements are calculated for the centroid and extrapolated to the grid points (nodes). Additional information necessary for the element's formulation is specified in the element property PSOLID.

R-TYPE (CONSTRAINT) ELEMENTS

R-type (sometimes referred to as constraint) elements are sometimes classified as 1D elements, but they are not considered structural elements in the true sense. Essentially, they are equations that define relationships between degrees of freedom of different nodes. While they are occasionally referred to as rigid elements, this description is not accurate as some R-type elements belong to the group of interpolation elements, which are not entirely rigid. [38][39]

Some R-type elements, such as rigid elements RROD or RBAR, can only connect DOFs on two nodes. However, the most commonly used R-type elements are those that can connect DOFs on multiple nodes, referred to as multipoint constraints (MPC) in Nastran. In these elements, one node (referred to as the independent node) controls the DOFs of other nodes (called dependent nodes). It is important to note that a dependent node should not be assigned as a dependent node for another MPC entry and cannot be constrained by a boundary condition. [37][38]

The most often, following elements are used [37]:

- RBE2- rigid element which distributes the forces and moments evenly among all the dependent nodes regardless of the position
- RBE3-interpolation element distributing the forces and moments in accordance with the distances of the dependent nodes (uses least square weighing function)

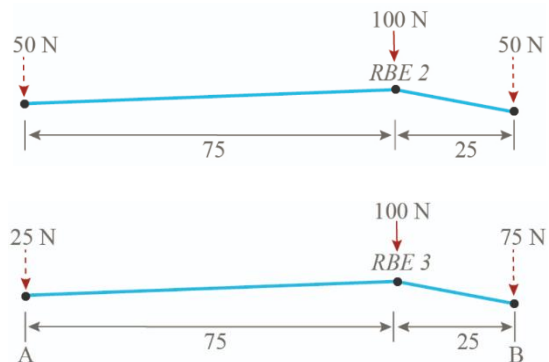


Fig. 34: RBE2 and RBE3 elements [37]

It should be noted that rigid elements (RBE2) introduce infinite local stiffness into a structure and should be used with caution. Typically, they are used to represent parts that are significantly stiffer, and do not require detailed modelling. They are also used for modelling the attachment of the structure to the launcher or for connecting mass elements. RBE2 elements are highly stiff, making them conservative for evaluating stresses. On the other hand, RBE3 elements have lower stiffness and are conservative for evaluating eigenvalues.

MASS ELEMENTS

Mass elements, also known as zero-dimensional or point elements, are typically placed at the center of gravity of the component they are representing. In addition to defining the total weight, the mass matrix representing inertia properties can also be defined, which is particularly important for dynamic analyses. The most commonly used mass element type is CONM2, which is usually attached to the structure using RBE2 or RBE3 elements, as previously

mentioned. This simplification is performed to reduce the complexity of the model and is typically used for components whose structure is clearly defined and not subject to design changes. Examples of parts usually represented by CONM2 elements include electronic boxes, reaction wheels, or satellites attached to the Dispenser structure, as shown in the Fig. 31.

SPRING ELEMENTS

Like R-type elements, spring elements are not true structural elements. They are mathematical equations that couple degrees of freedom (DOFs) between two connected nodes with pre-defined stiffness. The most commonly used spring element is the CBUSH element, which can be assigned stiffness in all six DOFs. The constants defining the stiffness connecting particular DOFs are defined in property PBUSH along with other parameters. The CBUSH element is commonly used for modelling bolt joints according to SAB Aerospace standard procedure. To avoid introducing unreal moments, these CBUSH elements are often modelled with zero length, which requires shifting mid-surfaces to the interface as mentioned in the section dedicated to 2D elements. To identify stiffnesses to relevant directions, a coordinate system (CS) must be assigned to the CBUSH elements. By convention, the axis of the bolt is assigned as the x-axis of the CS.

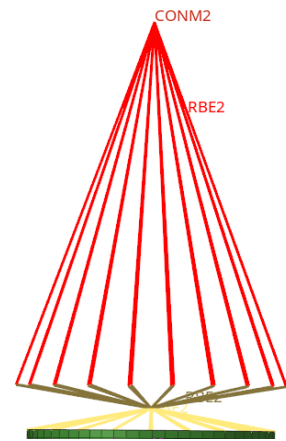


Fig. 35: Typical use of mass element

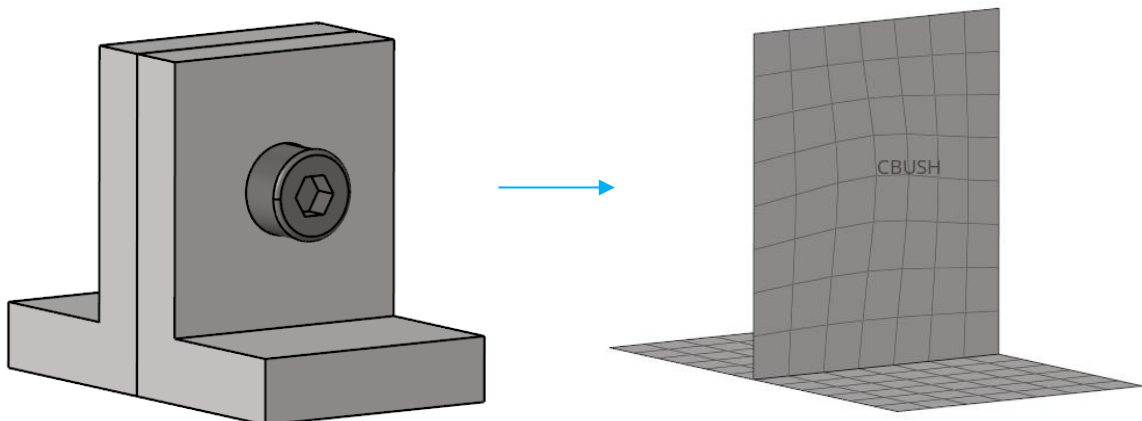


Fig. 36: Typical bolt joint of thin-walled structure represented by shell elements

3.4.4 MATERIAL MODELS

LINEAR ELASTIC ISOTROPIC (MAT1)

The simplest material model used in FE analyses is the linear elastic isotropic model, which is represented in Nastran by the material card MAT1. It is commonly used for the metallic parts of the structural model and can be fully defined by two elastic constants. These constants may be any combination of E, G, and ν , since the third constant is automatically calculated using the relation:

$$G = \frac{E}{2(1 + \nu)} \quad (2)$$

where E represents Young's modulus, G is the shear modulus, and ν is the Poisson's ratio. In addition, the MAT1 card allows for the specification of mass density, coefficient of thermal expansion, and reference temperature for thermo-elastic analyses.

TWO-DIMENSIONAL ORTHOTROPIC MATERIAL (MAT8)

This material model is used for modelling CFRP laminates with shell elements. An orthotropic material is one that has different material properties in three perpendicular directions. For thin-walled structures in laminate theory, the stress throughout the thickness is considered negligible, and therefore, a two-dimensional form of the general Hooke's law is generally applied [40]:

$$\begin{bmatrix} \varepsilon_1 \\ \varepsilon_2 \\ \gamma_{12} \end{bmatrix} = \begin{bmatrix} \frac{1}{E_1} & \frac{-\nu_{21}}{E_1} & 0 \\ \frac{-\nu_{12}}{E_1} & \frac{1}{E_2} & 0 \\ 0 & 0 & \frac{1}{G_{12}} \end{bmatrix} \begin{bmatrix} \sigma_1 \\ \sigma_2 \\ \tau_{12} \end{bmatrix} \quad (3)$$

where σ_1 , σ_2 , and τ_{12} are normal and shear stresses in the material CS, ε_1 , ε_2 , and γ_{12} are strains in the material coordinate system ν (Poisson's ratio), E (Young's modulus) and G (shear modulus) are material characteristics in specified material directions. Because the following relation [40]:

$$\nu_{21} = \nu_{12} \left(\frac{E_2}{E_1} \right) \quad (4)$$

is valid, it means that this material model has 4 independent material constants (E_1 , E_2 , G_{12} , ν_{12}). To define the MAT8 material model in Nastran, the following characteristics (symbols as per Nastran user manual) must be specified [39]:

- $E1$ – modulus of elasticity in the longitudinal direction.
- $E2$ – modulus of elasticity in the lateral direction
- $NU12$ – Poisson's ratio for uniaxial loading in direction 1
- $G12$ – in-plane shear modulus.
- $G1Z$ – transverse shear modulus for shear in the 1-Z plane.
- $G2Z$ – transverse shear modulus for shear in the 2-Z plane.

These additional transverse shear modules are necessary because Nastran using the PCOMP property entry creates equivalent PSHELL and MAT2 (two-dimensional anisotropic material) entries which are then used for the calculation itself. Using this combination of material models and particular material constants, the solver calculates also transverse shear stresses (Shear-1Z and Shear-2Z), if more than one ply is specified in the PCOMP property. In addition, mass density (RHO), coefficients of thermal expansion in two directions (A_1 , A_2), and reference temperature (TREF) can be specified. It should be noted that the MAT8 entry can be defined only for 2D elements. [38]

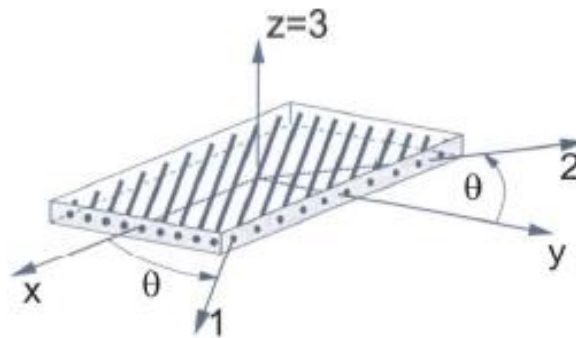


Fig. 37: General (element) and material (ply) coordinate systems (axis 1 represents the direction of the fibres, axis 2 represents direction perpendicular to the fibres, axis 3 is perpendicular to the plane of the ply)

Other material entries from the Nastran material library may be useful, though less frequently. For example, when modelling the core of the main deck of the SSMS Dispenser (as shown in Fig. 31) using solid elements, a three-dimensional anisotropic material with 21 material constants (MAT9) was used. This was necessary to accurately capture the orthotropic properties of the core using solid elements.

3.4.5 MASS DISTRIBUTION IN FE MODELS

Between the sections that cover material models and definitions of properties, it should be briefly noted that in FE models, there are two ways of specifying mass, which is particularly important for dynamic analyses where mass is a critical parameter. The traditional way of mass distribution is to include density in the material specification, which results in a distribution directly corresponding to the volume, as in the well-known formula $\text{mass} = \text{density} \times \text{volume}$. This method is preferred for components where the volumes of the FE model and of the component in the CAD are comparable.

However, sometimes the component in the FE model is considerably simplified, and the volumes are substantially different. In such cases, it is better to use the second method for specifying mass, which involves the use of non-structural mass (NSM). NSM is an additional parameter specified at the property level, representing the mass of the component obtained from the CAD model. This mass is then evenly distributed over the specified elements, ensuring that the component has the proper mass.

3.4.6 PROPERTIES

Properties, also known as P-entries, are bulk data entries that contain additional information about element definitions. They are primarily used to assign material entries, non-structural mass (NSM), and other data specific to a particular element type. The most commonly used properties are described in detail below.

PROD, PBAR, PBEAM

For 1D elements, the main information, apart from the material identification number (MID), relates to the properties of the cross-section. These include the area of the cross-section, the area moments of inertia, the polar moment of inertia, and the NSM. Typically, the cross-section properties are automatically generated by features in pre-processing software (such as HyperBeam in HyperMesh). There are also other advanced characteristics and coefficients that

describe properties such as torsional stiffness or the centre of shear, which are specific for each of these element types. [38]

PSHELL

PSHELL is a bulk data entry that contains additional information necessary for the analysis of shell elements. The most commonly specified parameters include MID, thickness, and, if applicable, NSM. More detailed descriptions of the shell element behaviour can also be specified for more complicated analyses, such as using material properties for specific loading types, although these options are not usually employed. When using PSHELL, it is important to note that calculated stress results are written in the element coordinate system (CS). [38]

PCOMP

PCOMP is property putting together different layers of materials in order to create composite material. The calculated stress results are then written separately for each layer in lamina CS. In contrast with the PSHELL property, which can also be used for shell elements, the PCOMP writes as an output also out-of-plane shear stress (Shear-1Z, Shear-2Z). The PCOMP contains information about the property belonging to each lamina which are MID, thickness, and angle of the fibres in element CS (θ in Fig. 37). Furthermore, there is specified allowable in-plane shear strength, NSM (if applicable), failure theory, damping coefficient and other advanced settings. [38]

PSOLID

The PSOLID entry is used to define the properties of solid elements. Apart from the MID, other additional parameters such as integration network or integration scheme can be assigned, but these are rarely used. [38]

PBUSH

The PBUSH property is associated with CBUSH spring elements, where the stiffness values in all DOFs (K1, K2, K3, K4, K5, K6) can be specified by the user. In addition to this, the damping coefficient can also be specified for all DOFs. Other parameters are usually not employed. [38]

3.4.7 REPRESENTATION OF CFRP PARTS

The use of composite components is mostly seen in sandwich panels or monolithic parts, and there are two ways to represent them in the FE model. The proper way involves a laminate model, where each lamina is characterized by its thickness, orientation, and assigned orthotropic material model MAT8 in the PCOMP property. However, this method is substantially time-consuming in all phases of structural analysis. To simplify this process, a method that uses only one ply instead of many laminas of material MAT8 is often used. The single ply is assigned material MAT1 with equivalent mechanical properties. It is important to note that this simplification can only be made if the CFRP plies are laid up in a quasi-isotropic configuration, as shown in Fig. 15. This second modelling approach is also called laminate modelling method.

This simplification is commonly employed during the early stages of spacecraft development when numerous design iterations are carried out, allowing significant time savings. The comparison of these two approaches is illustrated in the following picture. The monolithic component, represented by quasi-isotropic material, is split into two plies to utilize the PCOMP property, which by default gives non-zero out-of-plane shear stresses only if there is more than

one ply in the PCOMP property. These out-of-plane stresses are required to evaluate the interlaminar shear stress (ILSS), a criterion used to assess the strength of monolithic parts in shear. These two modelling approaches are important for software development and are referred to as ortho-skin composite and iso-skin composite.

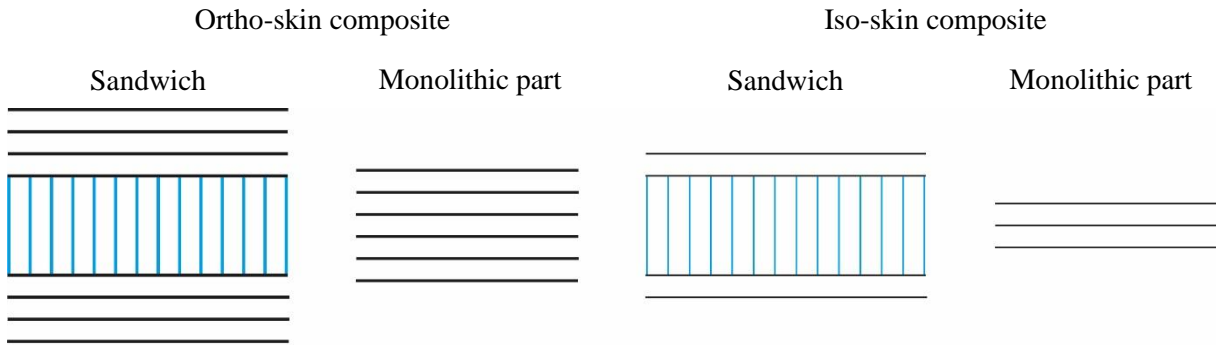


Fig. 38: Modelling approaches of CFRP components

3.4.8 MESH QUALITY CHECKS

Several checks must be performed prior to the actual analysis. These checks shall ensure the validity of the mathematical model and thus correct results will be calculated. The FE mesh verification is divided into pre-processor checks for which no calculation is required and mathematical checks for which the calculation in Nastran is used.

CHECKS IN THE PRE-PROCESSOR

The commercial pre-processors including HyperMesh usually offer features that simplify this control prior to the export. These checks usually include control of the geometric parameters of the FE mesh (warpage, skewness, aspect ratio), duplicate elements, and connectivity of the elements. Other aspects of the FE model to be checked are coherent units of the used physical quantities, correct orientation of elements and CS, correct assignment of MIDs and PIDs to the particular components, correct formulation of RBE2/RBE3 elements, etc. [41]

UNIT GRAVITY LOADING CHECK

This check is used to verify that the model provides correct displacements and reaction forces when subjected to the 1 g loading in all three axes. The results, obtained by linear static analysis (SOL 101), shall not indicate any large displacements and the reaction force obtained using SPCFORCES case control card must correspond to the applied force in the given axis according to the well-known Newton formula: force = mass × acceleration. [42]

From the ECSS follows an additional requirement that the ratio of residual work between external and internal nodal forces and the total applied load work of the nodal forces is lower than the predefined threshold value [43]:

$$\varepsilon_r = \frac{\delta W}{W} < 1 \cdot 10^{-8} \quad (5)$$

where δW is residual work, W is the work of applied load, and ε_r is the ratio.

FREE-FREE DYNAMICS CHECK

The Free-Free dynamics check verifies that the unconstrained FE model presents no other “rigid” degree of freedom rather than the expected 3 translations and 3 rotations. This is performed using modal analysis (SOL 103) where, in theory, the FE model without any constraints shall show zero eigenfrequencies for the first six modes, which correspond to the six degrees of freedom of the unconstrained body. Contrary to theory, there is always some small value of these 6 natural frequencies on the FE model related to numerical approximations, so the ECSS specifies a threshold of 0.005 Hz that must not be exceeded. [43][44]

At this check, the strain energy is also controlled using the stiffness matrix of the FE model. For this purpose, it is necessary to request GROUND-CHECK at the Nastran case control cards before running this check. In theory, the strain energy of the free body should be equal to zero, which does not happen at the real FE model. The ECSS puts the threshold value at 0.001 J. If this value is not met, it is an indicator that rigid elements or constraints in the model are probably incorrectly specified. [43][44]

3.4.9 EXPORT OF THE MODEL

RENUMBERING OF THE ELEMENTS

Before running any analysis using Nastran, the FE model must be exported to the BDF file. Prior to the export, it is common practice to renumber the elements to ensure that the EIDs (Element IDs) for each component fall within a predefined range. The range is determined by the ID numbers assigned to the components. For example, if a component has an ID of 100, the elements belonging to that component are consecutively numbered starting from 101, 102, and so on. It is crucial to verify that the range provides enough space to accommodate all the elements belonging to the component, preventing EIDs from overflowing into the next component. Commercial pre-processing software like HyperMesh offers features specifically designed for this operation. This procedure is done for several reasons:

- It helps engineers to orient in the assembly and to keep the model in a clearly arranged way (by looking at the EID one immediately knows to which component it belongs).
- At the projects on which several companies work, this is usually requested by the prime contractor because it allows him to easily integrate the sub-assemblies and maintain the main assembly.
- Some custom post-processing software require this pattern for proper functioning.

LONG AND SHORT FORMATS

The FE model can be exported in either short format or long format. The short format means that the line in the BDF file is divided into 8-character fields, whereas in the long format the field has 16 characters. The long format is used when more precision is required and is usually used for thermoelastic analyses.

SETS FOR STRESS EVALUATION

If the purpose of the structural analysis is to calculate element stresses, the elements for which the stress should be obtained need to be included in a set of elements, and the set ID must be specified in the analysis settings.

In stress evaluation, it is common practice to exclude elements that are adjacent to rigid or spring elements from the stress calculation. This is because the stiffness of such elements is significantly higher than that of the adjacent elements, leading to unrealistically high stress values. The evaluation of the excluded areas is addressed through the strength analysis of the bolts and/or inserts.

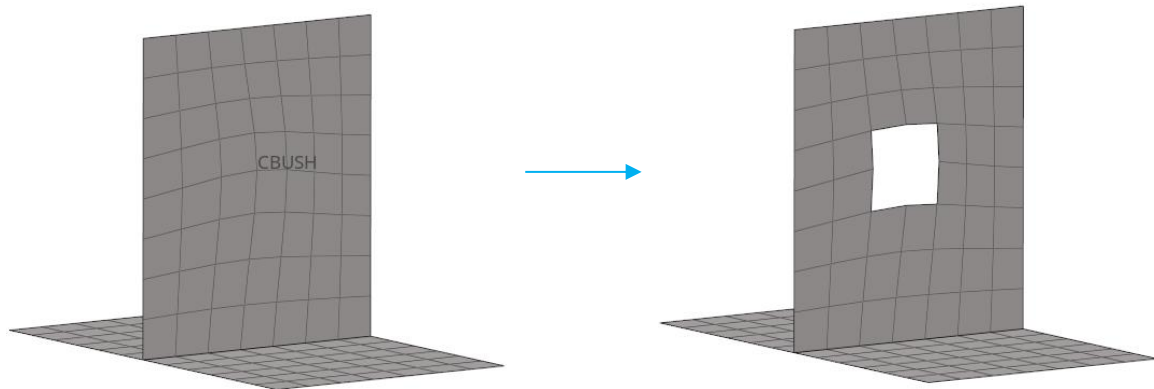


Fig. 39: Example of creation of set for stress evaluation

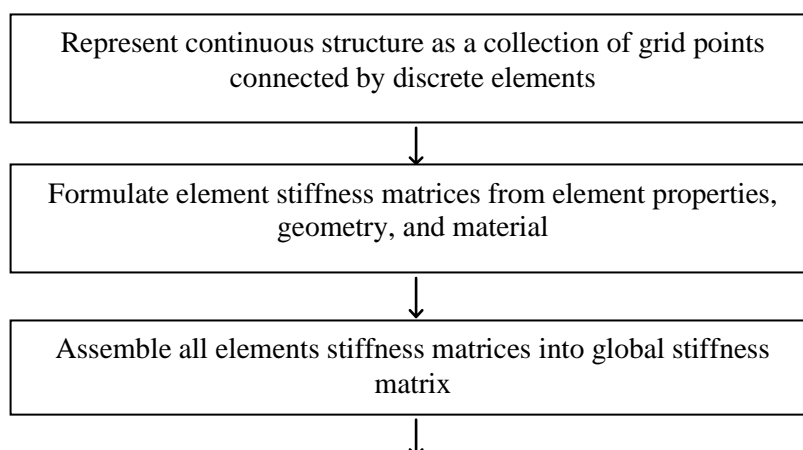
3.4.10 SOLUTION AND POST-PROCESSING

SOLUTION

An integral part of structural analysis using FEM is the solution. The mathematical formulation of the solution depends on the type of analysis being performed. As mentioned earlier, in Nastran, the type of analysis is specified by the solution sequence number (SOL). Here are some examples of the most commonly used solution sequences [39]:

- SOL 101 – Linear static
- SOL 103 – Modal (normal modes)
- SOL 105 – Buckling
- SOL 111 – Frequency response

The main focus of this thesis is the development of post-processing software linked to linear static analysis, which is commonly used for strength evaluation. The theory related to solving linear static material strength problems using FEM has been extensively described in the literature and is beyond the scope of this thesis, so it will not be further discussed. The workflow of the linear static analysis is illustrated in the diagram below:



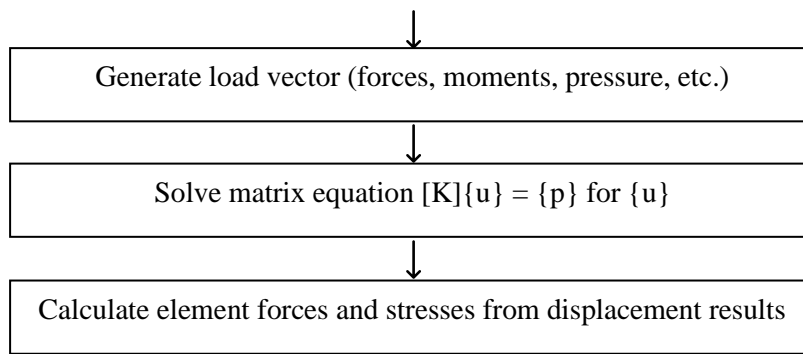


Fig. 40: Scheme of the solution of linear static FE analysis [38]

POST-PROCESSING

There are multiple approaches to further process the raw calculated data in order to streamline the evaluation process. Most commercial FEA software packages include powerful post-processing features, which are typically the primary tools used for this purpose in companies. However, certain features and operations in commercial software may be unfriendly to users or even unavailable, leading many companies to develop their own post-processing tools for achieving more efficient results. Given that the main objective of this thesis is to create a custom post-processing tool, the topic is further explored in detail below.

3.5 STRENGTH EVALUATION

Strength is a term expressing the ability of material to withstand a load without failure. The purpose of structural analysis is not to find the load at which the rupture occurs, but to find the design that will not fail. The most typical forms of failure are yielding and rupture, which occurs when the stress exceeds the limit value, which is material characteristic. To decrease the probability of failure, due to various uncertainties, on both load and stress, a safety factor (FoS) is given. The goal of structural analysis is to have some reserve, i.e., to have positive margin of safety (MoS). Prediction of failure is specific for different materials and types of the structure and in order to predict it, the following failure criteria are generally used. [17]

3.5.1 METALLIC PARTS

VON MISES CRITERION

This criterion, also known as the Maximum Distortion Energy Criterion, says that the yielding occurs when the distortion energy per unit volume in the material exceeds the distortion energy per unit volume required to cause yield in a tensile-test specimen of the same material. The distortion energy is the component of the strain energy density associated with changes in the shape of the material compared to the volumetric (hydrostatic) component, which is associated with volume change. [45]

The MoS is calculated with respect to both the yield strength (MoS_y) and the ultimate (MoS_u) strength for which separate factors of safety (FoS_y , FoS_u) are specified. It is important to note that the MoS_u is also calculated using the von Mises stress from linear static analysis with linear material model. This fact is considered and included in the value of FoS_u .

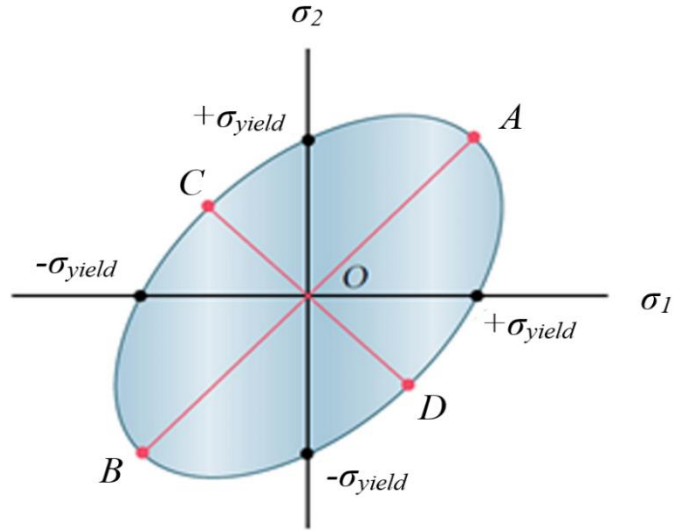


Fig. 41: von Mises criterion [45]

The formula for calculation of von Mises stress in condition of plane stress is:

$$\sigma_{Mises} = \sqrt{\sigma_x^2 + \sigma_y^2 - \sigma_x \sigma_y + 3\tau_{xy}^2} \quad (6)$$

where σ_x , σ_y , τ_{xy} are normal and shear components of stress.

Or using principal stresses:

$$\sigma_{Mises} = \sqrt{\sigma_1^2 - \sigma_1 \sigma_2 + \sigma_2^2} \quad (7)$$

where σ_1 , σ_2 are principal stresses.

The margins of safety are then calculated using the following formulas:

$$MoS_y = \frac{\sigma_{yield}}{FoS_y \cdot \sigma_{Mises}} - 1, \quad MoS_u = \frac{\sigma_{ultimate}}{FoS_u \cdot \sigma_{Mises}} - 1 \quad (8)$$

where σ_{yield} , $\sigma_{ultimate}$ are yield and ultimate strengths, σ_{Mises} is calculated von Mises stress and FoS_y , FoS_u are factors of safety.

3.5.2 COMPOSITE COMPONENTS

When evaluating composite parts, it is crucial to differentiate between the modelling of the composite part as an iso-skin or ortho-skin composite, as previously discussed. This differentiation is necessary because different evaluation criteria are used for each modelling method.

ORTHO-SKIN COMPOSITES

To evaluate ortho-skin composites, the Tsai-Hill criterion is commonly utilized, which is a quadratic criterion that considers biaxial loads. To apply this criterion, it is essential to first

determine the stress in the material CS for each ply of the laminate. The criterion is usually expressed in the following form, where FoS_u is employed:

$$FI_{Tsai-Hill} = \frac{(FoS_u \cdot \sigma_1)^2}{X^2} - \frac{(FoS_u \cdot \sigma_1) \cdot (FoS_u \cdot \sigma_2)}{X^2} + \frac{(FoS_u \cdot \sigma_2)^2}{Y^2} + \frac{(FoS_u \cdot \tau_{12})^2}{S_{12}^2} \quad (9)$$

where if $\sigma_1 > 0$, $X = X_T$ (tensile strength in direction 1), otherwise $X = X_C$ (strength in compression of direction 1). If $\sigma_2 > 0$, $Y = Y_T$ (tensile strength in direction 2), otherwise, $Y = Y_C$ (compression strength in direction 2), $\sigma_1, \sigma_2, \tau_{12}$ are stresses in the ply, and FoS_u is factor of safety with respect to ultimate strength of the composite material.

QUASI-ISOTROPIC SKIN COMPOSITES

For the failure evaluation of quasi-isotropic skin CFRP composites, the maximum stress between the von Mises stress and principal stresses is used. The von Mises formula was introduced above at the metallic components; the principal stresses for plane stress are calculated using the well-known formulas:

$$\sigma_{1,2} = \frac{\sigma_x + \sigma_y}{2} \pm \sqrt{\left(\frac{\sigma_x - \sigma_y}{2}\right)^2 + \tau_{xy}^2} \quad (10)$$

where $\sigma_x, \sigma_y, \tau_{xy}$ are normal and shear components of stress.

Because the material is a composite that does not indicate yielding, the MoS is calculated only with respect to the ultimate strength:

$$MoS_u = \frac{\sigma_{ultimate,equiv.}}{FoS_u \cdot \max(\sigma_{Mises}, |\sigma_1|, |\sigma_2|)} - 1 \quad (11)$$

where σ_1, σ_2 are principal stresses, σ_{Mises} is von Mises stress, FoS_u is factor of safety with respect to the ultimate strength of the quasi-isotropic composite, and $\sigma_{ultimate,equiv.}$ is equivalent strength considering the simplification to the isotropic material.

CORE SHEAR STRENGTH

Evaluation of the sandwich honeycomb is performed separately. The principal purpose of the core of the sandwich is to carry the out-of-plane shear load. Thus, for the evaluation is necessary to know the out-of-plane shear stresses as well as the out-of-plane shear allowables in the directions specified for L and W directions separately as shown in the Fig. 42. For the evaluation is used FI calculated using the following formula:

$$FI_{core} = \left(\frac{\tau_{1Z}}{\tau_{LOL}}\right)^2 + \left(\frac{\tau_{2Z}}{\tau_{LOW}}\right)^2 \quad (12)$$

where τ_{1Z}, τ_{2Z} are out of plane shear stresses and τ_{LOL}, τ_{LOW} are allowables in the L and W directions.

The MoS is then calculated using the following formula:

$$MoS_{core} = \frac{1}{FoS_{core} \cdot \sqrt{FI_{core}}} - 1 \quad (13)$$

where FI_{core} is failure index of the core and FoS_{core} is factor of safety for the core.

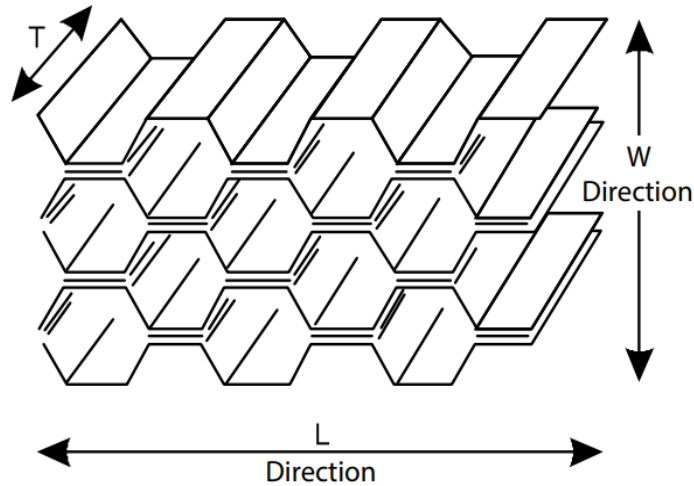


Fig. 42: Hexagonal honeycomb core [46]

CORE LOCAL INSTABILITIES

One of the key requirements for the new post-processing tool was to assess core local instabilities. The requirement applied to iso-skin composite model, as it focused on the overall strength, stiffness, and thickness of the skin, rather than properties specific to individual plies. More specifically, the objective was to evaluate the occurrence of core local instabilities, which are illustrated in the image below.

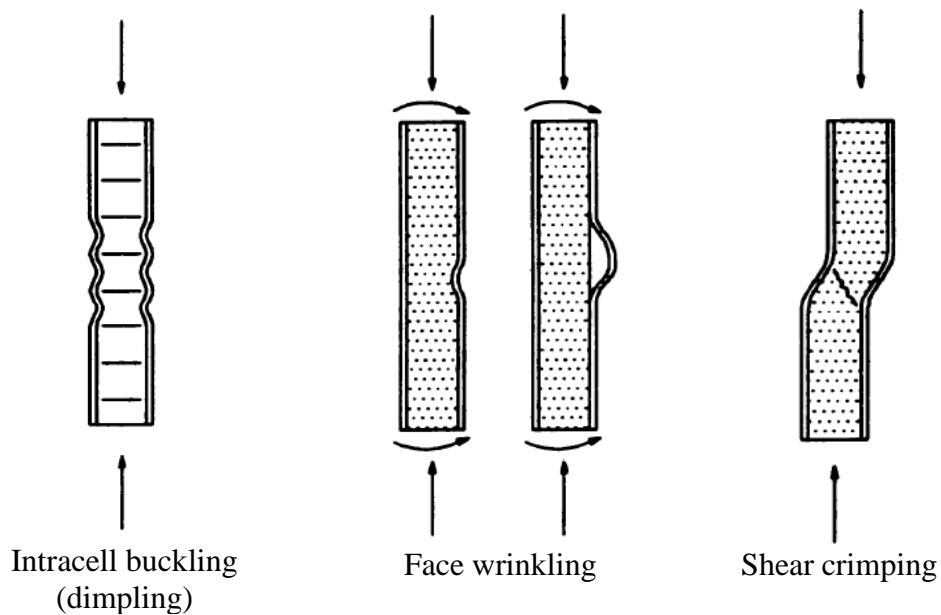


Fig. 43: Core local instabilities [47]

1. **Intracell buckling (or dimpling)** – critical for sandwich panels with core where the core does not provide continuous support of the thin faces, i.e. the core cells are large and faces too thin. [47]

The company specified that the evaluation in the post-processing tool should be done using the following formulas which are based on the sources [47][48]:

$$\sigma_{crit} = 2.25 \cdot \frac{E_f}{(1 - \nu_f^2)} \cdot \left(\frac{t_f}{S_c}\right)^2 \quad (14)$$

where E_f is Young's modulus of face skins (note that the skin is modelled as isotropic and therefore has only one Young's modulus), ν_f is Poisson's ration of the face skins, t_f is face skin thickness, and S_c is core cell size.

$$MoS_{compr} = \frac{\sigma_{crit}}{\max(|\sigma_1|, |\sigma_2|) \cdot FoS_{inst}} - 1 \quad (15)$$

where σ_{crit} is critical normal stress calculated using eq. 14, $|\sigma_1|, |\sigma_2|$ are principal stresses in the skin, and FoS_{inst} is factor of safety.

$$\tau_{crit} = \frac{\sigma_{crit}}{\sqrt{3}} \quad (16)$$

where σ_{crit} is critical normal stress calculated using eq. 14.

$$MoS_{shear} = \frac{\tau_{crit}}{\tau_{12} \cdot FoS_{inst}} - 1 \quad (17)$$

where τ_{crit} is critical shear stress calculated using the eq. 16, τ_{12} in-plane shear stress in the skin, and FoS_{inst} factor of safety.

$$MoS_{comb} = \frac{2}{R_a + \sqrt{R_a^2 + 4R_s^2}} - 1 \quad (18)$$

where R_a and R_s are calculated in the following way:

$$R_a = \frac{\max(|\sigma_1|, |\sigma_2|) \cdot FoS_{inst}}{\sigma_{crit}} \quad (19)$$

$$R_s = \frac{\tau_{12} \cdot FoS_{inst}}{\tau_{crit}} \quad (20)$$

where σ_{crit} critical normal stress calculated using eq. 14, τ_{crit} is critical shear stress calculated using eq. 16, FoS_{inst} is factor of safety, σ_1 and σ_2 are principal stresses in the skin, and τ_{12} is in-plane shear stress in the skin.

2. **(Face sheet) wrinkling** – critical for low density cores; as wrinkling is considered inward or outward buckling of a face elastically supported by the core. [47]

The company specified that for the evaluation of the wrinkling shall be used following formulas derived based on the sources [47][48]:

$$\sigma_{crit} = 0.33 \sqrt{\frac{E_c E_f t_f}{(1 - \nu_f^2) t_c}} \quad (21)$$

where E_c is Young's modulus in the through-thickness direction, E_f is Young's modulus of the skins (skin is modelled as isotropic and therefore has only one Young's modulus), ν_f is Poisson's ratio of the skins, t_f is face skin thickness, and t_c is core thickness.

$$MoS_{compr} = \frac{\sigma_{crit}}{\max(|\sigma_1|, |\sigma_2|) \cdot FoS_{inst}} - 1 \quad (22)$$

where σ_{crit} is critical normal stress calculated using eq. 21, $|\sigma_1|, |\sigma_2|$ are principal stresses in the skin, and FoS_{inst} is factor of safety.

$$\tau_{crit} = \frac{\sigma_{crit}}{\sqrt{3}} \quad (23)$$

where σ_{crit} is critical normal stress calculated using eq. 21.

$$MoS_{shear} = \frac{\tau_{crit}}{\tau_{12} \cdot FoS_{inst}} - 1 \quad (24)$$

where τ_{crit} is critical shear stress calculated using the eq. 23, τ_{12} is in-plane shear stress in the skin, and FoS_{inst} is factor of safety.

$$MoS_{comb} = \frac{2}{R_a + \sqrt{R_a^2 + 4R_s^2}} - 1 \quad (25)$$

where R_a and R_s are calculated in the following way:

$$R_a = \frac{\max(|\sigma_1|, |\sigma_2|) \cdot FoS_{inst}}{\sigma_{crit}} \quad (26)$$

$$R_s = \frac{\tau_{12} \cdot FoS_{inst}}{\tau_{crit}} \quad (27)$$

where σ_{crit} is critical normal stress calculated using eq. 21, τ_{crit} is critical shear stress calculated using eq. 23, FoS_{inst} is factor of safety, $|\sigma_1|, |\sigma_2|$ are principal stresses in the skin, and τ_{12} is in-plane shear stress of the skin.

3. **Shear crimping** – occurs often as a consequence of a global buckling of the sandwich panels; it is caused by low shear modulus of the core, or low adhesive shear strength. [47]

The company specified that for the shear crimping evaluation shall be used following formulas derived based on the source [48]:

$$\sigma_{crit} = \frac{\min(G_{LZ}, G_{WZ}) \cdot (t_c + 2t_f)}{2t_f} \quad (28)$$

where G_{LZ}, G_{WZ} are shear modules of the core in L and W directions, t_c is core thickness, and t_f is thickness of the skin.

$$MoS = \frac{\sigma_{crit}}{\max(|\sigma_1|, |\sigma_2|) \cdot FoS_{inst}} - 1 \quad (29)$$

where σ_{crit} is critical normal stress calculated using eq. 28, $|\sigma_1|, |\sigma_2|$ are principal stresses and FoS_{inst} is factor of safety.

MONOLITHIC PARTS

For evaluation of out-of-plane shear strength at the monolithic CFRP components is used interlaminar shear strength (ILSS). The evaluation is in SAB Aerospace performed using the approach defined by Zhang in the following manner using FI and MoS [40]:

$$FI_{ILSS} = \frac{\tau_{1Z}^2 + \tau_{2Z}^2}{\tau_{ILSS}^2} \quad (30)$$

$$MoS_{ILSS} = \frac{1}{FoS_{ILSS} \cdot \sqrt{FI_{ILSS}}} - 1 \quad (31)$$

where τ_{1Z}, τ_{2Z} are out of plane shear stresses and τ_{ILSS} is allowable for interlaminar shear strength given for the specific material.

4 DEVELOPMENT OF THE SOFTWARE

4.1 REQUIREMENTS AND POSSIBLE APPROACHES

4.1.1 INTRODUCTION

In section 3.3, which discusses loads, it was explained that during the development of a spacecraft, it is typically necessary to analyse a considerable number of load cases. The number of load cases can range from several tens to several thousand, depending on the purpose of the structure and the customer's structural requirements. The need to calculate such a large number of load cases presents a significant challenge for the overall design of the structure. This is because each load case requires solving one structural analysis, which increases the demands on both computational time and the time spent evaluating the results.

4.1.2 POSSIBLE APPROACHES

While it is possible to run all structural analyses using a single DAT file (which can specify the boundary conditions for each load case) directly through Nastran and save the results for all load cases in PCH or OP2 file, this method is impractical due to the enormous amount of data generated. Although obtaining these results is not difficult, the challenge lies in evaluating the vast number of results and determining the load cases in which failure occurs. While some commercial software offers features to address this issue, they are not user-friendly enough, prompting companies in this field to search for alternative methods to conduct solving and post-processing more efficiently. The following potential methods were discussed at the beginning of this project:

- Utilizing Nastran's proprietary programming language, known as the Direct Matrix Abstraction Program (DMAP)
- Exploring advanced options in the HyperView post-processing software, as well as its capability to add functionalities to the main software using the Tcl programming language
- Developing a standalone software application using one of the commonly used programming languages

4.1.3 CHOICE OF APPROACH

Although the first two options may appear more convenient, as they involve commercial software commonly used for these purposes and could potentially be less challenging in terms of programming length and complexity, they come with significant drawbacks. These disadvantages stem from the fact that the post-processing algorithm would be strictly dependent on the commercial software, regardless of its future development, cost, version compatibility, and other factors.

In contrast, a standalone application can be easily customized for different solvers or pre/post-processing software, making it much more adaptable for the future development of engineering methods in this field. The downside to this approach includes demands on the code for reliability, speed, comprehensibility, user-friendliness, and so on. Another reason for choosing this option was that a similar approach had been used in the company prior to the start of this project, and as a result, the structural team was already accustomed to employing this method.

The decision was made to replace the previous post-processing tool due to its slow speed, user-unfriendliness, and lack of documentation, which would have complicated its further

development. Considering the aforementioned factors, the selected approach involved developing a standalone software application.

4.1.4 REQUIREMENTS ON THE NEW SOFTWARE APPLICATION

DESCRIPTION OF THE PREVIOUS SOFTWARE TOOL

The requirements for the new software application are partly derived from the shortcomings of the previous tool, which was created using the VBA programming language. The main routine of this tool involves reading inputs (model data from the BDF file and result stresses of subcases calculated by Nastran from the PCH file), combining the subcase results using the principle of superposition according to the matrix with load cases, generating the output files, and preparing the data for visualization in HyperView.

One of the primary issues with this tool was its inability to post-process data from all elements in a single run using one PCH file. Instead, it required multiple separate Nastran runs for the evaluation of shell elements, composite sandwich parts with orthotropic skins, composite sandwich parts with isotropic skins, panel cores, and interlaminar shear stress in composite components without cores.

This meant that a structural analyst, in order to analyse the behaviour of a single structure, had to export, prepare, and run five separate structural analyses in Nastran, followed by running the post-processing tool with specific settings as many times. This was because the tool was unable to read and process stress data for all the aforementioned element and component types from a single PCH file. For instance, to post-process isotropic shell element stresses, the data in the PCH file had to be requested in the SORT1 format, while data for shell elements with PCOMP properties needed to be requested in the SORT2 format (the difference between these formats is explained in Section 2.4.2). Another issue that required separate runs to be carried out was the presence of unresolved bugs, such as the tool's inability to recognize the ply representing the core of a sandwich panel unless specific settings were applied to the material models.

It is also worth noting that the previous tool was unable to evaluate core local instabilities, necessitating the use of a separate Excel tool for this purpose. The same issue applied to solid elements, as their evaluation was not incorporated into the previous tool either. Another drawback was that the input matrix containing the load cases had to be prepared in a separate TXT file, and the outputs, before being processed through another Excel tool, were stored in individual CSV files. This meant that the data during the post-processing routine was stored in numerous separate files, necessitating several manual operations, which ultimately made the tool significantly less user-friendly.

PROPOSED CHANGES AND IMPROVEMENTS

As previously mentioned, the requirements for the new tool stemmed from the shortcomings of the existing one. While there were many ways to create a better software solution, the main steps remained consistent. The items listed in each of the following steps describe the requirements for the new tool:

1. Reading the inputs (BDF file, PCH file, matrix with load cases):
 - Develop a PCH file parser capable of reading all necessary element, property, and material types from a single PCH file containing element stresses in the SORT1 format

- Read the matrix with load cases from an Excel sheet to avoid creating a separate TXT file
2. Assigning element stresses to the model data:
 - Create two algorithms that allow the structural analyst to choose whether the PCH stress data should be assigned to components read from the BDF file based on EID or PID (explained below in section 4.3.1)
3. Calculating the superposition of subcase stress results:
 - Accelerate this routine, which requires most of the calculation operations
4. Evaluation and writing of the results into table:
 - Write the evaluated data directly to Excel sheets from the new tool's code, eliminating the need for a separate CSV file
5. Preparing visualization of the envelopes:
 - Prepare data for visualization in HyperView using the Altair ASCII format, written to a TXT file that can be directly read by HyperView

These requirements were determined after a series of meetings with the company's structural team. They were derived from the team's extensive experience with structural analyses in the aerospace industry and should serve as the foundation for the development of the new software tool.

4.2 CHOICE AND DESCRIPTION OF THE PROGRAMMING LANGUAGE

4.2.1 CHOICE OF THE PROGRAMMING LANGUAGE

Arguably, one of the crucial decisions at the beginning of any software development process is the choice of the programming language. This process involves many requirements that often conflict with each other. Here is a list of the most important factors, along with an explanation of their significance for this task:

- **Code speed** – the software needs to handle gigabytes of data on a daily basis
- **Language comprehensibility** – the tool will be developed and likely modified by structural analysts who do not have a strong background in computing
- **Compatibility with other software** – in this case, the software tool must work closely with MS Excel
- **Availability of advanced libraries** – some programming languages offer a variety of supporting libraries that significantly simplify the programmer's work
- **Prevalence of the language and access to learning/support materials** – it must be considered that the programmer is a novice in the field of software development

After carefully considering each of the aforementioned requirements, Python was chosen as the programming language.

4.2.2 PYTHON

Python is a high-level, interpreted, interactive, object-oriented language that features dynamic typing, modules, exceptions, high-level data types, and classes. In addition to object-oriented programming, it supports procedural and functional programming. Python emphasizes readability, which is primarily demonstrated through significant indentation. First created in the early 1990s, Python gained considerable popularity during the 2000s and is currently one of the most widely used programming languages. For the purpose of creating the new tool, version 3.9 was utilized, as it was the most recent version available when the project began. [49]

Python is utilized for a variety of purposes, such as scientific computing, machine learning, web frameworks, image processing, desktop GUI applications, and more. It has been successfully integrated into numerous commercial software applications across various industries and research fields. The widespread use of Python is largely due to its status as a free open-source software. For more information about the extensive usage of Python, please refer to source. [50]



Fig. 44: Official logo of Python

One of Python's strengths is the availability of a vast number of libraries designed for various purposes. The libraries frequently used in the development of the software tool will be described in greater detail.

NUMPY

NumPy is one of the most essential packages for scientific computing in Python. It is particularly useful for operations involving multi-dimensional arrays, including mathematical, logical, shape manipulation, sorting, selecting, and basic linear algebra. One of the biggest advantages of NumPy, compared to Python's standard data structures, is its speed. NumPy is fast because it is pre-compiled and optimized in the C programming language. Due to its speed and ease of manipulation, NumPy is frequently used when working with large data sets, making it the most utilized Python package during the development of the new post-processing application. [51]



Fig. 45: Logo of NumPy

OPENPYXL

The OpenPyXL module is a Python package used for working with Microsoft Excel. It enables manipulation of data in Excel without needing to launch the application. The module can iterate through Excel cells to read or write data, as well as add, remove, or rename sheets, format and style sheets, and create charts. Direct access to Excel using this package is necessary because the table with load cases is typically stored in an Excel sheet, and the post-processed data is also stored in an Excel sheet for reporting purposes. [52]



Fig. 46: Logo of OpenPyXL

QT DESIGNER AND PYQT5

Due to the need for user-friendliness in the new software, it was decided to create a graphical user interface (GUI) for operating the code. While there are several options for creating a GUI for Python code, Qt Designer and the PyQt5 library were chosen for this purpose. The rationale behind this choice was the high efficiency and ease of use associated with these tools.

Qt Designer is a tool for creating GUIs using Qt Widgets. Users can design and style their GUI in Qt Designer by dragging and dropping desired features, while seeing the actual design. The Qt Designer platform is programming language-independent, meaning it can be used to create GUIs for various programming languages. The current version of the library that connects Qt Designer with Python is called PyQt5. The content created in Qt Designer has a .ui extension and can either be directly translated into Python code using `pyuic5` or loaded and integrated into the Python code without such direct translation. [53]



Fig. 47: Logo of Qt Designer

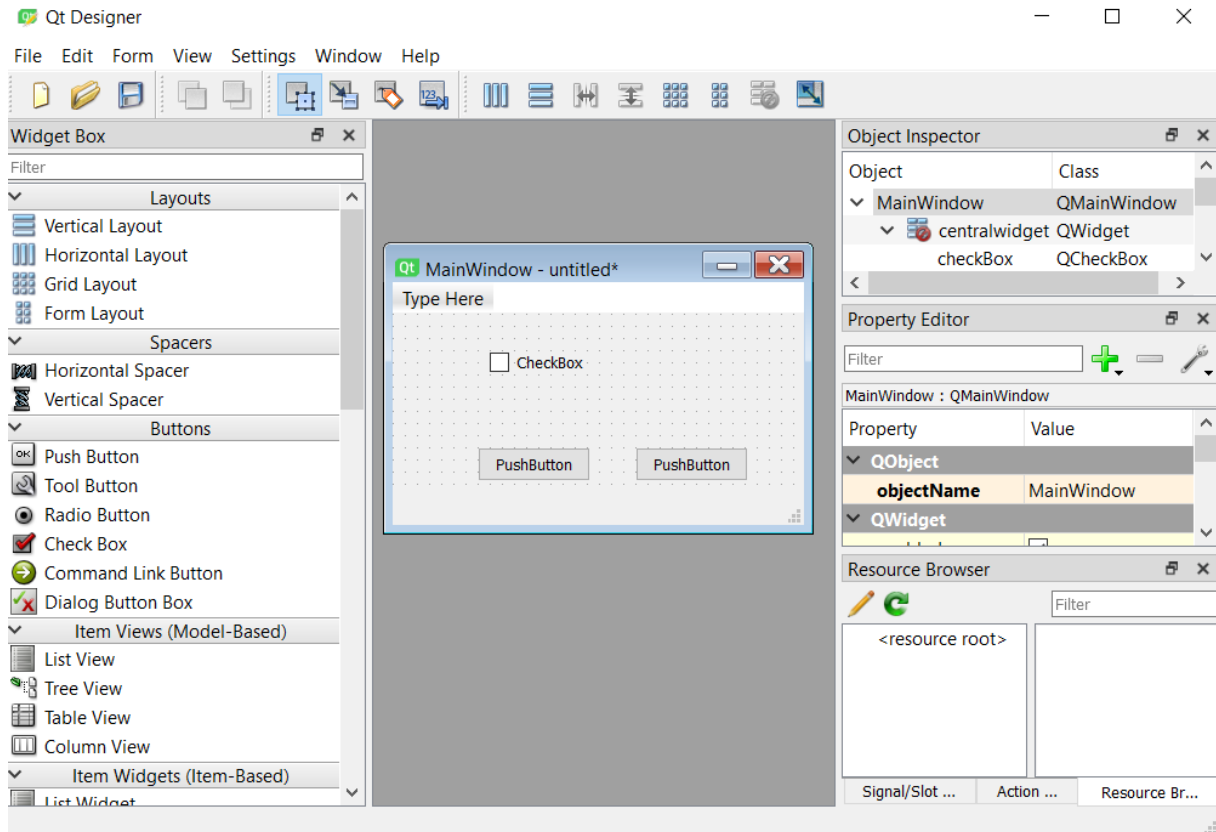


Fig. 48: Creation of GUI using Qt Designer

4.2.3 FREQUENTLY USED DATA STRUCTURES

In programming, a data structure is a method for storing and organizing data in computer memory. To access and organize data more efficiently for specific purposes, various data structures are available, differing from one language to another. Before delving into the structure of the code, it is helpful to explain the properties of the most commonly used data structures in this Python code.

PYTHON LIST

A list is a data structure used for storing multiple items within a single variable. Essentially, it is an ordered collection of data. Python lists are highly flexible, implemented as mutable dynamic arrays, which means they allow for the removal or appending of items. Another advantage is that a single list can store different data types and even various data structures, such as another list, dictionary, or numpy array. When a user creates a list of lists (multi-dimensional list), the nested lists do not need to have the same length. These properties grant the programmer significant freedom in organizing data, but at the cost of slower processing speed when working with this data type. [54]

```
list = [45, "engineering", [2.2, 258, "component"]]
print(list[2][1])

# Output:
258
```

Fig. 49: Sample Python list

PYTHON DICTIONARY

Like a list, a dictionary can store multiple data types and/or data structures. The primary distinction between a dictionary and a list is that data in a dictionary is accessed using a key instead of a numerical index. In essence, a dictionary consists of key-value pairs, with the key being any data type. The advantage of using a dictionary is that one doesn't need to know the position or iterate through a sequence of data to access a specific value; it can be directly accessed using the corresponding key. [54]

```
dict = {'material_ID': 252, 15: [5, 5.8, 'laminate'], 5.5: 'part'}
print(dict[15])

# Output:
[5, 5.8, 'laminate']
```

Fig. 50: Sample Python dictionary

NUMPY ARRAY

A NumPy array is the primary data structure of the Python library NumPy. Unlike a Python list, it has a fixed size defined at the beginning, meaning that the dimensions cannot be changed dynamically by deleting or appending items inside. When resizing a NumPy array is necessary, a new array is created and the original one is deleted. Additionally, it cannot hold different data types or data structures. While these properties may limit the flexibility of this data structure compared to a Python list, the significant advantages of a NumPy array are its simple operations and high speed. [51]

```
np_array = numpy.zeros([2,2,3])
print(np_array)

# Output:
[[[0. 0. 0.]
  [0. 0. 0.]]

 [[0. 0. 0.]
  [0. 0. 0.]]]
```

Fig. 51: Sample NumPy array

4.3 READING AND SORTING OF THE INPUT DATA

The code begins by reading the input data required for further post-processing. Although there are some open-source codes for reading Nastran files available on the internet, the decision was made to create custom reading functions to ensure full understanding and control over the entire code.

The necessary input data are stored in three separate files, each of which must be read individually:

- Excel sheet – contains the matrix with load cases
- BDF file- contains necessary information about the model:
 - Names and ID numbers of the components, materials and properties
 - Material properties necessary for the strength evaluation (nomenclature as in MSC Nastran QRG):
 - MAT8: E1, E2, NU12, G12, G1Z, G2Z, Xt, Xc, Yt, Yc, S
 - MAT1: E, NU, yield strength (position ST), ultimate strength (position SC)
 - Information about the properties:
 - PSHELL: thickness of the shell elements and corresponding material
 - PCOMP: order of the plies, thickness of the plies, angle of the plies, material corresponding to the plies, interlaminar shear strength allowable
 - List of elements, its ID numbers and assigned properties
- PCH file – contains stresses for the subcases necessary for evaluation (nomenclature as in MSC Nastran QRG):
 - PSHELL- Normal x at Z1 (Z1 = top surface), Normal y at Z1, Shear xy at Z1, Normal x at Z2 (Z2 = bottom surface), Normal y at Z2, Normal xy at Z2
 - PCOMP- Normal-1, Normal-2, Shear-12, Shear-1Z, Shear-2Z

Reading the table with load cases was performed quite easily using a short function called “reading_loadcases”, which utilized the Pandas library (the only instance of this package being used in the code). This function takes two arguments: the path to the Excel file and the name of the Excel sheet (both specified in the GUI). The function returns three variables: a 2D NumPy array containing the load cases table, and two integers representing the number of subcases (the number of columns in the table) and the number of load cases (the number of rows in the table). Reading the BDF and PCH files is more complex and will be explained in further detail below.

	1L	2L	3L
1	3.3	0	1.35
2	3.19	0.85	1.35
3	2.86	1.65	1.35
4	2.33	2.33	1.35
5	1.65	2.86	1.35
6	0.85	3.19	1.35
7	0	3.3	1.35
8	-0.85	3.19	1.35
9	-1.65	2.86	1.35
10	-2.33	2.33	1.35

Tab. 8: First 10 load cases from input matrix of L-QSL for PLATO SVM development

4.3.1 READING DATA FROM THE BDF FILE

Although the information in the BDF file varies from model to model, the file structure always remains consistent, which is crucial for writing the parser. The function for reading the BDF file is called “read_bdf” and has only one argument: the path to the BDF file (specified by the user in the GUI). The function processes the file line by line, searching for keywords that

indicate where to stop and read specific data. For the code's subsequent functions, it is important to read data from the following sections of the BDF file, listed in order from the top to the bottom of the file. It is worth noting that the names of components, properties, and materials appear in the model only if exported from HyperMesh with HM comments, which is one of the export options available in that software.

GROUP DEFINITIONS

```

$$$$-----
$$$                               Group Definitions
$$$$-----
$$$
$$$  CTRIA3 Elements
$$$
$
$      EID      PID      G1      G2      G3      G4
CTRIA3 10000003|10000000|60000003|20000001|40000009|
CTRIA3 10000004|10000000|40000009|40000008|60000003|
CTRIA3 20000002|20000000|20000001|60000002|60000003|
$$$
$$$  CQUAD4 Elements
$$$
CQUAD4 10000001|10000000|60000001|60000003|40000008|40000005|
CQUAD4 10000002|10000000|20000001|20000002|40000007|40000009|
CQUAD4 20000001|20000000|50000001|50000002|20000001|20000002|
CQUAD4 30000001|30000000|40000009|40000007|40000001|40000002|
    
```

Fig. 52: Structure of the element data in Group Definitions

This section of the BDF file contains elements and their associated information. They are organized according to element types and always listed in consecutive order from the lowest to the highest EID. The elements to be searched for, based on the requirements, are CQUAD4, CTRIA3, CTETRA, CHEXA, and CPENTA. The EID, PID, and individual grid points are stored in eight-digit fields in the order illustrated in the following image.

Going through this part of the BDF file is necessary to assign elements to their corresponding components for both EID and PID algorithms. The EID approach utilizes predefined ranges of component IDs, as explained in section 3.4.9. It assigns an element to the component with the closest lower component ID, which means this algorithm requires a properly renumbered model; otherwise, it will not work. On the other hand, the PID assigning approach does not require proper numbering but does require coincident PID and component IDs for every component.

HYPERMESH NAME AND COLOR INFORMATION FOR GENERIC COMPONENTS

This section of the BDF file is essential to read because it contains information about the component ID and its name. While the component ID appears on every line with a new component in the same eight-digit slot, the component name varies in length and is enclosed in quotation marks.


```

$$$$-----$$$$
$$$   HyperMesh name and color information for generic components   $$$
$$$$-----$$$$
$HMNAME COMP
$HWCOLOR COMP
$
$HMNAME COMP
$HWCOLOR COMP
$
$HMNAME COMP
$HWCOLOR COMP

```

Fig. 53: Component names and IDs position in the BDF file

Below the last component, there is a line with the name of the following section, "Property Definition for Surface and Volume Elements". When this line is encountered, it indicates that all component names and IDs have been read, and the elements can be assigned to these components using either the EID or PID algorithm, as previously mentioned. Components that do not contain any elements necessary for evaluation, such as those with RBE2 elements, are subsequently deleted.

PROPERTY DEFINITION FOR SURFACE AND VOLUME ELEMENTS

In this section, component properties need to be read, specifically PIDs and values corresponding to each property type.

For the PSHELL property, it is essential to read the PID, MID, and thickness, with their specific positions in the BDF file marked in the following illustration.

```

$$$$-----$$$$
$$$   Property Definition for Surface and Volume Elements   $$$
$$$$-----$$$$
$$$
$$$ PSHELL Data
$
$HMNAME PROP
$HWCOLOR PROP
PSHELL
$$$$

```

Fig. 54: PSHELL data structure in the BDF file

For the PSOLID property, it is necessary to read the PID and MID at the positions indicated in the following image.

```

$HMNAME PROP
$HWCOLOR PROP
PSOLID

```

Fig. 55: PSOLID data in the BDF file

For the PCOMP property, reading the property is more complex because it stores the lay-up of the composite material. From the PCOMP, it is necessary to read the PID, allowable ILSS value, and MID for each ply. The order of the plies is arranged from top to bottom according to the element normal.

		MID	Thickness				22"Sandwich_panel" 4	
\$HMNAME	PROP							
\$HWCOLOR	PROP							
PCOMP		22				7.123E+7		HILL
	Ply 1		40.000125		0.0	YES	2	40.000125 45.0 YES
	3	12	0.018		0.0	YES	4	40.000125 45.0 YES
	5		40.000125		0.0	YES		

Angle of the ply ILSS allowable

Fig. 56: PCOMP property data structure

MATERIAL DEFINITION CARDS

In the material definition cards, there is a description of the materials used, which are assigned to the component properties. Although the Nastran definition of MAT8 includes slots for assigning the allowable values of orthotropic materials in a commonly used sense, MAT1 does not have default slots for defining yield and ultimate tensile strength. Therefore, it was decided to place these values in the positions ST and SC, where the allowable values for tension and compression should be placed by default. In the ST position, the yield tensile strength should be specified, while the ultimate tensile strength should be specified in the SC position.

Name	Value
Solver Keyword	MAT1
Name	Alu_6082
ID	100000
Color	
Include	[Master Model]
Defined	<input type="checkbox"/>
Card Image	MAT1
User Comments	Do Not Export
E	7000000000
G	
NU	0.33
RHO	
A	
TREF	
GE	
ST	280000000.0
SC	310000000.0
SS	

Fig. 57: Definition of the allowables for MAT1 in HyperMesh

The values of yield and ultimate strength are also used to distinguish quasi-isotropic composite materials. The agreement with the structural team is that if MAT1 represents a quasi-isotropic composite material, then the same value should be placed in both the ST and SC positions. This is because carbon fiber does not exhibit yielding, and therefore, there is only one limit value.

For the further post-processing operation at the MAT1 it is necessary to read from the BDF file material name, MID, Young's modulus, yield strength, and ultimate strength.

```

$$$$-----
$$$
$$$                               Material Definition Cards
$$$$-----
$$$$
$$$  MAT1 Data
$
$HMNAME MAT      MID      E      NU
$HWCOLOR MAT
MAT1             17.0E+10  0.3      2700.0
+
+ 4.5E+8  5.7E+8

```

Yield Strength Ultimate Strength

Fig. 58: MAT1 data structure

For MAT8, it is necessary to read the material name, MID, E1, E2, NU12, G12, G1Z, G2Z, and the allowable values for the extended Tsai-Hill failure criterion. These include:

- X_t , X_c – Allowable stresses in tension and compression, respectively, in the direction of the fibres' longitudinal orientation
- Y_t , Y_c – Allowable stresses in tension and compression, respectively, in the direction of the fibres' transverse orientation
- S – Allowable stress for in-plane shear

```

MID      E1      E2      NU12      G12      G1Z      G2Z
$HMNAME MAT      4"CFRP" "MAT8"
$HWCOLOR MAT      4      33
MAT8      42.05E+11 6.4E+9  0.36  1.8E+10 1.8E+10 1.8E+10
+
+      20.0  1.853E+9 4.44E+8 2.22E+7 1.24E+8 6.9E+7
Xt      Xc      Yt      Yc      S

```

Fig. 59: MAT8 data structure

It is important to note that there is an agreement with the structural team that if the MAT8 ply represents the core, the previously mentioned allowables should be replaced with characteristics for evaluating core local instabilities in the designated slots. These characteristics include τ_{LOL} and τ_{LOW} , which are out-of-plane shear allowables in L and W directions, E_c (Young's modulus in through-thickness direction), and S_c (honeycomb cell size).

4.3.2 READING OF THE PCH FILE

As previously mentioned, the PCH file is essentially a text file containing stress values for a specific set of elements specified in the DAT file for particular subcases. As explained earlier, the new tool should be capable of reading stress values for various element types from a single PCH file, organized in SORT1 format. Similar to the BDF file, the PCH file is read line by line from top to bottom, looking for keywords. This is done in the "read_pch" function. To recognize and read all desired stresses and assign them to the corresponding plies, elements, and subcases, a rather complex part of the code was created. This code must be able to anticipate all possible changes caused by different types of models, which may lead to changes in the order of elements in the file.

STRESS OUTPUT FOR SHELL ELEMENTS WITH PSHELL PROPERTY

The code is designed to work with a large amount of data, thus only the information necessary for further evaluation is read and kept in memory. For shell elements, Nastran calculates stresses

on both surfaces of the shell element. Stresses from both sides are read and evaluated during further analysis, as it is unclear at this stage which side of the shell element will be critical. Shell elements are identified based on the information in the line with the element type. "74 TRIA3" represents a triangular shell element, while "33 QUAD4" denotes a rectangular shell element. Stresses at shell elements are marked with X and Y, indicating that they are evaluated in the element coordinate system. The information read by the code and its location in the PCH file are shown in the following image.

```

    $TITLE =
    $SUBTITLE= 1 G X
    $LABEL =
    $ELEMENT STRESSES
    $REAL OUTPUT
    $SUBCASE ID =
    $ELEMENT TYPE =
    EID 10000003 74 TRIA3
    -CONT- -4.000000E-03
    -CONT- 1.415908E+03
    -CONT- -2.441814E+03
    -CONT- 2.682571E+03
    -CONT- -3.937347E+01
    -CONT- 1.176749E+04
    -CONT- 10000004 -4.000000E-03
    -CONT- 1.238103E+02
    -CONT- -7.934334E+03
    -CONT- 7.964713E+03
    -CONT- -3.054577E+01
    -CONT- 1.365381E+04
  
```

	Shear xy at Z1	Normal x at Z1	Normal y at Z1
VONM	-1.002880E+03	-1.002880E+03	-1.048564E+03
	4.453788E+01	4.453788E+01	3.903698E+02
	2.658581E+03	2.658581E+03	4.000000E-03
	4.890276E+01	4.890276E+01	-6.618320E+03
	8.113789E+03	8.113789E+03	-5.382316E+03
	-7.932227E+03	-7.932227E+03	-6.560512E+02
	8.902544E+01	8.902544E+01	-6.539451E+02
	7.628412E+03	7.628412E+03	4.000000E-03
	7.408815E+02	7.408815E+02	-6.540689E+03
	1.182451E+04	1.182451E+04	-3.118919E+03
		Normal y at Z2	Shear xy at Z2

Normal x at Z2

Fig. 60: Isotropic shell element stresses structure in PCH file

STRESS OUTPUT FOR SHELL ELEMENTS WITH PCOMP PROPERTY

For composite elements, the reading process is more complex because each element contains a specific number of plies and stresses are recorded for each of these plies. Unlike shell elements, stresses for composite plies are marked with 1, 2, and Z, indicating that they are in the ply coordinate system. Rectangular shell elements with PCOMP are designated as "95 QUAD4LC", while triangular elements are labelled "97 TRIA3LC". The necessary information for further evaluation of shell elements with composite properties is indicated in the following image.

```

    $TITLE =
    $SUBTITLE= 5 G Z
    $LABEL =
    $ELEMENT STRESSES
    $REAL OUTPUT
    $SUBCASE ID =
    $ELEMENT TYPE =
    EID 20000001 95 QUAD4LC
    -CONT- 1.130558E+04
    -CONT- 2.816844E+01
    -CONT- 1.358336E+04
    -CONT- 20000001 2 -5.588817E+03
    -CONT- -6.689146E+00
    -CONT- 2.415435E+04
    -CONT- 20000001 3 3.917217E-05
    -CONT- 4.392070E+01
    -CONT- 3.919998E-05
  
```

	Shear-12	Normal-1	Normal-2
	1.130558E+04	1.363961E+04	-1.419137E+03
	2.816844E+01	1.447539E+02	1.246509E+01
	1.358336E+04	1.969359E+04	-7.473120E+03
	-5.588817E+03	4.496116E+04	-2.036607E+03
	-6.689146E+00	1.948532E+02	1.506533E+02
	2.415435E+04	4.561663E+04	-2.692069E+03
	3.917217E-05	7.138025E-07	-2.239203E-06
	4.392070E+01	1.948532E+02	1.506533E+02
	3.919998E-05	3.843728E-05	-3.996268E-05

Fig. 61: Structure of composite shell element stresses in PCH file

- **Component property** – assigned based on the EIDs and their corresponding PIDs, or directly based on the PID if it corresponds to the component ID, as explained above
- **Material data** – assigned based on the MID, which is always specified in the component property
- **Component type** – this fact is distinguished based on the component property and corresponding material data. This process is explained in more detail below. With the current abilities of the code can be distinguished these types of the components:
 - Isotropic shell component
 - Composite with orthotropic plies with core (sandwich)
 - Composite with orthotropic plies without core (monolithic part)
 - Composite with isotropic plies with core (sandwich)
 - Composite with isotropic plies without core (monolithic part)
 - Solid element component
- **Core ply number** – this is determined based on the materials assigned to the plies, as described below

RECOGNITION OF THE COMPONENT TYPE AND PLY WITH CORE

Identifying a component as defined above is essential because different component types require distinct procedures. Recognizing isotropic shell and solid element components is straightforward, as they are characterized by the assignment of PSHELL and PSOLID properties to these components.

For composite components, the distinction is less clear, as orthotropic and quasi-isotropic composites, with or without a core, all have the PCOMP property. The differentiation between orthotropic and quasi-isotropic composites is based on the material type of the top ply. If it is MAT8, the composite is considered orthotropic, while if it is MAT1, the composite is deemed quasi-isotropic.

The presence of a core is determined differently for iso-skin and ortho-skin composites. For quasi-isotropic composites, the core is the ply with the MAT8 material (as the other plies have MAT1). In the case of orthotropic material composites, the core is identified as the only ply with a different MID from the other plies. The code not only checks for a change in material from one ply to another, but also ensures that it is the only ply with a different material in the component. This is due to the potential change in material from a doubler to the skin of a sandwich (a doubler is an additional layer applied to the skin for reinforcement). However, since a doubler typically consists of multiple plies, the first ply with a different MID will not be considered as a core. The composite elements at which the core was not found are considered to be monolithic.

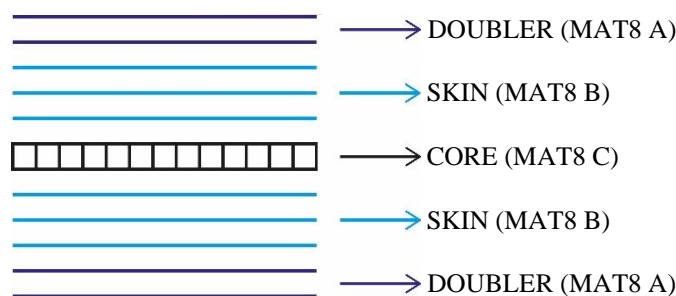


Fig. 63: Constitution of the ortho-skin composite with doubler

LIMITATIONS

Based on the previously mentioned approaches, two important limitations arise; otherwise, an error will occur:

- The orthotropic composite (with or without core) must have at least 3 plies
- Orthotropic and quasi-isotropic skins should not be used on the same component (e.g., placing an orthotropic doubler on an isotropic skin)

Users should be aware of the approaches used in this part of the code and these limitations, as they may cause problems in some special cases. Nevertheless, these automated recognition processes are reliable for the vast majority of cases and allow for the simultaneous post-processing of all element and component types.

4.4.2 ORGANISATION AND USED DATA STRUCTURES

Once the model data has been read from the BDF and the resulting stresses from Nastran have been read from the PCH file, the PCH data must be assigned to the specific components. This is done based on the EID, as it is the only information logically connecting components from the BDF and stress data in the PCH. Throughout the entire process of reading and assigning data, it is crucial to use appropriate data structures and organize the data in a clearly arranged way.

The fundamental unit for organizing data is the component. Data fully describing a component consists of various pieces of information of different types (name, ID, component property, etc.). Therefore, a Python list was chosen as the data structure representing a component because it can hold different data types and structures. At the same time, it is not common for the structure to consist of more than hundreds or thousands of components, which means that when iterating through the components, the code will not be significantly slowed down. The components are stored in superordinate lists, where all components of the same kind are grouped together.

ORGANISATION OF THE ISOTROPIC SHELL AND SOLID ELEMENT COMPONENTS DATA

Isotropic shell and solid element component data are organized in a similar way, as shown schematically below. The only differences are that solid element data do not include thickness, and the stress components for these two element types are different.

List with components = [[Component 1],[Component 2],[Component 3],...]

Component = ['Name', ID, 'Iso_shell/solid', [Material data], Thickness (for shell), Stresses]

Material data = ['Name', MID, [Yield strength, Ultimate strength]]

Stresses = [[Subcase 1], [Subcase 2], ...]

Subcase = [[Element 1], [Element 2], ...]

Shell element = [EID, Normal x at Z1, Normal y at Z1, Shear xy at Z1,
Normal x at Z2, Normal y at Z2, Shear xy at Z2]

Solid element = [EID, Normal x, Shear xy, Normal y, Shear yz, Normal z, Shear zx]

It is important to note that the stresses are stored in a multidimensional NumPy array, which maintains the data in a predefined format to take advantage of the NumPy library's speed when working with large datasets.

ORGANISATION OF THE COMPOSITE COMPONENTS

The structure of the data for iso-skin composites and ortho-skin composites are very similar to each other and is in simplified manner depicted in the following scheme:

Composite shell = [[Component 1], [Component 2], [Component 3], ...]

Component = ['Name', ID, [Type], [Materials], [Properties], [Stresses]]

Type = ['Ortho/Iso', 'Sandwich/Monolithic']

Materials = [[Material 1], [Material 2], ...]

Material = [Name, ID, MAT8/MAT1, [Material characteristics]]

Material characteristics – are in different format depending on whether the material represents an isotropic ply, orthotropic ply, or core as explained above

Properties = [ILSS allowable, [[Ply prop 1], [Ply prop 2], ...], Number of ply with core/ 'NO_CORE']

Ply prop= [MID, Thickness, Angle, MAT8/MAT1, Material characteristics]

Stresses = [[Element 1], [Element 2], ...]

Subcase = [[Element 1], [Element 2], ...]

Element = [[Ply stress 1], [Ply stress 2], ...]

Ply stress= [EID, Ply number, Normal-1, Normal-2, Shear-12, Shear-1Z, Shear-2Z]

4.5 COMBINATION FUNCTION

After reading and organizing the input data, the combination of subcase stresses into loadcase stresses must be carried out. This operation requires a large number of mathematical calculations, so the subcase stresses for each component are stored in a NumPy array. While the same function can be used for isotropic shell and solid elements, since they have the same dimensions, a separate function must be developed for composite elements due to the additional dimension caused by multiple plies belonging to one element.

Before combining stresses for each component, an empty (zero) NumPy array is prepared to store the results. This array has three dimensions:

1. Number of load cases
2. Number of elements in the current component
3. 7 – the length of the field necessary to store information about a single element

The EID, which is in the zero position of the third dimension, is assigned in advance and is not subject to combination.

The linear combination of isotropic shell and solid subcase stresses occurs within three nested loops. The outermost loop iterates through the components, the second loop goes through load cases in the load case NumPy array, and the third loop iterates through the subcases.

Once the combination is complete, the resulting NumPy array containing the load case stresses replaces the NumPy array holding the subcase stresses at the end of the component list.

4.5.1 COMBINATION OF THE COMPOSITE STRESSES

The linear superposition of the composite subcase stresses according to the load cases table takes place almost in the same way as for the shells. The only significant difference is another dimension due to plies that are specified for every element. Therefore, the pre-defined NumPy array for the saving of the results from the combination has to have for every component 4 dimensions:

1. Number of load cases
2. Number of elements
3. Number of plies
4. 7 – the length of the field necessary for storing information about one ply

The EID and ply number, which are located in the zero and first positions of the third dimension, are assigned beforehand and are not subject to linear combination.

After linear superposition, the NumPy arrays containing the load case stresses replace the arrays with subcase stresses at the end of the component list. The composite components are then separated into two lists for quasi-isotropic and orthotropic composites, as the evaluation process differs for each type.

4.6 EVALUATION AND TABULAR OUTPUTS

The primary goal of this software is to identify the highest stress levels across the entire structure and all load cases. As a result, the outputs should be presented in a manner that allows the user to determine the highest stress for each component, along with the EID where it occurred and the specific load case at which it occurred.

In addition to the stresses used to determine the MoS, which is typically the most sought-after information, there are various other types of stresses that can help in understanding the structure's behaviour under load. Since it is rare for a structural analyst to require an evaluation of all the stresses for all element types, each potential result has been incorporated into a GUI as a checkbox. This makes all the results optional and, since running time is critical when

working with large models and numerous load cases, can save a significant amount of computational time.

The evaluated results are written into Excel sheets using the OpenPyXL package. In total, there are four Excel sheets for the results, specifically for shell components, quasi-isotropic composite components, orthotropic composite components, and solids. The format of the result tables is predefined, and the data is either written (if the user requested it in the GUI) or marked as 'Not_requested' in the cells.

Since the results of the analyses are typically reported both internally within the company and externally to customers, it is important to present the most crucial results in a format that can be easily and quickly incorporated into reports. To achieve this, additional report tables are automatically generated on separate sheets for each component type and are labelled as SHELL_SUM, QI_SUM, ORT_SUM, and SOLID_SUM. Similar to the result tables, the code either creates or overwrites these tables based on whether they are found in the specified Excel workbook.

4.6.1 STRUCTURE OF THE TABULAR OUTPUT DATA

ISOTROPIC SHELL COMPONENTS TABULAR OUTPUT DATA

The Excel sheet that contains the result data for shell elements is named SHELL_RES. If the code detects a sheet with this name in the Excel workbook specified by the user, the data within the sheet will be overwritten. If no sheet named SHELL_RES is found, a new one is automatically created, with data written and formatted accordingly. The same process applies to the Excel summary sheet named SHELL_SUM. Due to space limitations in this thesis, the structure of the tables can be found in Appendix A.

ORTHOTROPIC COMPOSITE COMPONENTS TABULAR OUTPUT DATA

The results for orthotropic composite components are written into the Excel sheet ORTHO_RES, which contains result data for both sandwich panels and monolithic parts. If a component is monolithic, "N/A" is written in the cells pertaining to the evaluation of the core. Conversely, for sandwich composites where ILSS is not applicable, "N/A" is written as well. The most critical data are then automatically written into the summary table named ORTHO_SUM. The structure of both tables can be found in Appendix A.

QUASI-ISOTROPIC COMPOSITE COMPONENTS TABULAR OUTPUT DATA

The result data for quasi-isotropic composites are written in the Excel sheet named QI_RES. The output data are quite similar to those of orthotropic composites, with the exception that the result table also evaluates core local instabilities. The output data which are written in QI_RES and QI_SUM sheets can be found in Appendix A.

SOLID ELEMENT COMPONENTS TABULAR DATA OUTPUT

The result and summary data are automatically written into the SOLID_RES and SOLID_SUM Excel sheets, and their structure and evaluated data are similar to the isotropic shell element component results. The structure of these output data can also be found in Appendix A.

4.7 DISPLAY OF THE EVALUATED DATA IN THE HYPERVIEW

The requirement for visualizing the results in HyperView specified that the code should be able to display the envelopes of the result data, which are maps showing the extreme values on every element of the structure across all load cases. During the development process, this matter was revisited, and it was decided to also include the possibility of visualizing individual load case results.

4.7.1 ALTAIR ASCII FILE

The most convenient method for incorporating custom results directly into HyperView is by using the Altair ASCII file. HyperView has a Generic ASCII Reader capable of reading TXT files in a specific format and assigning the predefined results directly to the elements. Loading the model and the result TXT file into HyperView can be done directly through HyperView's GUI. More information about the ASCII file format can be found in the source [55].

4.7.2 VISUALISATION OF ISOTROPIC SHELL ENVELOPES RESULTS

To seamlessly assign data, it is essential to maintain a specific format for the ASCII file. To illustrate, the format of the ASCII data will be demonstrated using a simple model consisting of three elements with the EIDs 1, 2, and 3.

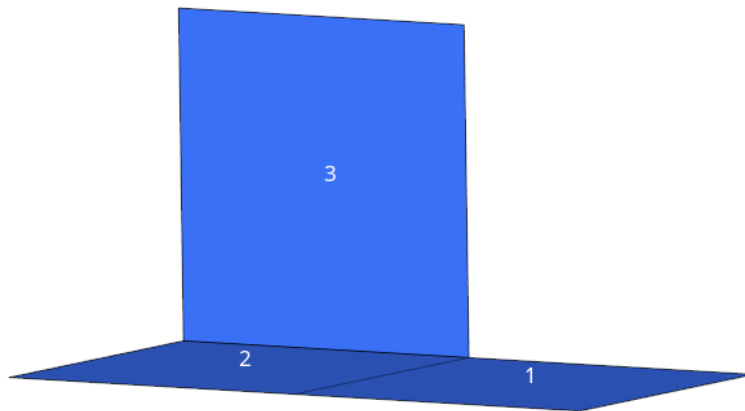


Fig. 64: Simple model for the demonstration of the Altair ASCII format

For each dataset that needs to be assigned to the elements in HyperView, it is necessary to write an individual header. This header always starts with the line: ALTAIR ASCII FILE. The next piece of information that must be specified in the header is the delimiter, for which the tabulator was chosen because it clearly separates data in the columns. Additional lines in the header specify that the data are to be assigned to the elements based on their EIDs. When writing the data for the visualization of the shell envelopes, two separate datasets must be written for each element: the maximum value that appeared on the element throughout all the load cases and the load case number in which it occurred. The dataset name is in the header line \$RESULT _TYPE. It was decided to use the extension "strs" for stress data and "LCs" for the dataset showing the numbers of load cases. The following scheme shows an example Altair ASCII file with dummy data for the three-element model:

```
ALTAIR ASCII FILE
$DELIMITER =
$title = Static Analysis
$SUBCASE_ID = 1 SHELL_ENVELOPES
$BINDING = ELEMENT
$COLUMN_INFO = ENTITY_ID
$result type = 17_Max_Mises_strs
1 86000000
2 75000000
3 95000000
ALTAIR ASCII FILE
$DELIMITER =
$title = Static Analysis
$SUBCASE_ID = 1 SHELL_ENVELOPES
$BINDING = ELEMENT
$COLUMN_INFO = ENTITY_ID
$result type = 18_Max_Mises_LCs
1 6
2 64
3 42
```

The header must always start with this line

As a delimiter was chosen tabulator (not visible)

Generic information, it can always be the same

Subcase ID has to be specific for each dataset.

The name of the dataset appear in the drop down menu in Results tab as shown in Fig. 66

These two lines specify that the data are to be assigned to element according to its EID

The result type name appear in the result type drop down menu (see Fig. 66)

In the first column are EIDs and in the second are the values to be assigned

Fig. 65: Illustration of the Altair ASCII file using shell element envelopes results

The name of the result type begins with a number because HyperView maintains the order of the datasets in the result type dropdown menu according to this number. After loading the ASCII file along with the corresponding BDF file into HyperView, the names of the datasets appear in the dropdown menus, as shown in the following image.

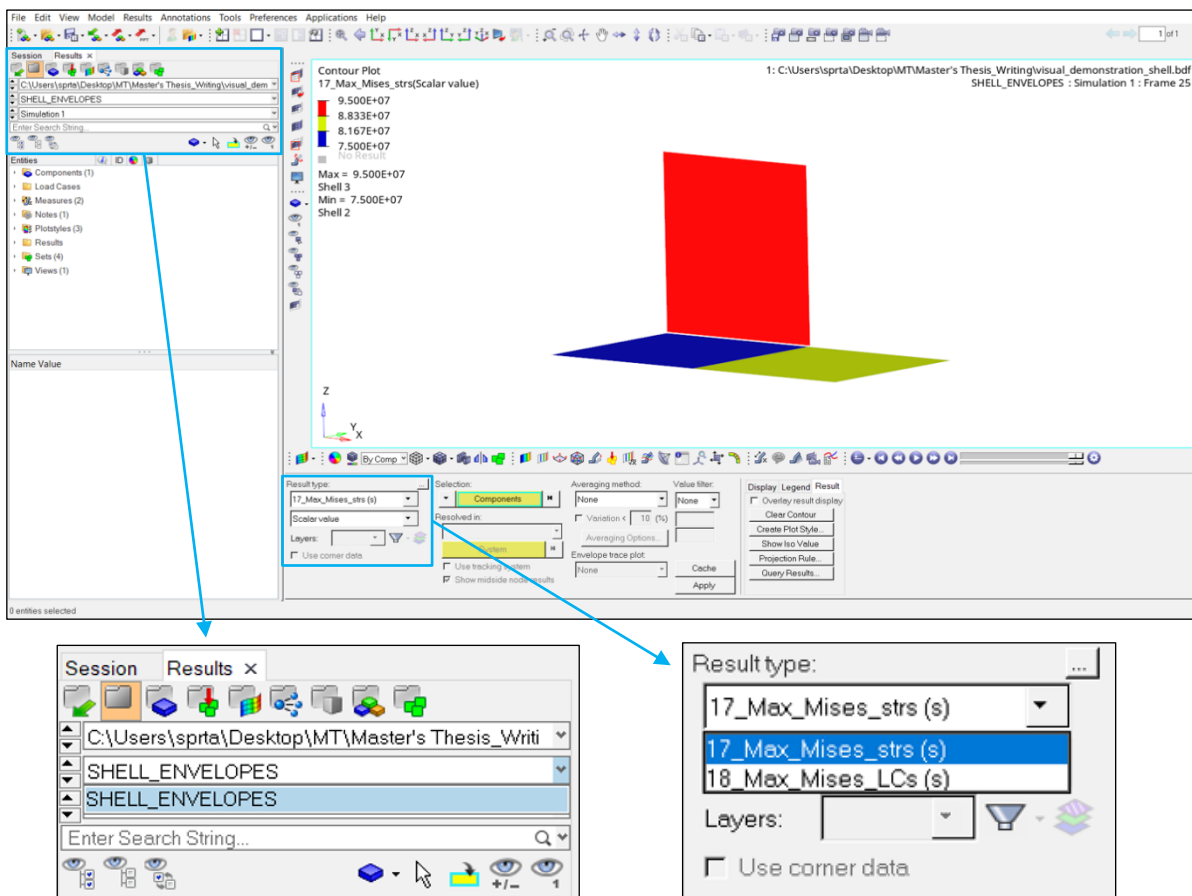


Fig. 66: GUI of HyperView and menus with user input data

After selecting the Result dataset and Result type, and confirming with the Apply button, the data will appear on the FE model in the main window. The data from the illustrative ASCII file in Fig. 65, when applied to the simple model in Fig. 64, are visualized in the following image.

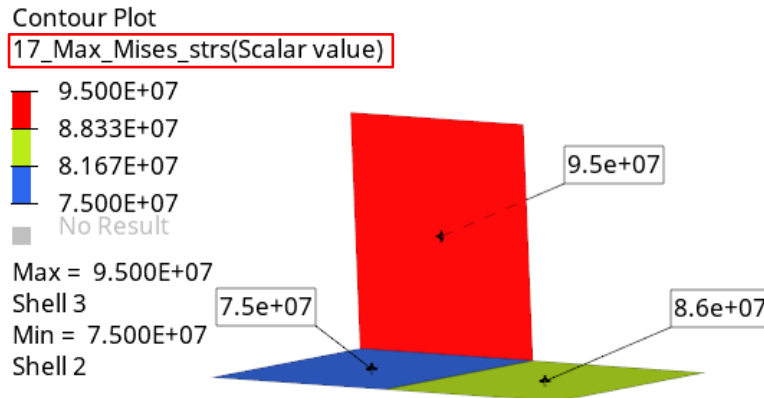


Fig. 67: Visualisation of Max_Mises_strs from ASCII file from Fig.38

4.7.3 VISUALISATION OF THE LOAD CASE RESULTS FOR ISOTROPIC SHELL COMPONENTS

If the user wants to visualize results for a specific element type and particular load cases, they can choose and specify this in the GUI (see section 4.8). In the case of visualizing data related to individual load cases, the header is written in the same way as for visualizing envelopes. The element type, along with the load case number, is visible in the top drop-down menu, and the specific dataset for visualization can be selected from the bottom drop-down menu.

4.7.4 VISUALISATION OF ENVELOPES FOR SHELL ELEMENTS WITH PCOMP PROPERTY

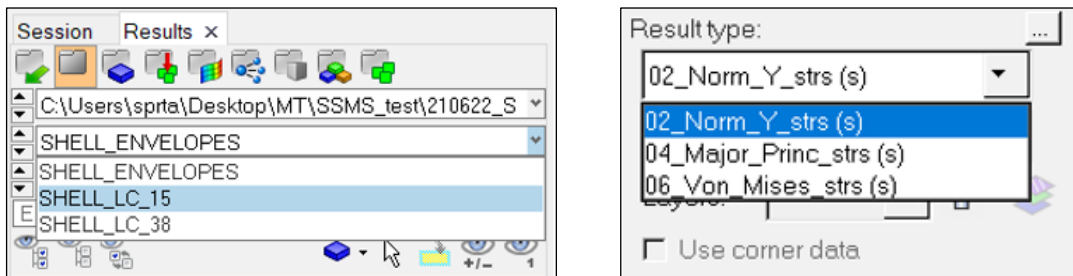


Fig. 68: Visualisation of load case results for shell elements with PSHELL property in HyperView

In principle, the visualization of envelopes for composite elements is similar to that of envelopes for shell elements with PSHELL properties. Envelopes for composites with quasi-isotropic skin can be found under the name QI_ENVELOPES, while composites with orthotropic skin are named ORTHO_ENVELOPES. Similar to shell elements, it offers two datasets for each requested data selected in the GUI, which are maximum values and the load cases at which these maximum values occurred (with the extension LCs). The exception is the Hill failure index (FI), for which the numbers of plies where the maximum FI occurred on every element are automatically prepared as well.

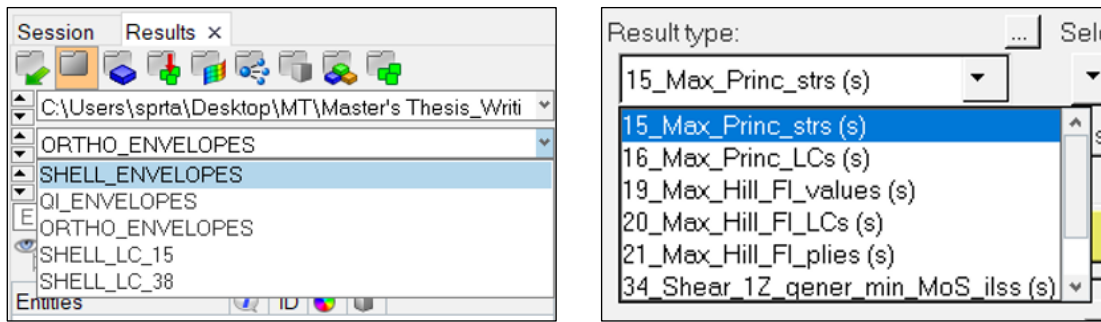


Fig. 69: Results dropdown menu and Result type dropdown menu results for ORTHO_ENVELOPES

4.7.5 VISUALISATION OF LOAD CASE RESULTS FOR COMPOSITE SHELL ELEMENTS

The naming of the load case result in the upper results dropdown menu follows a similar format as for standard shell elements, consisting of the composite type name and the load case number. The difference between visualizing standard shell element results and composite results using Altair ASCII files is that for composites, it is necessary to visualize the stresses for each ply separately. HyperView has a special dropdown menu called Layers, located below the Result type dropdown menu, for this purpose (see the image below). To view the evaluated data for each ply in this dropdown menu, the Altair ASCII file must have the following structure.

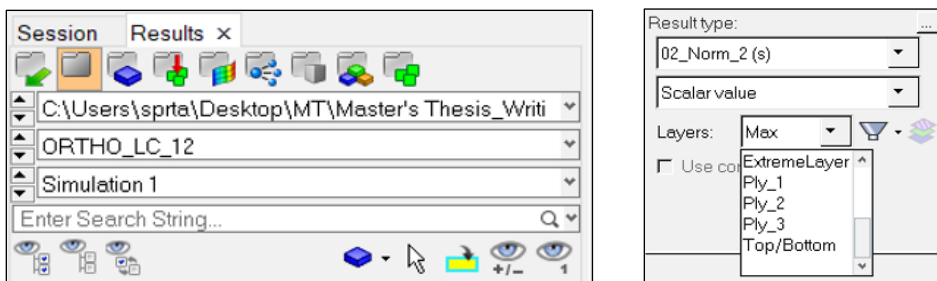


Fig. 70: Above ASCII file loaded into HyperMesh

To visualize the results for composite components (including results for plies), the Altair ASCII file must follow a predefined format, as shown in the image below. Each element's EID is repeated as many times as there are plies, in consecutive order from the first to the last ply. However, a problem arises when parts have differing numbers of plies. In such cases, it is necessary to pad the NumPy arrays in the code with NaN data type and write it as such in the TXT file. As a result, there is an empty space in the TXT file, but this allows the remaining plies on other components to be displayed. Elements without any assigned data are displayed in grey, and if the element contour value is requested, they indicate an N/A value, as shown in Fig. 72.

```

ALTAIR ASCII FILE
$DELIMITER =
$title = Static Analysis
$SUBCASE_ID = 101 ORTHO_LC_12
$BINDING = ELEMENT
$LAYER_INFO =3 "Ply_1" "Ply_2" "Ply_3"
$COLUMN_INFO = ENTITY_ID
$RESULT_TYPE = 02_Norm_2
1 120000000
1 61500000
1
2 92000000
2 55000000
2 83000000
3 133000000
3 76000000
3 124000000

```

Name of the component type and the number of the load case
 Total number of plies and the name to be assigned to every ply
 Name of the dataset which appears in the Result type drop-down menu
 Dataset, in the first column are EIDs and in the second column are values to be assigned

Fig. 71: Altair ASCII file for visualisation of the results of composite shell elements

It is important to note that when requesting and loading a dataset with values belonging to the skin of a sandwich component in HyperView, the ply numbering skips the presence of the core. In other words, the numbers for the bottom skin are one lower because the core ply is not included. The structural analyst working with the tool should be aware of this fact to ensure accurate evaluation of the skin results.

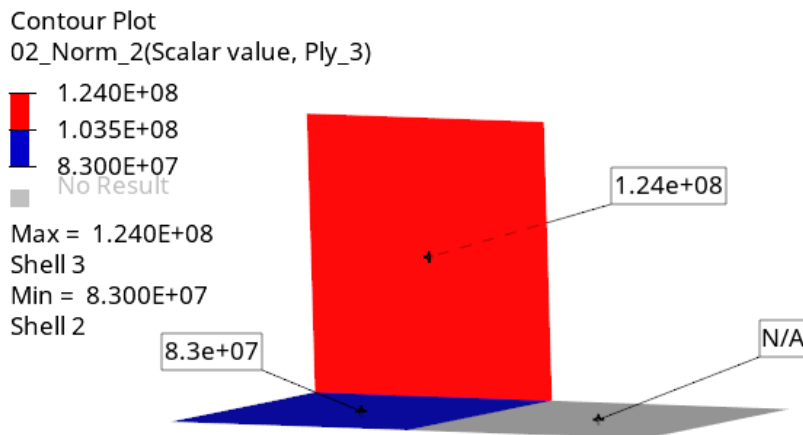


Fig. 72: Visualisation of the Ply_3 from the ASCII file in the Fig. 71

4.7.6 VISUALISATION OF RESULTS FOR ISOTROPIC SOLID ELEMENTS

The visualization of results for solid elements follows the same method as for isotropic shell elements, as explained in detail above.

4.8 GRAPHICAL USER INTERFACE OF THE NEW TOOL

To enhance user-friendliness while working with the new tool, a GUI was developed using Qt Designer and the PyQt5 library, as discussed in more detail earlier. At the top of the GUI, there are browse buttons and line edit input widgets where users can enter the paths to the specified

files. When the browse button is clicked, the Windows file explorer appears, allowing the user to find the requested file. Since Excel files containing load cases typically have multiple sheets, user can specify the name of the Excel sheet they want to read the matrix with the load cases from, in the second line.

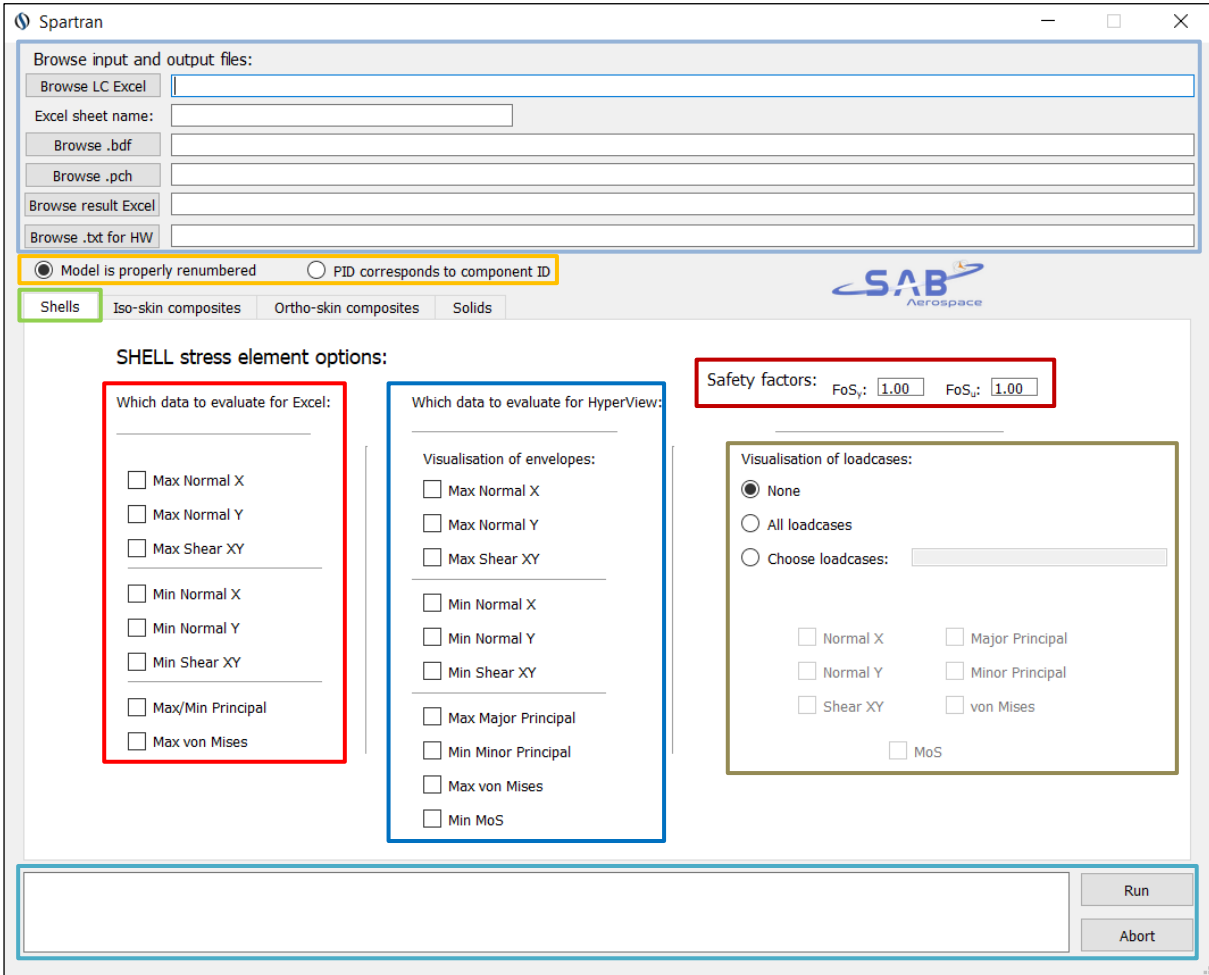


Fig. 73: GUI tab with shell element options

Below the definition of the paths to the input and result files are two radio buttons specifying which of the assigning algorithms shall be used for the particular run. Below these sections which are common to all the element types are the tabs with the stress element options for each component type. In these tabs is a number of checkboxes whose meaning is to save computational time because the user can particularly specify which data they want to evaluate.

The area in the particular tabs is always divided into four sections. On the left are data which are to be evaluated and written in the result and summary Excel tables. In the middle column are checkboxes with the data which are to be visualised in HyperView as an envelopes and on the right are the options for the visualisations of the individual load cases. The user can specify using the radio buttons whether they want to visualise none, all load cases or choose which load cases specifically they want to visualise and by the check boxes can also specify which outputs for these load cases are to be visualised. In the top right corner of the tabs are the line edit input widgets for specifying the factors of safety.

At the bottom of the GUI is output window into which are written comments regarding the run. If the run is successful there are displayed running times of individual parts of the code and if there is a problem there is displayed error message which can help the structural analyst to avoid the issue e.g., Error, the allowables for MAT1 are missing. Next to the output window are Run and Abort buttons which serves for start of the run and abort in the case that the run is to be for some reason terminated.

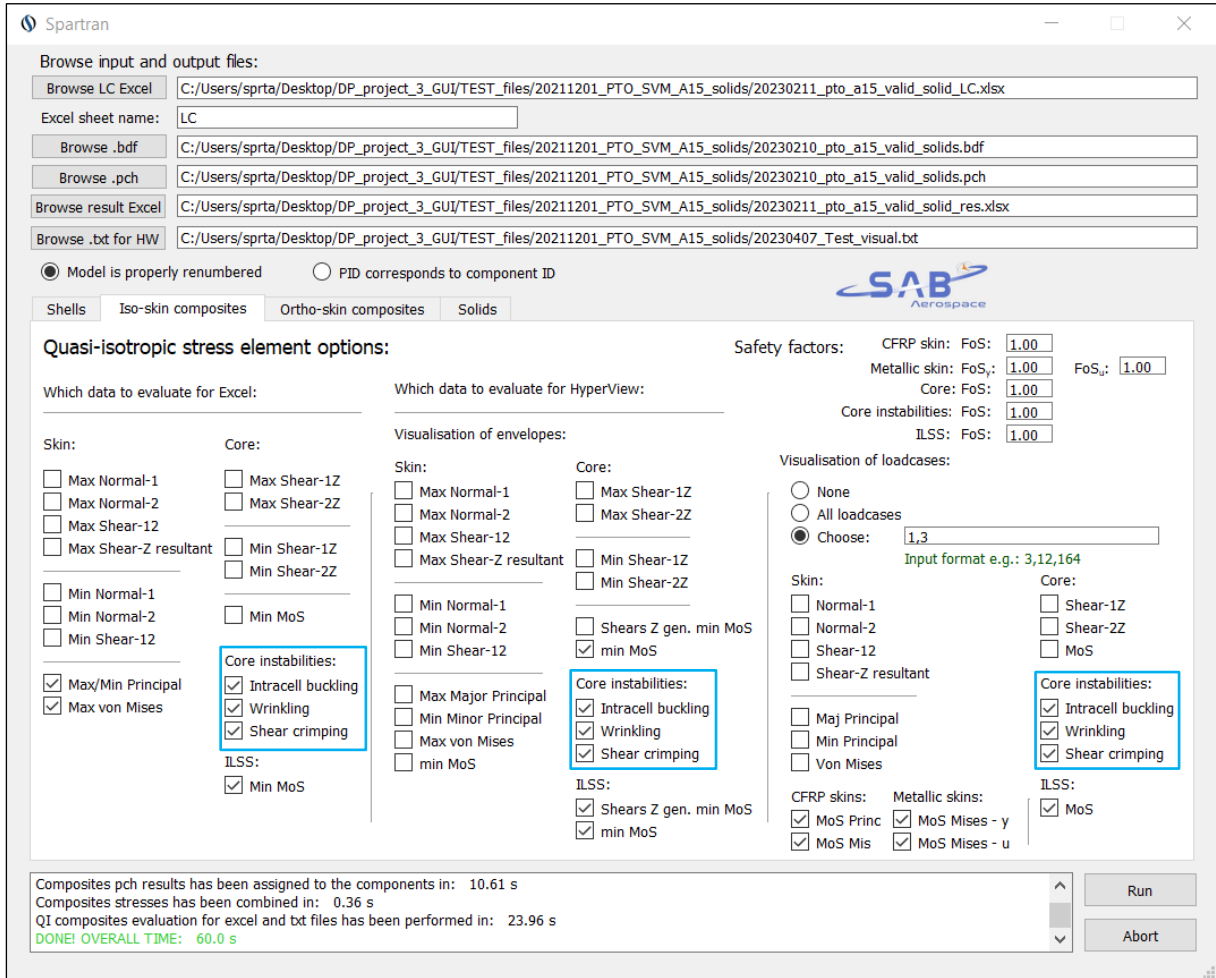


Fig. 74: GUI tab with iso-skin composite element options

At the composites there are more evaluation options because evaluation of skin, core shear strength and ILSS are performed separately. The biggest difference between GUI of the iso-skin composites (image above) and ortho-skin composites (Fig. 75) is that the first contain the checkboxes for evaluation core instabilities. The images showing the tabs with the ortho-skin composite element options and solid element options are shown in the following page.

The application was compiled using python package PyInstaller into the EXE file which means that the software can be installed directly to computer with Windows operation system without necessity to install Python and other libraries used for the development of the code.

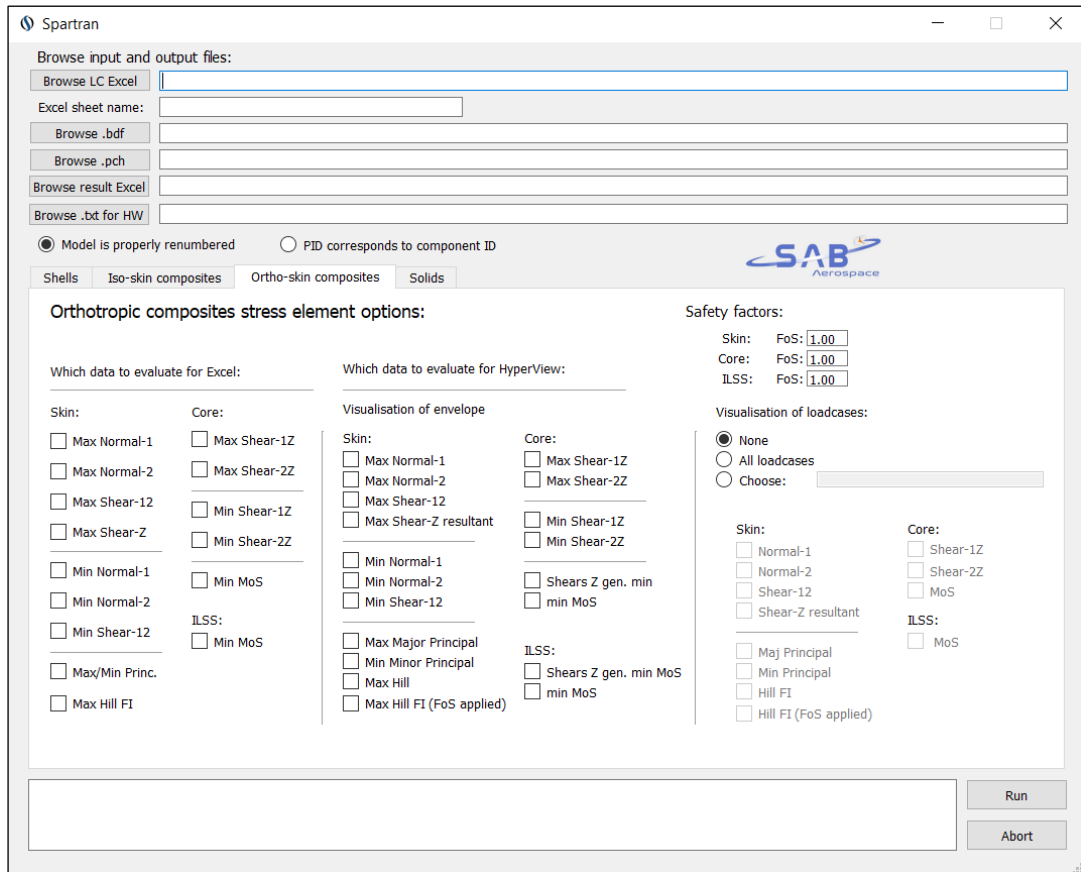


Fig. 75: GUI tab with ortho-skin composite element options

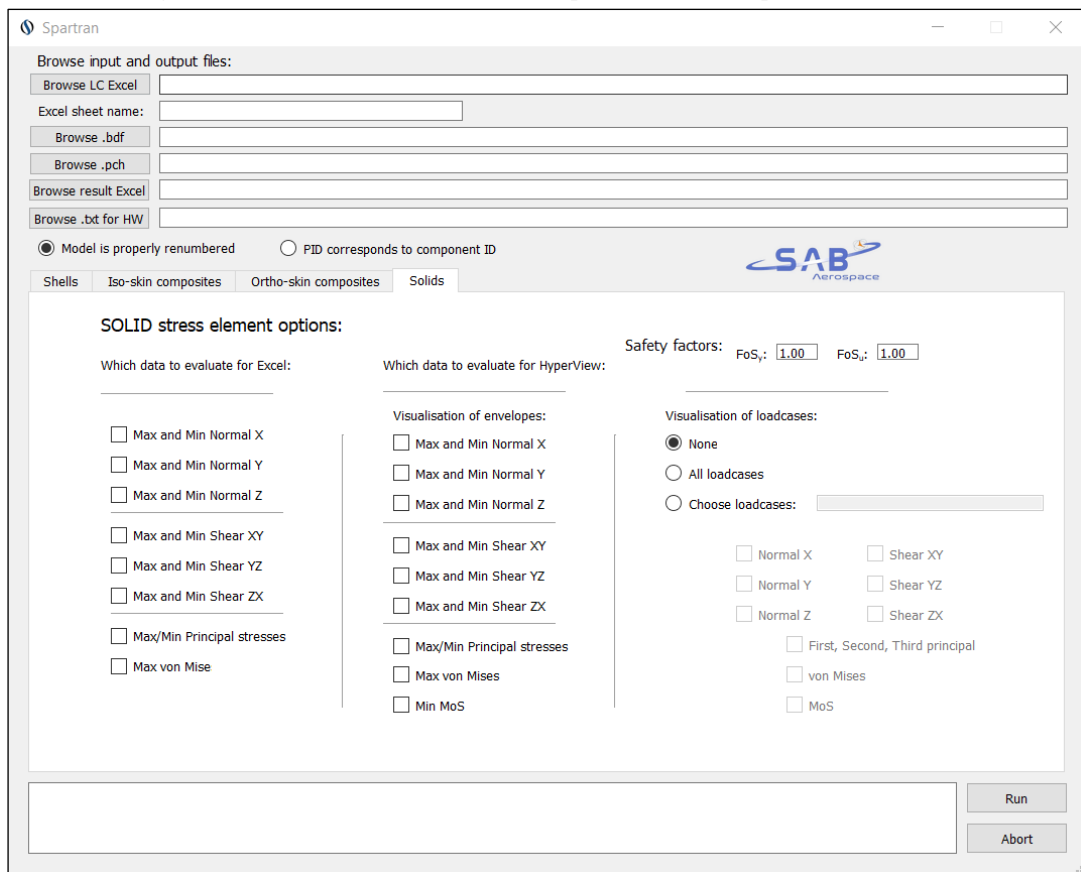


Fig. 76: GUI tab with solid element options

5 VALIDATION OF THE FUNCTIONALITY OF THE TOOL

5.1 DESCRIPTION OF THE FE MODEL

Although the first testing of the new tool was performed on much simpler models for the illustration and verification of the new tool functionalities in this thesis the FE model of PLATO SVM was chosen. This is because it includes all element types that the new tool is able to post-process and at the same time the model is rather complex and therefore it shows the power of the new tool. Although the mesh is rather coarse, and for the evaluation of stresses are often used sub-models, it will serve well for the illustration.

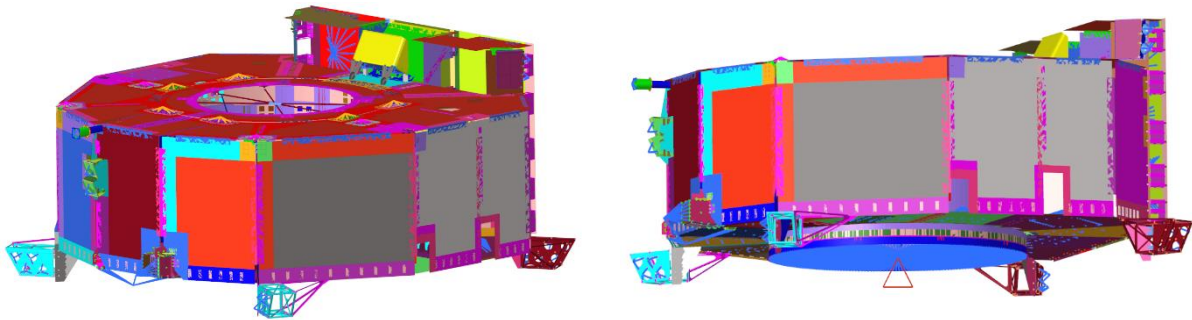


Fig. 77: FE model of the PLATO SVM constrained by SPC

For demonstration and verification of the results, only first three load cases of the Launch Quasi-Static Loads (L-QSL) will be used, combined of three subcases which are 1 g accelerations in all three axes. The movement of the model is constrained by SPC constraining all 6 degrees of freedom on the launch vehicle adapter ring where the structure will be attached to the launcher.

	1L	2L	3L
1	3.30	0.00	1.35
2	3.19	0.85	1.35
3	2.86	1.65	1.35

Tab. 9: Load cases used for the validation

The outputs from the new tool will be compared directly with the outputs from the Nastran (saved in OP2 file) because in the previous custom tool might have been undetected bugs. Although during the verification testing all the stress outputs were carefully checked, because of the limited scope of the master’s thesis, only some of the outputs will be investigated and illustrated on the following pages.

5.2 VALIDATION OF THE STANDARD SHELL ELEMENTS

The MoS for standard shell elements with PSHELL property is determined based on von Mises stress whose evaluation will be more closely investigated.

5.2.1 VISUALISATION OF INDIVIDUAL LOAD CASES

The comparison of the outputs from Nastran and new tool for the first of the load cases from the table above is in the following pictures.

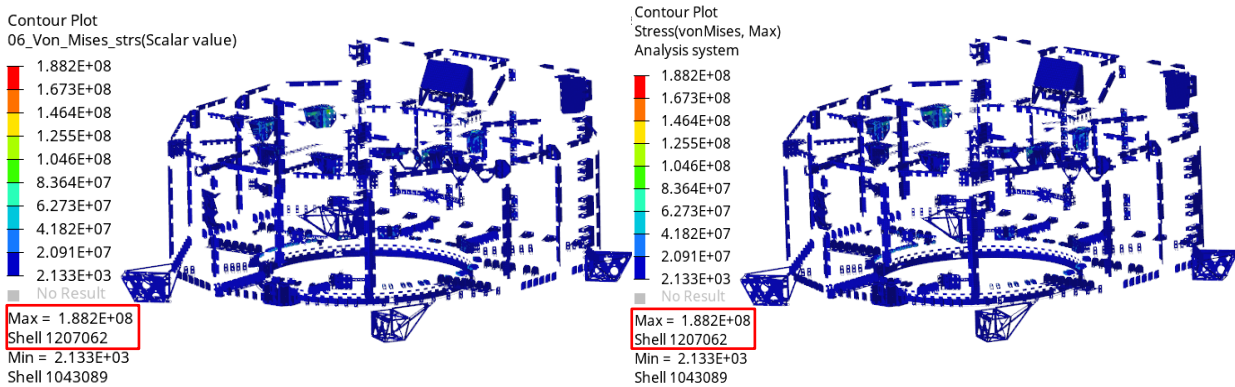


Fig. 78: Comparison of von Mises stress on metallic parts at the first load case, new tool (left), Nastran (right)

In the picture above can be seen that all standard shells with PSHELL property have, apart from another elements, assigned value according to the expectation. For more detailed investigation will be used Payload module (PLM) bracket, which indicates the highest stress at the first load case on the element with EID 1207062. For comparison, in the Fig. 80 and Fig. 81 there are shown the stresses for all three load cases calculated using the new tool and Nastran to validate the results separately.

Subcase 1: 1 G X			
1207062	-1.000000E-03	8.705584E+06	-8.052247E+06
-CONT-	2.901973E+07	3.694745E+01	3.053181E+07
-CONT-	-2.987848E+07	5.231787E+07	1.000000E-03
-CONT-	6.765812E+06	-1.458519E+06	2.708073E+07
-CONT-	4.068284E+01	3.004481E+07	-2.473752E+07
-CONT-	4.751704E+07		
Subcase 2: 1 G Y			
1207062	-1.000000E-03	-3.459259E+06	5.105155E+06
-CONT-	-1.249401E+07	-5.445934E+01	1.403043E+07
-CONT-	-1.238453E+07	2.289083E+07	1.000000E-03
-CONT-	-2.826917E+06	1.217774E+06	-1.106812E+07
-CONT-	-5.017737E+01	1.044679E+07	-1.205594E+07
-CONT-	1.950453E+07		
Subcase 3: 1 G Z			
1207062	-1.000000E-03	2.094307E+06	-1.087469E+06
-CONT-	6.456095E+06	3.807858E+01	7.152636E+06
-CONT-	-6.145798E+06	1.152778E+07	1.000000E-03
-CONT-	1.505363E+06	-7.603042E+04	6.078016E+06
-CONT-	4.129397E+01	6.843898E+06	-5.414565E+06
-CONT-	1.064017E+07		

Fig. 79: Shell element stresses at element 1207062 for all three subcases

For demonstration, the stress for the element 1207062 at the first load case will be calculated manually. The stresses from the subcases 1,2, and 3 in PCH file were showed in the picture above. As it was mentioned in the section 4.3.2, the stresses are in PCH file specified for both surfaces of the shell element. Therefore, the calculation must be performed for each surface separately as follows.

Top side:

$$\sigma_{x,top} = 8705584 \cdot 3.30 - 3459259 \cdot 0.00 + 2094307 \cdot 1.35 = 31555742 \text{ Pa}$$

$$\sigma_{y,top} = -8052247 \cdot 3.30 + 5105155 \cdot 0.00 - 1087469 \cdot 1.35 = -28040498 \text{ Pa}$$

$$\tau_{xy,top} = 29019730 \cdot 3.30 - 12494010 \cdot 0.00 + 6456095 \cdot 1.35 = 104480837 \text{ Pa}$$

$$\begin{aligned} \sigma_{Mises,top} &= \sqrt{\sigma_{x,top}^2 + \sigma_{y,top}^2 - \sigma_{x,top}\sigma_{y,top} + 3\tau_{xy,top}^2} = \\ &= \sqrt{31555742^2 + (-28040498)^2 - 31555742 \cdot (-28040498) + 3 \cdot 104480837^2} = \\ &= 188190353 \text{ Pa} \end{aligned}$$

Bottom side:

$$\sigma_{x,bot} = 6765812 \cdot 3.30 - 2826917 \cdot 0.00 + 1505363 \cdot 1.35 = 24359420 \text{ Pa}$$

$$\sigma_{y,bot} = -1458519 \cdot 3.30 + 1217774 \cdot 0.00 - 76030 \cdot 1.35 = -4915754 \text{ Pa}$$

$$\tau_{xy,bot} = 27080730 \cdot 3.30 - 11068120 \cdot 0.00 + 6078016 \cdot 1.35 = 97571731 \text{ Pa}$$

$$\begin{aligned} \sigma_{Mises,bot} &= \sqrt{\sigma_{x,bot}^2 + \sigma_{y,bot}^2 - \sigma_{x,bot}\sigma_{y,bot} + 3\tau_{xy,bot}^2} = \\ &= \sqrt{24359420^2 + (-4915754)^2 - 24359420 \cdot (-4915754) + 3 \cdot 97571731^2} = \\ &= 171166640 \text{ Pa} \end{aligned}$$

From the values calculated for both sides is chosen the higher one (188190353 Pa) which is then written into the result table in excel and also to be visualised in HyperView.

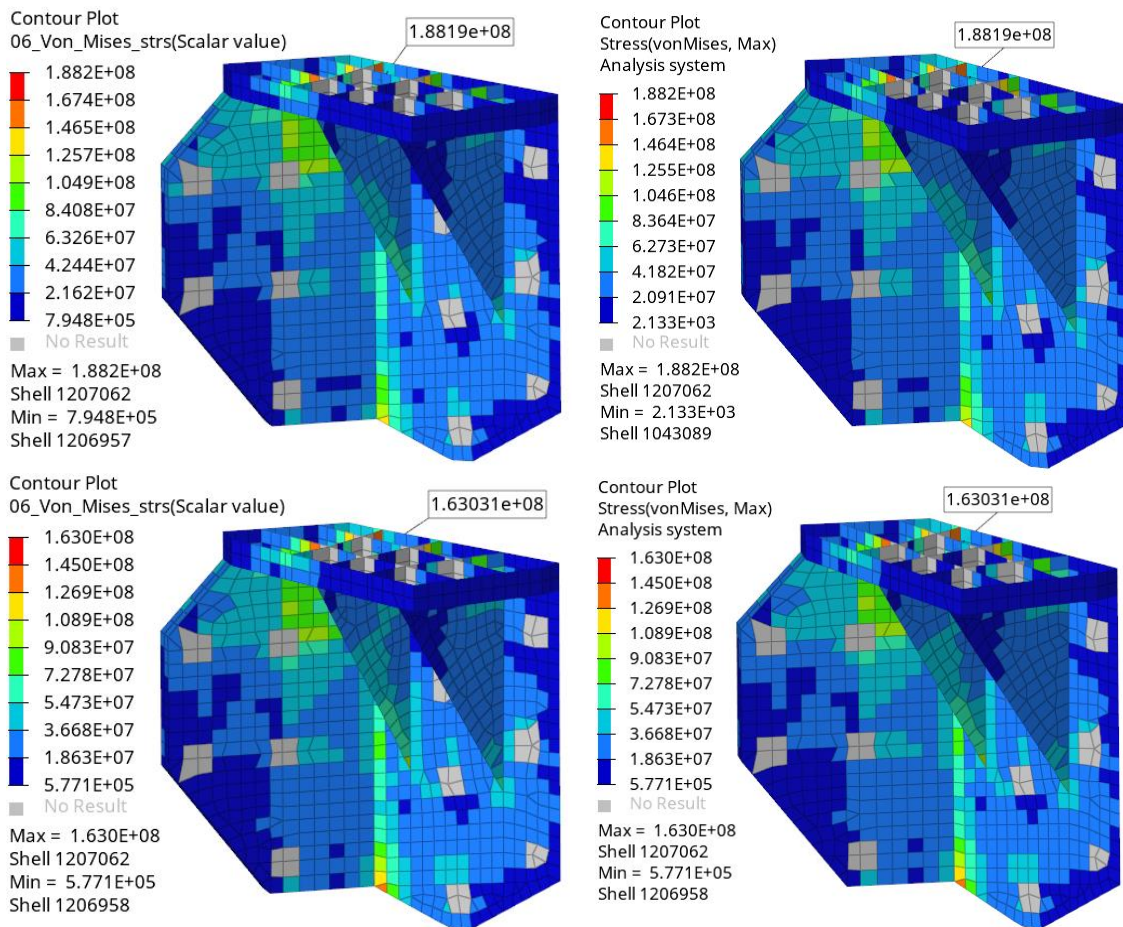


Fig. 80: Load cases 1 and 2 from the top, new tool on the left, Nastran on the right

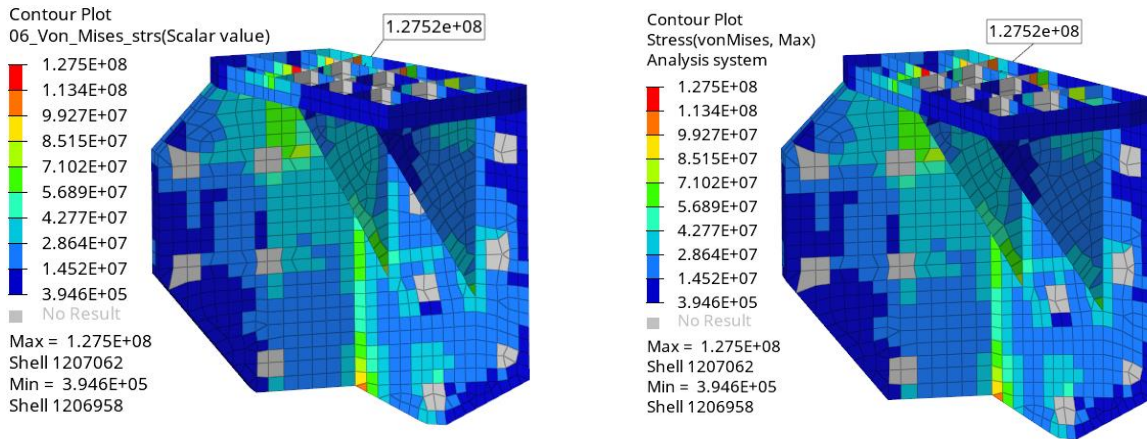


Fig. 81: Load case 3, new tool on the left, Nastran on the right

5.2.2 VISUALISATION OF ENVELOPE

The illustration of visualisation of envelope is shown in the following pictures. The maximum value on the element 1207062 is 1.8819×10^8 Pa which corresponds to the maximum value on this element throughout all the calculated load cases shown in the pictures above.

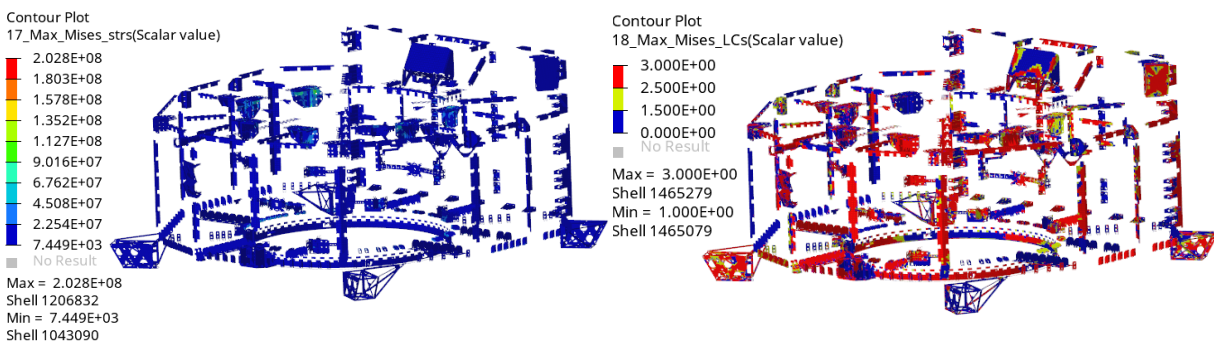


Fig. 82: The von Mises stress envelope and the load cases at which the maximum values at the elements occurred

In the following figure there is detail of the envelopes displayed on the PLM bracket. The maximum value is displayed correctly on the element 1207062 and it is correctly indicated that this value corresponds to the load case 1.

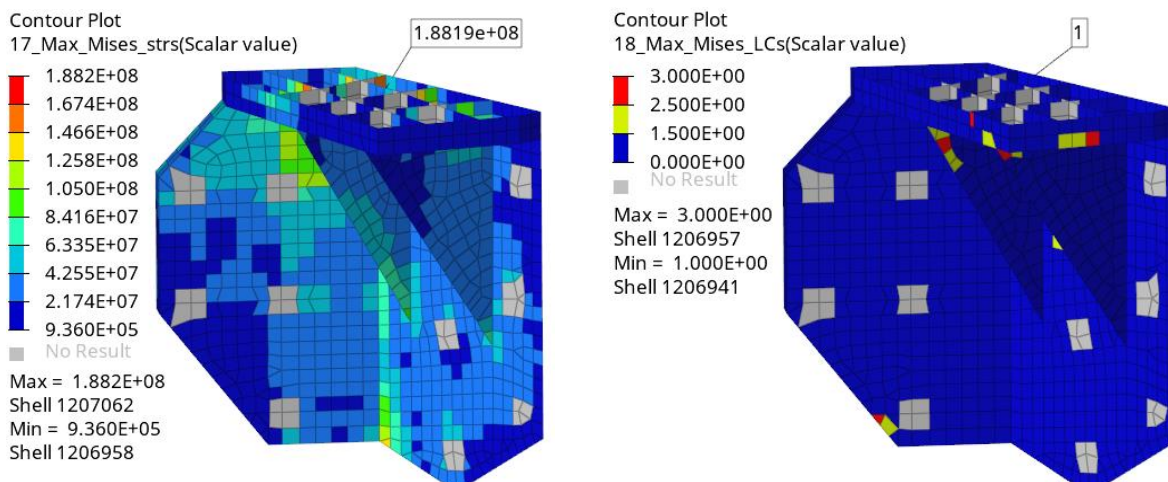


Fig. 83: Visualisation of the envelope of the von Mises stress (left) and map of the load cases at which they occurred (right)

5.3 VALIDATION OF THE EVALUATION OF ISO-SKIN COMPOSITE SHELL ELEMENTS

Evaluation of MoS at shell elements with PCOMP property and isotropic skins depends on the type of the component and the material. For the sandwich panels with quasi-isotropic composite skin is for the determination of the MoS of the skin used absolute maximum value from major and minor principal stresses and from von Mises stress. If the skin is metallic then the MoS is determined based on maximum von Mises stress. The core shear strength is calculated according to the formulas 12 and 13 as it will be shown below. Interlaminar shear strength on iso-skin composites was evaluated on different FE models because PLATO SVM does not contain any monolithic parts with quasi-isotropic skins. The correctness of the evaluation of core local instabilities will be demonstrated using shear crimping.

5.3.1 QUASI-ISOTROPIC CFRP SKINS

VISUALISATION OF THE INDIVIDUAL LOAD CASES

The comparison of visualisation of individual load cases will be performed using von Mises stress in the top ply (Ply 1) of the sandwich panels. The maximum value at first load case is $4.854e+07$ Pa and it is on element 2674545.

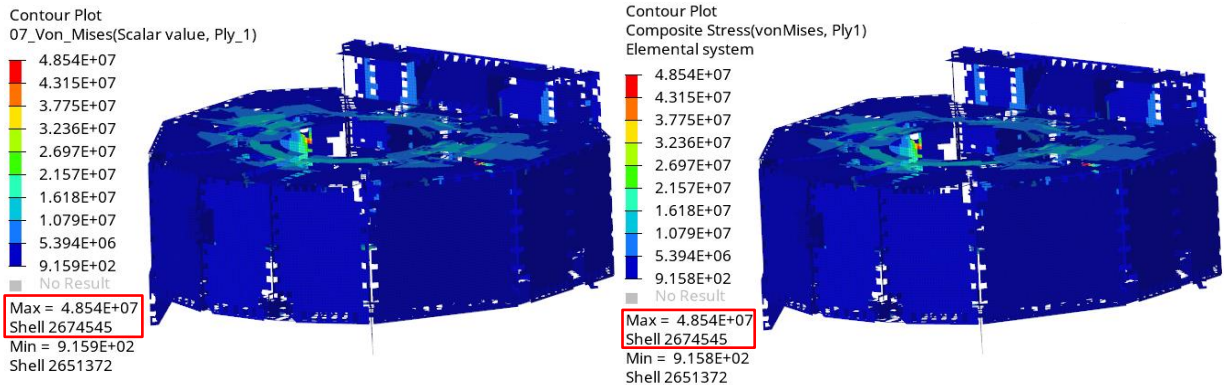


Fig. 84: Comparison of von Mises stress in the first ply at the first load case, new tool (left), Nastran (right)

The correctness of the results will be further investigated using one of the shear panels which indicates the highest values of the von Mises stress on the whole model.

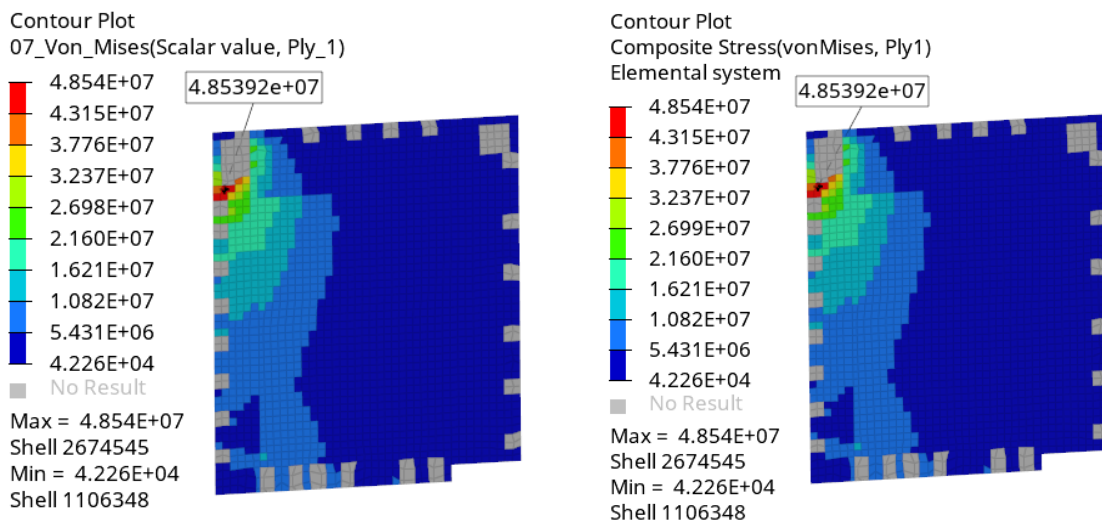


Fig. 85: Load case 1 on the top skin, new tool on the left, Nastran on the right

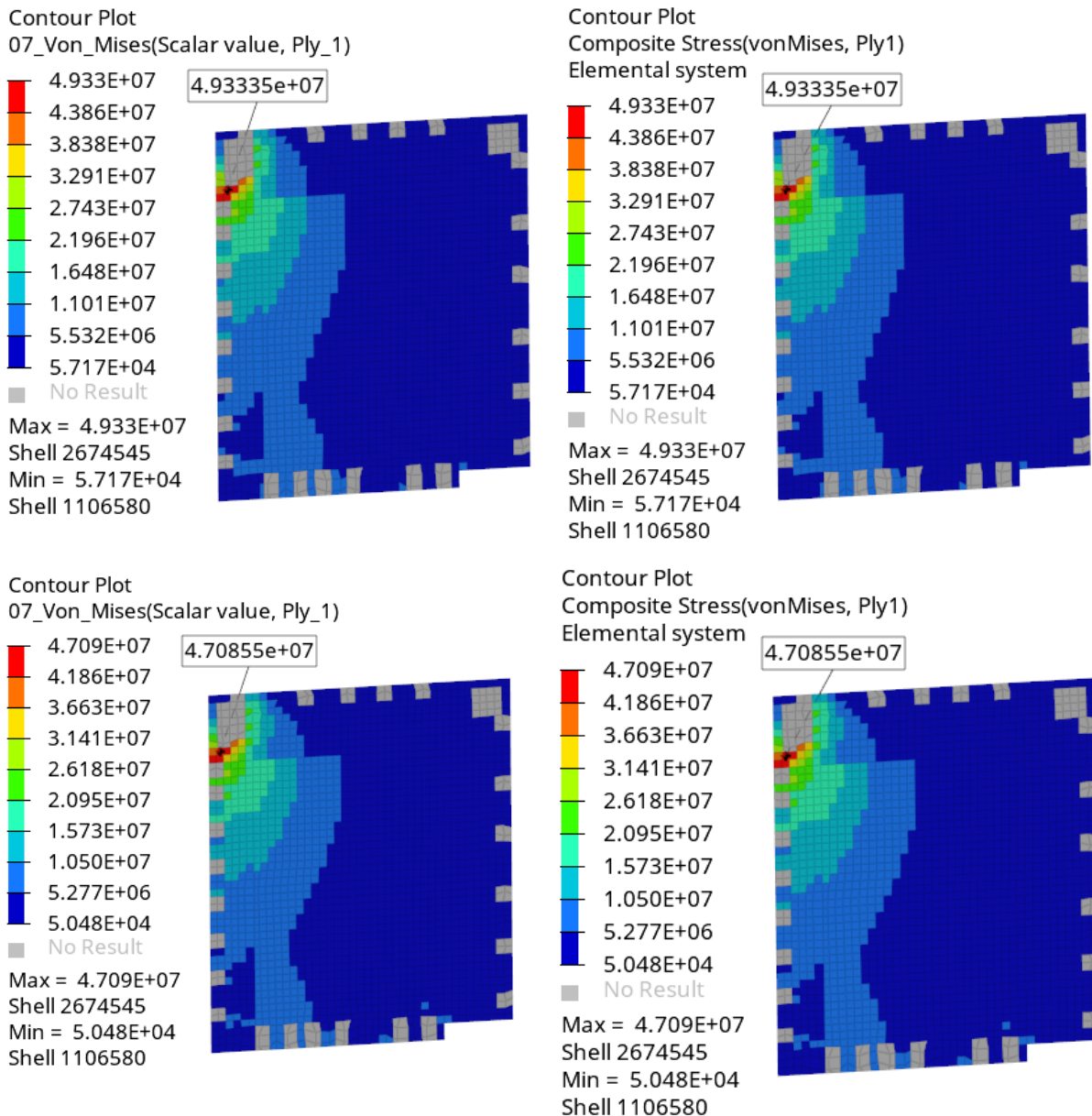


Fig. 86: Load case 2 and 3 (from top) on the top skin, new tool on the left, Nastran on the right

VISUALISATION OF ENVELOPE

From the previous pictures can be seen that the maximum value is indicated for all three load cases on the element 2674545 and the highest value can be found at the load case 2 where the maximum value in the first ply is 4.93335×10^7 Pa. This value is maximum also when results from the bottom side of the sandwich panel are included. The envelope showing the highest stresses throughout all the 3 load cases as well as the map showing at which load cases it occurred are shown in the following figure.

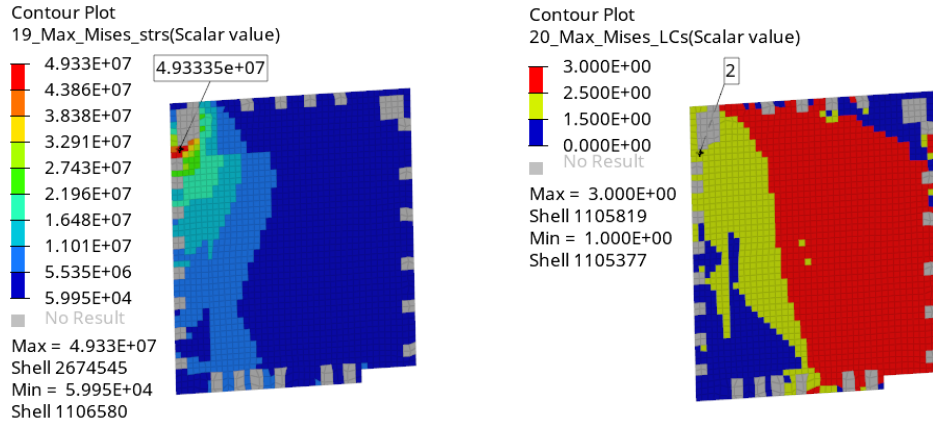


Fig. 87: Visualisation of the envelope of the von Mises stress (left) and map of the load cases at which they occurred (right)

5.3.2 METALLIC SKINS

VISUALISATION OF THE INDIVIDUAL LOAD CASES

The radiator panels with metallic skins are at the bottom and rear side of the PLATO structure as it can be seen in the following picture.

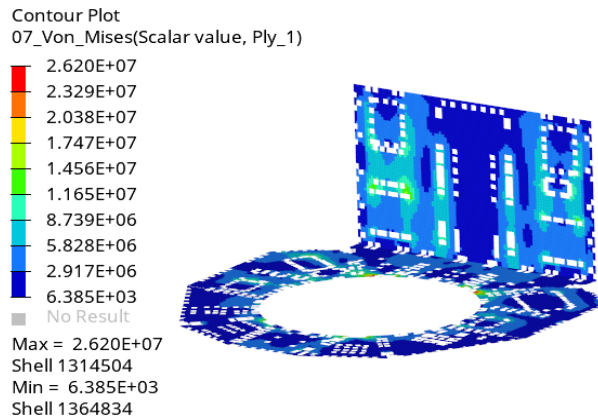


Fig. 88: The results on the top skin of the radiator panels at the load case 1

The evaluation is closely investigated and compared to the direct Nastran output on the radiator panel on which are located the highest values.

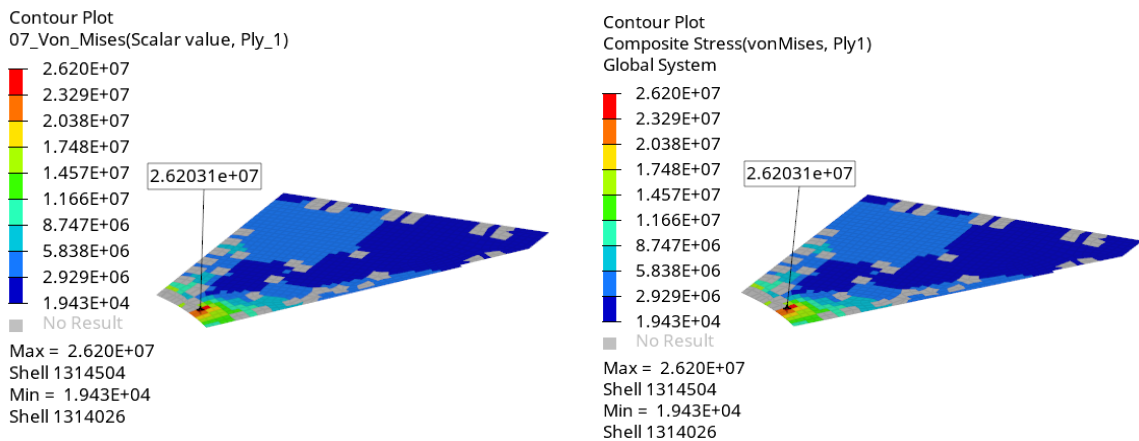


Fig. 89: Von Mises at load case 1 in the top skin, new tool on the left, Nastran on the right

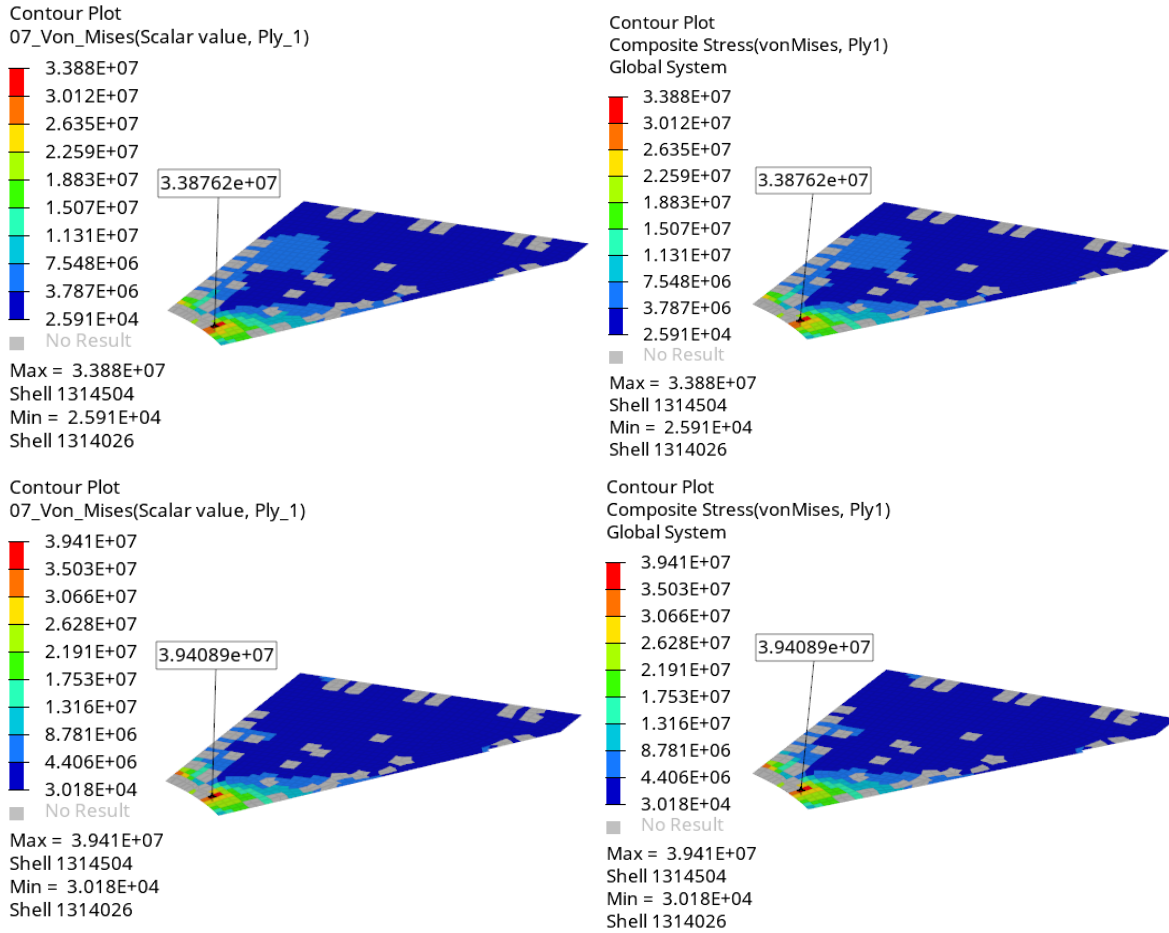


Fig. 90: Von Mises at load cases 2 and 3 (from top) in the top skin, new tool on the left, Nastran on the right

VISUALISATION OF THE ENVELOPES

From the previous figures is apparent that the maximum is $3.94089e+07$ Pa and that it occurred at the load case 3. This is exactly what the envelope throughout all the load cases indicates as it can be seen in the following figure.

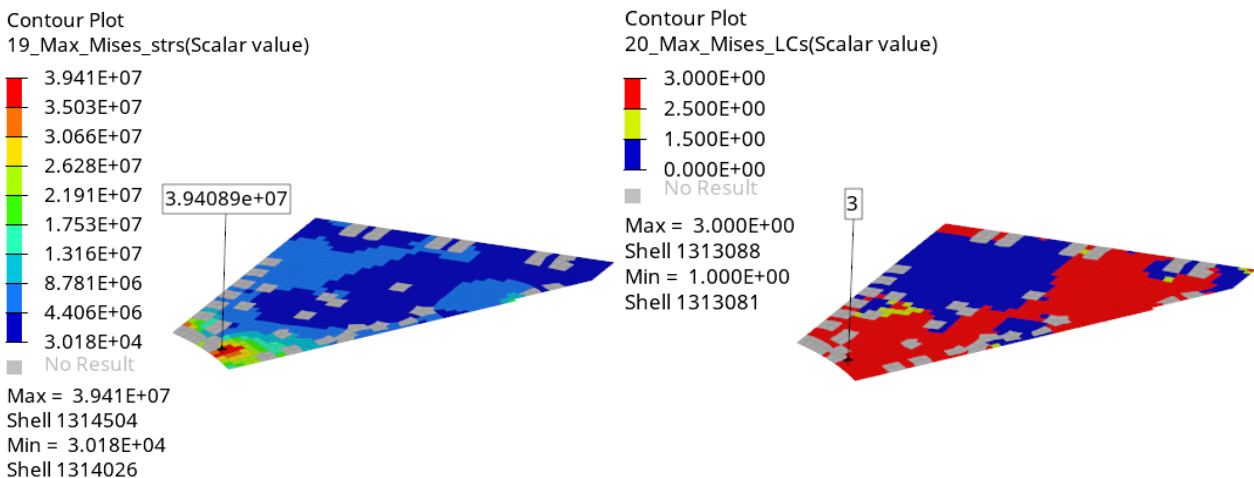


Fig. 91: Visualisation of the envelope of the von Mises stress (left) and map of the load cases at which they occurred (right)

5.3.3 CORE STRENGTH EVALUATION

The core strength evaluation is performed based on formulas that cannot be directly requested from Nastran. Therefore, the verification of the correctness of the evaluation will be performed using calculation.

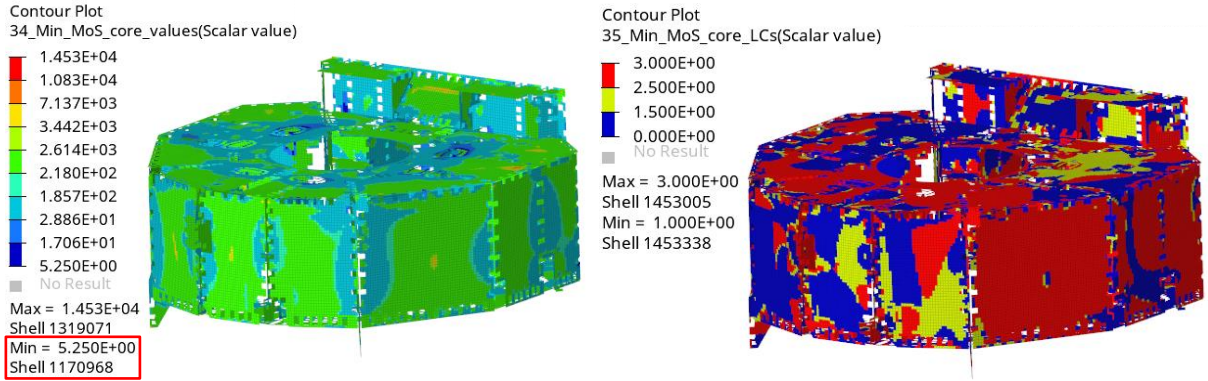


Fig. 92: Visualisation of the envelope of min MoS for core shear strength (left) and map of the load cases at which they occurred (right)

From the above picture can be seen that the minimum MoS is 5.25 and can be found on the element 1170968. The envelope in the vicinity of this element can be closely investigated in the following figure.

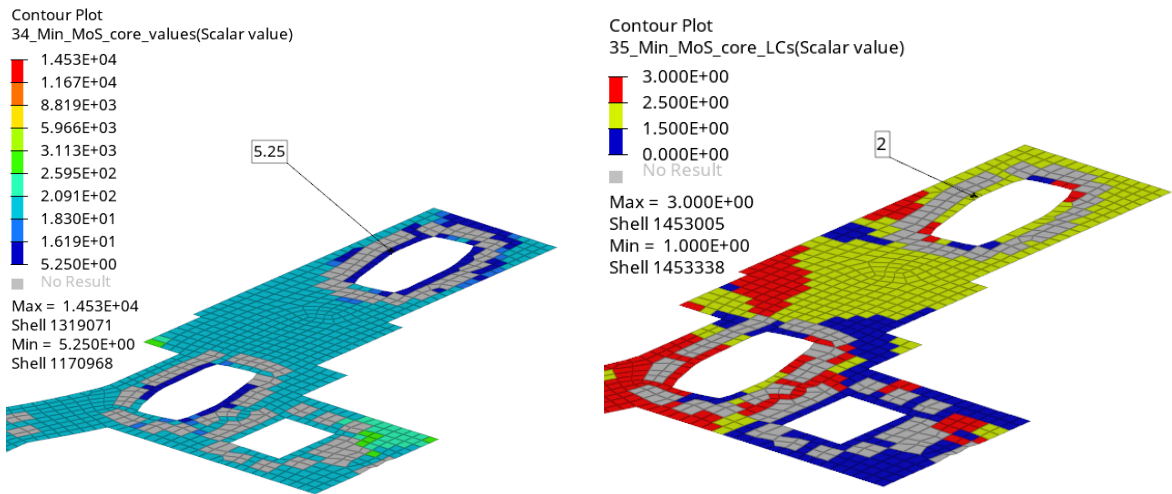


Fig. 93: Detail of platform top panel where the minimum MoS value can be found at the load case 2

For the element 1170968, the MoS is calculated manually based on following PCH data:

Subcase 1: 1 G X			
1170968	2	-1.584614E-04	-1.304226E-03
-CONT-	1.259441E-03	-2.767282E+03	2.655004E+04
-CONT-	3.277031E+01	6.522692E-04	-2.114957E-03
-CONT-	1.383613E-03		
Subcase 2: 1 G Y			
1170968	2	9.427514E-04	1.172123E-02
-CONT-	-3.788021E-03	-9.374909E+02	6.913447E+03
-CONT-	-7.244858E+01	1.291933E-02	-2.553458E-04
-CONT-	6.587338E-03		
Subcase 3: 1 G Z			
1170968	2	-4.852757E-04	-5.763439E-03
-CONT-	2.330846E-03	-4.564849E+02	7.660295E+03
-CONT-	2.072553E+01	3.966648E-04	-6.645380E-03
-CONT-	3.521022E-03		

Fig. 94: PCH stresses of subcases for core ply (ply 2) of the element 1170968

Based on the data from the Fig. 94 is calculated linear superposition of the stresses τ_{1Z} and τ_{2Z} and then the FI and MoS for core based on the equations 12 and 13.

$$\tau_{1Z,LC_2} = -2767.3 \cdot 3.19 - 937.5 \cdot 0.85 - 456.5 \cdot 1.35 = -10240.8 \text{ MPa}$$

$$\tau_{2Z,LC_2} = 26550.0 \cdot 3.19 + 6913.4 \cdot 0.85 + 7660.0 \cdot 1.35 = 100912.5 \text{ MPa}$$

$$FI_{core} = \left(\frac{\tau_{1Z,LC_2}}{\tau_{LOL}} \right)^2 + \left(\frac{\tau_{2Z,LC_2}}{\tau_{LOW}} \right)^2 = \left(\frac{-10240.8}{1379000} \right)^2 + \left(\frac{100912.5}{758000} \right)^2 = 0.0178 [-]$$

$$MoS_{core} = \frac{1}{FoS_{core} \cdot \sqrt{FI_{core}}} - 1 = \frac{1}{1.2 \cdot \sqrt{0.0178}} - 1 = 5.25 [-]$$

The manually calculated value for load case 2 corresponds with the value shown in the Fig. 93 and also with the value written with the result and report tables indicating that the evaluation of core is calculated flawlessly.

5.3.4 CORE LOCAL INSTABILITIES EVALUATION

Because of the limited scope of the thesis, the verification of evaluation will be performed only on one failure mode-Shear Crimping. The evaluation of Shear Crimping cannot be directly requested from Nastran and therefore it will be verified by comparison with manual calculation.

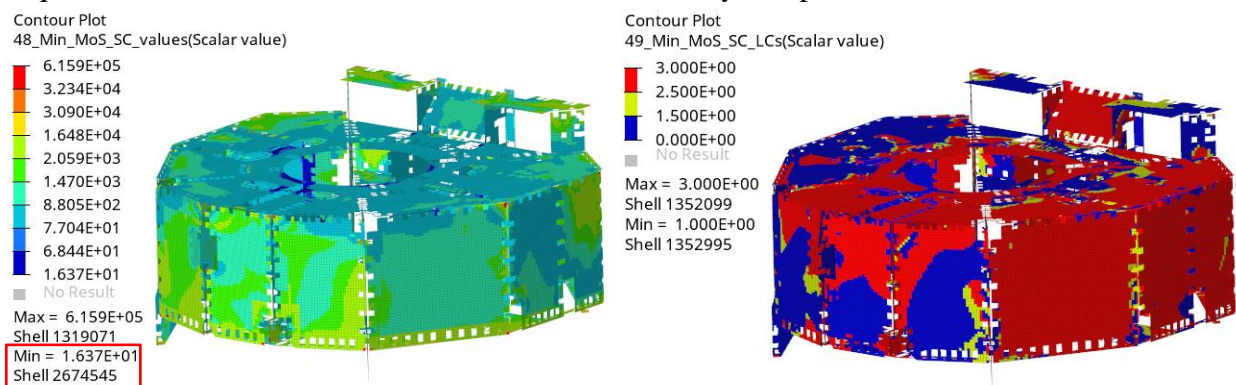


Fig. 95: Visualisation of the envelope of min MoS for Shear Crimping (left) and map of the load cases at which they occurred (right)

In the following picture is detail of the component indicating the minimum value.

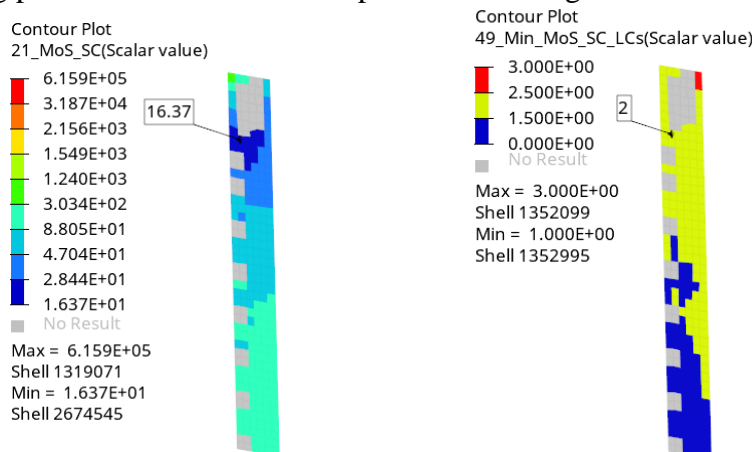


Fig. 96: Detail of shear panel where is minimum MoS value at the load case 2

The Shear Crimping (as well as Face Wrinkling and Intracell buckling) is evaluated on both skins of the sandwich panel with skins represented by isotropic material. The results from all subcases for top and bottom skin (ply 1 and 3) copied from PCH file are shown in the following figure.

Subcase 1: 1 G X			
2674545	1	1.216956E+07	-6.961661E+05
-CONT-	-2.445784E+06	-1.587037E+04	8.765995E+03
-CONT-	-1.040844E+01	1.261882E+07	-1.145424E+06
-CONT-	6.882122E+06		
2674545	3	1.021678E+07	-7.015280E+05
-CONT-	-2.221279E+06	0.000000E+00	0.000000E+00
-CONT-	-1.107047E+01	1.065139E+07	-1.136137E+06
-CONT-	5.893764E+06		
Subcase 2: 1 G Y			
2674545	1	2.375800E+06	-1.750564E+05
-CONT-	-5.555174E+05	3.607486E+02	2.667362E+03
-CONT-	-1.176785E+01	2.491528E+06	-2.907848E+05
-CONT-	1.391157E+06		
2674545	3	2.305858E+06	7.018982E+03
-CONT-	-3.184829E+05	0.000000E+00	0.000000E+00
-CONT-	-7.743533E+00	2.349165E+06	-3.628802E+04
-CONT-	1.192727E+06		
Subcase 3: 1 G Z			
2674545	1	3.309455E+06	-1.493190E+05
-CONT-	-7.385001E+05	-3.405055E+03	1.147205E+03
-CONT-	-1.156197E+01	3.460537E+06	-3.004005E+05
-CONT-	1.880469E+06		
2674545	3	2.847434E+06	-2.253978E+05
-CONT-	-7.770726E+05	0.000000E+00	0.000000E+00
-CONT-	-1.341445E+01	3.032766E+06	-4.107297E+05
-CONT-	1.721748E+06		

Fig. 97: PCH composite stresses for plies 1 and 3 of element 2674545 for all three subcases

The linear superposition of the components of the stress is performed for both skins in the following way (the notation of normal stresses in ply CS is changed to avoid confusion with principal stresses):

$$\sigma_{norm-1,top} = 12169560 \cdot 3.19 + 2375800 \cdot 0.85 + 3309455 \cdot 1.35 = 45308091 \text{ Pa}$$

$$\sigma_{norm-2,top} = -696166 \cdot 3.19 - 175056 \cdot 0.85 - 149319 \cdot 1.35 = -2571148 \text{ Pa}$$

$$\tau_{12,top} = -2445784 \cdot 3.19 - 555517 \cdot 0.85 - 738500 \cdot 1.35 = -9271215 \text{ Pa}$$

$$\sigma_{norm-1,bot} = 10216780 \cdot 3.19 + 2305858 \cdot 0.85 + 2847434 \cdot 1.35 = 38395543 \text{ Pa}$$

$$\sigma_{norm-2,bot} = -701528 \cdot 3.19 + 7019 \cdot 0.85 - 225398 \cdot 1.35 = -2536195 \text{ Pa}$$

$$\tau_{12,bot} = -2221279 \cdot 3.19 - 318483 \cdot 0.85 - 777073 \cdot 1.35 = -8405639 \text{ Pa}$$

From the combined stresses are calculated principal stresses using the equation 10 as it is for illustration performed for the major principal stress in the top ply:

$$\begin{aligned} \sigma_{1,top} &= \frac{\sigma_{norm-1,top} + \sigma_{norm-2,top}}{2} + \sqrt{\left(\frac{\sigma_{norm-1,top} - \sigma_{norm-2,top}}{2}\right)^2 + \tau_{12,top}^2} = \\ &= \frac{45308091 - 2571148}{2} + \sqrt{\left(\frac{45308091 + 2571148}{2}\right)^2 + (-9271215)^2} = \end{aligned}$$

$$= 47040651 \text{ Pa}$$

Other principal stresses are calculated accordingly, thus, for the element 2674542 there are calculated four principal stresses:

$$\sigma_{1,top} = 47040651 \text{ Pa}$$

$$\sigma_{2,top} = -4303709 \text{ Pa}$$

$$\sigma_{1,bot} = 40054469 \text{ Pa}$$

$$\sigma_{2,bot} = -4195121 \text{ Pa}$$

The biggest absolute value from the above principal stresses is 47040651 Pa which will be used for the calculation of the MoS using formulas 28 and 29:

$$\sigma_{crit} = \frac{\min(G_{LZ}, G_{WZ}) \cdot (c + 2t_f)}{2t_f} = \frac{137900000 \cdot (0.0165 + 2 \cdot 0.00135)}{2 \cdot 0.00135} = 980622222 \text{ Pa}$$

$$MoS = \frac{\sigma_{crit}}{\max(|\sigma_1|, |\sigma_2|) \cdot FoS_{inst}} - 1 = \frac{980622222}{47040651 \cdot 1.2} - 1 = 16.37 [-]$$

The result corresponds with the value displayed on the figures above from which can be concluded that the calculations inside of the tool are correct.

5.4 VALIDATION OF THE ORTHOTROPIC COMPOSITE SHELL ELEMENTS

5.4.1 VISUALISATION OF THE LOAD CASES

The Tsai-Hill failure index can be directly requested from Nastran which means that this method can be used for the verification of the correctness of the evaluation. The evaluation of orthotropic composite shell elements will be used central tube of the PLATO model which was created using this modelling approach. The comparison of the results from the new tool and Nastran for the ply 13 (ply with the highest stresses) at the 3rd load case is shown in the following pictures. The values correspond to each other which means that the code works according to the expectations.

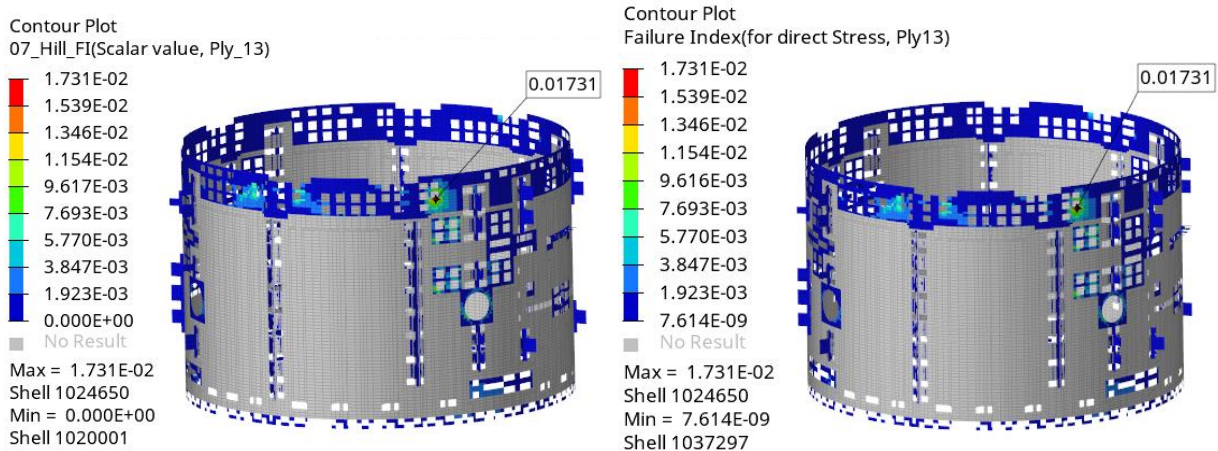


Fig. 98: Tsai-Hill FI at load case 1 in the ply 13, new tool on the left, Nastran on the right

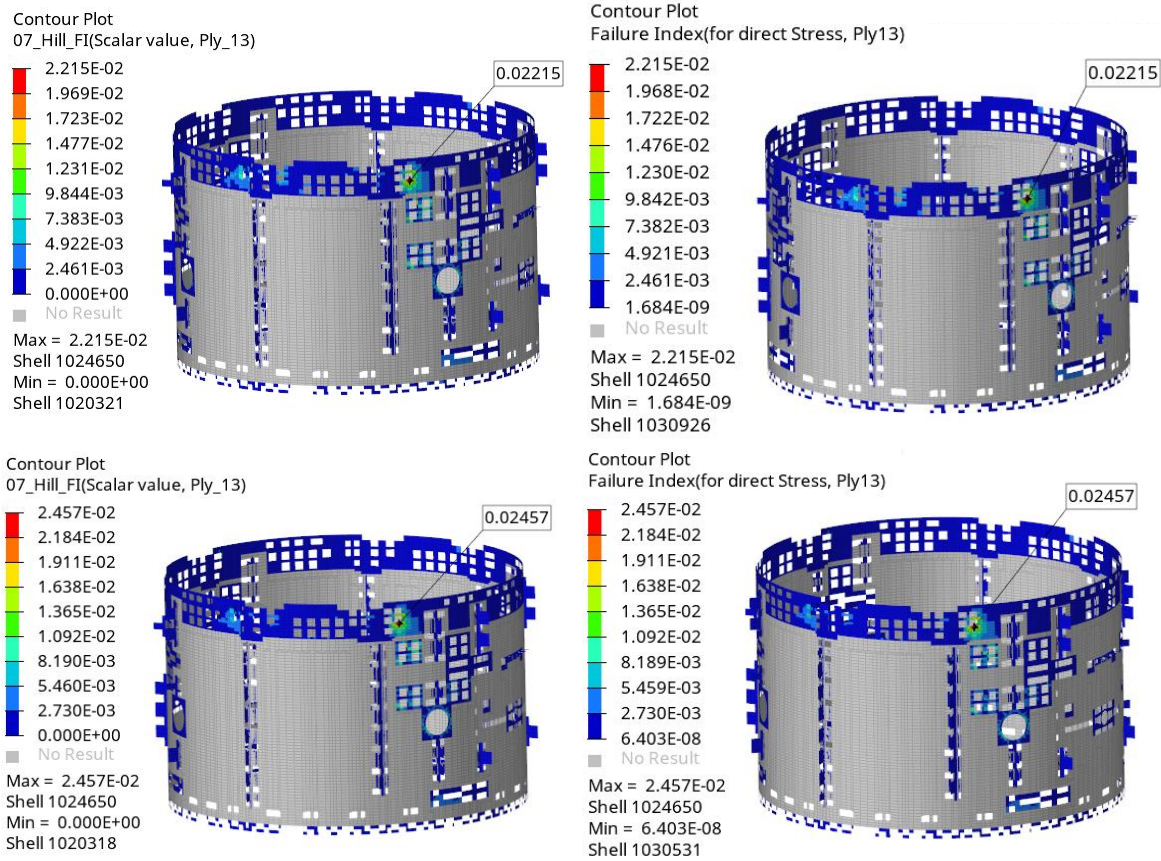


Fig. 99: Tsai-Hill FI at load cases 2 and 3 in the ply 13, new tool on the left, Nastran on the right

5.4.2 VISUALISATION OF THE ENVELOPE

From the previous figures can be seen that the maximum value of the Tsai-Hill FI in the ply 13 is 0.02457 and this value is reached at the load case 3. These data correspond with the following pictures in which are shown the maps throughout all the load cases. Since there are usually many plies when the structure is represented using orthotropic plies, there is an additional map showing at which ply the maximum value was reached. The reason why in the pictures above displaying the results in the ply 13 are many elements without result is that these elements have only 10 plies in their PCOMP property.

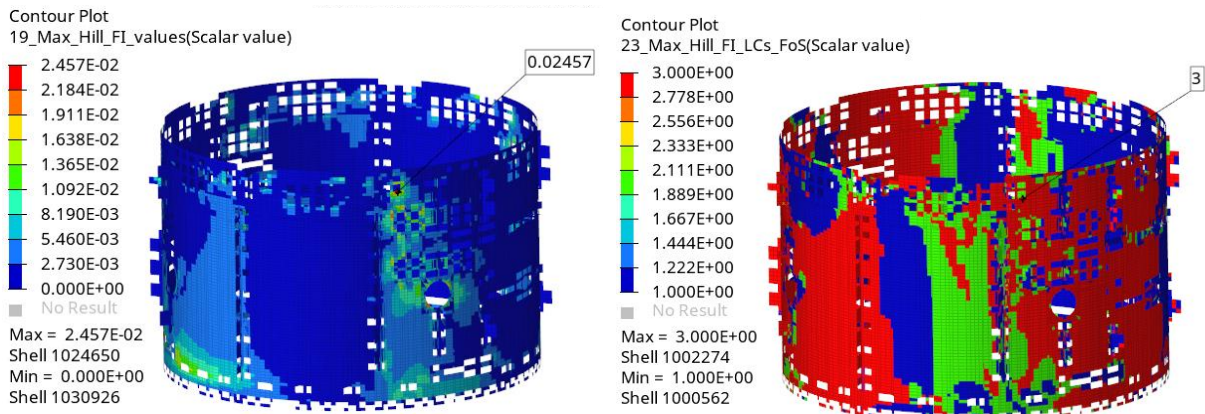


Fig. 100: Visualisation of the envelope of max Tsai-Hill FI (left) and map of the load cases at which they occurred (right)

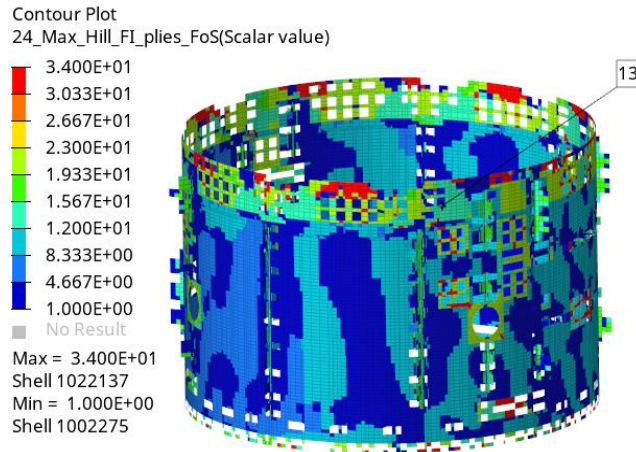


Fig. 101: Map showing at which ply the maximum value was reached

5.4.3 EVALUATION OF ILSS

The values of the interlaminar shear strength cannot be requested directly from Nastran and therefore the correctness of the evaluation will be verified by hand calculation. The envelope showing the minimum MoS with respect to ILSS together with the map showing at which load cases the values were reached are shown in the following figure.

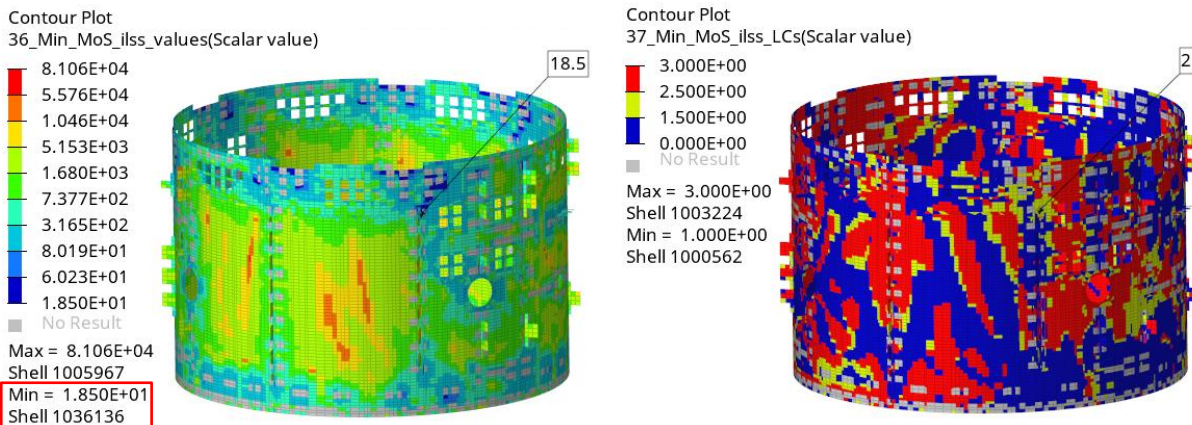


Fig. 102: Visualisation of the envelope of min MoS of ILSS (left) and map of the load cases at which it occurred (right)

From the figure above can be seen that the minimum value of MoS is 18.5 and it was reached on the element 1036136 at the load case 2. This value belongs to ply 8 for which the composite stresses copied from PCH file for all subcases are shown in the following figure.

Subcase 1: 1 G X			
1036136	8	2.148968E+05	-4.942638E+05
-CONT-		2.002854E+05	3.658942E+04
-CONT-		1.473001E+01	2.675528E+05
-CONT-		4.072363E+05	
Subcase 2: 1 G Y			
1036136	8	-1.543950E+04	-7.502757E+04
-CONT-		6.311311E+04	1.461080E+03
-CONT-		3.236462E+01	2.455865E+04
-CONT-		6.979219E+04	
Subcase 3: 1 G Z			
1036136	8	5.235556E+04	-1.155268E+05
-CONT-		6.804748E+04	1.229587E+03
-CONT-		1.951509E+01	7.647261E+04
-CONT-		1.080582E+05	

Fig. 103: PCH composite stresses for plies 8 of element 1036136 for all three subcases

The out of plane shear stresses from the previous figure are combined according to the linear superposition for the load case 2 in the following way.

$$\tau_{1Z,LC_2} = 36589 \cdot 3.19 + 1461 \cdot 0.85 + 1230 \cdot 1.35 = 119622 \text{ Pa}$$

$$\tau_{2Z,LC_2} = -674804 \cdot 3.19 - 111558 \cdot 0.85 - 142280 \cdot 1.35 = -2439527 \text{ Pa}$$

The FI and MoS for ILSS are calculated using formulas 30 and 31 in the following way.

$$FI_{ILSS} = \frac{\tau_{1Z}^2 + \tau_{2Z}^2}{\tau_{ILSS}^2} = \frac{119622^2 + (-2439527)^2}{57200000^2} = 0.00182 [-]$$

$$MoS_{core} = \frac{1}{FoS_{core} \cdot \sqrt{FI_{core}}} - 1 = \frac{1}{1.2 \cdot \sqrt{0.00182}} - 1 = 18.5 [-]$$

The result matches well with the corresponding visualisations from which can be concluded that the calculation works correctly.

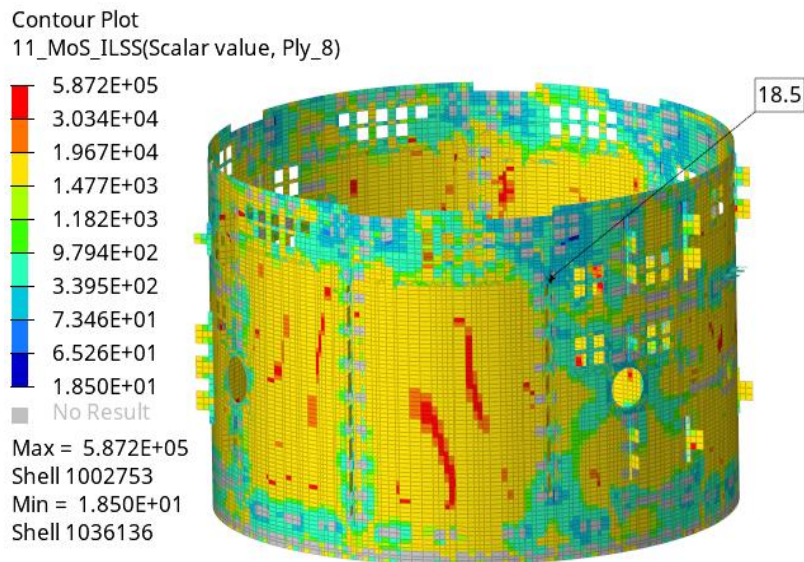


Fig. 104: Visualisation of the min MoS for ply 8 at the load case 2

5.5 SOLID ELEMENTS

Solid elements are on the used PLATO SVM model present in limited number for modelling of small brackets. Because the von Mises stress for solid elements can be requested from Nastran directly, the verification will be performed with comparison with OP2 file from Nastran.

5.5.1 VISUALISATION OF LOAD CASES

The results from the new tool and Nastran can be compared using following pictures. The agreement between these two result files proves that the linear superposition of the solid element stresses and the following calculation is performed correctly.

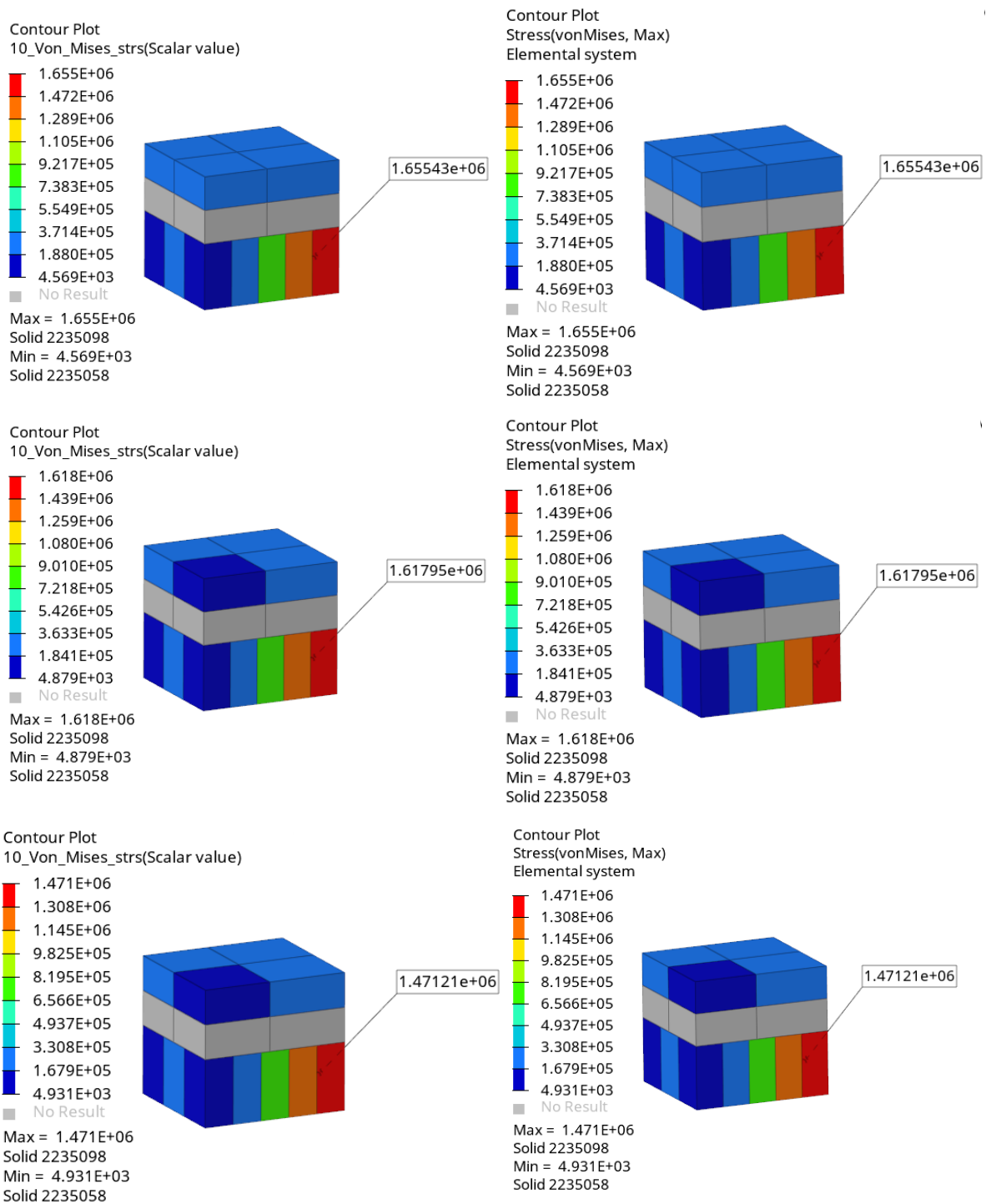


Fig. 105: Von Mises stress for all three load cases new tool on the left, Nastran on the right

5.5.2 VISUALISATION OF ENVELOPES

In the following figure can be seen that the maximum von Mises stress through all the load cases is $1.65543e+06$ Pa, this value is on element 2235098, and that this value was reached at load case 1. These data correspond with the values that can be seen in the figure above which proves the correctness of the calculation.

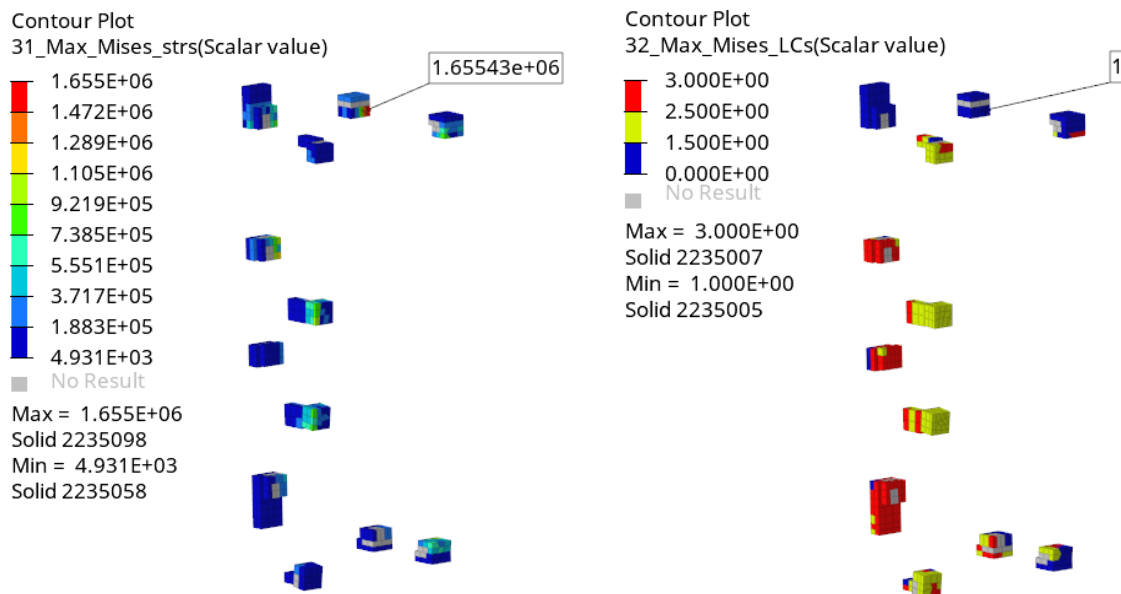


Fig. 106: Envelope of von Mises stress (left) and map showing load cases at which it occurred (right)

CONCLUSION

This thesis begins with a description of the problem situation, outlining the main aspects of the project's development. In the second chapter, the European space programme is discussed as the driving force behind the project, providing a brief overview of its history, organization, projects, and engineering standards.

In order to understand the requirements for the new post-processing tool, chapter three is important as it offers a comprehensive overview of the fundamental aspects of structural development in the space industry. This chapter covers various topics, including the classification and requirements for spacecraft structures, details regarding loading environments, finite element analysis, and the criteria for strength evaluation. The aim of this rather long theoretical section is to serve as a concise introductory resource for interns or engineers who are new to the structural departments of space companies.

The specific requirements for the new tool are outlined in the initial section of the fourth chapter. Additionally, various approaches for problem resolution are discussed, and based on the presented factors, the decision was made to develop a standalone software application. This chapter also covers the selection of the programming language and utilized libraries. The development process itself is the central focus of this chapter, providing insights into the employed data structures, data organization, graphical user interface, and other pertinent aspects.

The final chapter is dedicated to validating the created application. The validation process involved using a real spacecraft structure, specifically the PLATO service module, which is currently being developed as part of a project by the European Space Agency. The validation results demonstrated that the tool performs reliably and meets the established requirements and expectations.

In conclusion, all the requirements have been successfully met, and additional functionalities have been incorporated beyond the initial scope. The software has been fully implemented across all structural departments of the company, and rough estimates suggest that it has increased the efficiency of post-processing by 40 %, resulting in significant time savings for structural analyses. Alongside this thesis, comprehensive documentation is being prepared, covering all the essential aspects of the software's development. This documentation is necessary to support future maintenance and further enhancements of the software.

BIBLIOGRAPHY

- [1] ESA Facts. *European Space Agency* [online]. © ESA [cit. 2022-07-27]. Available at: https://www.esa.int/About_Us/Corporate_news/ESA_facts
- [2] History of Europe in space. *European Space Agency* [online]. © ESA [cit. 2022-07-27]. Available at: https://www.esa.int/About_Us/ESA_history/History_of_Europe_in_space
- [3] ESA's Purpose. *European Space Agency* [online]. © ESA [cit. 2022-07-28]. Available at: https://www.esa.int/About_Us/Corporate_news/ESA_s_Purpose
- [4] Our Missions. *European Space Agency* [online]. © ESA [cit. 2022-07-28]. Available at: https://www.esa.int/ESA/Our_Missions
- [5] Elements of Ariane 5. In: *European Space Agency* [online]. 10. 9. 2019 [cit. 2023-05-06]. Available at: https://www.esa.int/Enabling_Support/Space_Transportation/Launch_vehicles/Ariane_5
- [6] Member States & Cooperating States. *European Space Agency* [online]. © ESA [cit. 2022-07-27]. Available at: https://www.esa.int/About_Us/Corporate_news/Member_States_Cooperating_States
- [7] Funding. *European Space Agency* [online]. © ESA [cit. 2022-07-27]. Available at: https://www.esa.int/About_Us/Corporate_news/Funding
- [8] ECSS: *European Cooperation for Space Standardization* [online]. Noordwijk, The Netherlands: ECSS Secretariat, 2022 [cit. 2022-08-03]. Available at: <https://ecss.nl/>
- [9] Requirements and standards. *The European Space Agency* [online]. ESA [cit. 2022-08-03]. Available at: https://www.esa.int/Enabling_Support/Space_Engineering_Technology/Requirements_and_standards
- [10] ECSS. *ECSS-S-ST-00C: ECSS System*. Rev.1. Noordwijk, The Netherlands: ECSS Secretariat, 2020
- [11] European Space Agency. *Czech Space Portal* [online]. The Coordination Council for Space Activities [cit. 2022-07-28]. Available at: <https://www.czechspaceportal.cz/esa-gsa/evropska-kosmicka-agentura-esa/>
- [12] Coordination of Czech Space Activities. *Czech Space Portal* [online]. The Coordination Council for Space Activities [cit. 2022-07-28]. Available at: <https://www.czechspaceportal.cz/en/national-space-strategy/coordination-of-czech-space-activities/>
- [13] S.A.B. Aerospace s.r.o. *Czech Space Portal* [online]. [cit. 2023-01-15]. Available at: <https://www.czechspaceportal.cz/catalog/s-a-b-aerospace-s-r-o-2/>
- [14] *SAB Aerospace* [online]. S.A.B. Aerospace, 2023 [cit. 2023-05-06]. Available at: <https://www.sabaerospace.cz/en/>

- [15] Satellites being integrated onto the SSMS payload dispenser. In: *European Space Agency* [online]. [cit. 2023-05-06]. Available at: https://www.esa.int/Enabling_Support/Space_Transportation/Rideshare_service_for_light_satellites_to_launch_on_Vega
- [16] WIJKER, Jacob. *Spacecraft Structures*. Springer-Verlag Berlin Heidelberg, 2008. ISBN 978-3540755524.
- [17] SARAFIN, Thomas, ed. *Spacecraft Structures and Mechanisms: From Concept to Launch*. Torrance, California: Microcosm, 1995. ISBN 978-1881883036.
- [18] In: *NASA* [online]. National Aeronautics and Space Administration, Aug 7, 2017 [cit. 2023-05-06]. Available at: <https://www.nasa.gov/content/goddard/nasas-science-mission-directorate-cubesat-initiative>
- [19] Sentinel-1. In: *ESA* [online]. ESA/ATG medialab, 06/05/2013 [cit. 2022-08-02]. Available at: https://www.esa.int/Space_in_Member_States/Czech_Republic/Seznameni_se_s_druzici_Sentinel-1A
- [20] ECSS. *ECSS-E-HB-32-26A: Space engineering*. Noordwijk, The Netherlands: ECSS Secretariat, 2013.
- [21] Coupled dynamic analysis. In: *European Space Agency* [online]. [cit. 2023-05-06]. Available at: https://www.esa.int/TEC/Structures/SEMUGM91M9H_1.html
- [22] Launcher-Spacecraft Coupled Loads Analysis. *The European Space Agency* [online]. ESA, 12 March 2013 [cit. 2022-08-04]. Available at: https://www.esa.int/TEC/Structures/SEMUGM91M9H_0.html
- [23] MACDONALD, Malcolm a Viorel BADESCU, ed. *The International Handbook of Space Technology*. Berlin: Springer-Verlag Berlin Heidelberg, 2014. ISBN 978-3-642-41100-7.
- [24] RANA, Sohel a Raul FANGUEIRO, ed. *Advanced Composite Materials for Aerospace Engineering: Processing, Properties and Applications*. Elsevier, 2016. ISBN 978-0-08-100054-0.
- [25] In: *Abet Laminati* [online]. [cit. 2023-05-07]. Available at: <https://ch.abetlaminati.com/collezioni/metalleido/>
- [26] *APCO Technologies catalogue*. Available at: <https://www.apco-technologies.eu/catalogue-datasheets/>
- [27] BATCHU, Surya. Solid Metal Versus Sandwich Panels. *Stress Ebook LLC*. [online]. Feb 28, 2015 [cit. 2023-05-07]. Available at: <https://www.stressebook.com/solid-metal-versus-sandwich-panels/>
- [28] Standard mission. In: *Ariane Space: Ariane Group* [online]. [cit. 2023-05-07]. Available at: <https://www.arianespace.com/vehicle/ariane-5/>

- [29] GRIFFIN, Michael a James FRENCH. *Space Vehicle Design*. 2nd edition. Reston, Virginia: American Institute of Aeronautics and Astronautics, 2004. ISBN 1-56347-539-1.
- [30] YUNIS, Isam. The Standard Deviation of Launch Vehicle Environments. *NTRS - NASA Technical Reports Server* [online]. Apr 18, 2005, 7 [cit. 2023-05-07]. Available at: <https://ntrs.nasa.gov/citations/20120001364>
- [31] WIJKER, Jaap. *Mechanical Vibrations in Spacecraft Design*. Springer, 2004. ISBN 3-540-40530-5.
- [32] SCEO / Hispasat 36W-1. In: *Space Structures* [online]. [cit. 2023-05-07]. Available at: https://spacestructures.de/references_sc-struct.php
- [33] NASA STRuctural ANalysis (NASTRAN): Design and Integration Tools. *NASA's Technology Transfer Program* [online]. NASA [cit. 2022-08-09]. Available at: <https://software.nasa.gov/software/LAR-16804-GS>
- [34] NAGY, Dennis. Analysis Origins - MSC and NASTRAN. *NAFEMS: The International Association for the Engineering Modelling, Analysis and Simulation Community*. [online]. © NAFEMS [cit. 2022-08-09]. Available at: <https://www.nafems.org/blog/posts/analysis-origins-msc-and-nastran/>
- [35] MSC Nastran: Multidisciplinary Structural Analysis. *Hexagon: MSC Software is Hexagon* [online]. Hexagon AB and/or its subsidiaries, 2022 [cit. 2022-08-09]. Available at: <https://www.mscsoftware.com/product/msc-nastran>
- [36] MSC Nastran Files. *MSC Nastran 2021.3 - Online Help* [online]. Hexagon, 2022 [cit. 2023-01-13]. Available at: https://help.hexagonmi.com/cs-CZ/bundle/MS_C_Nastran_2021.3/page/Nastran_Combined_Book/getstart/GS-Files/GS-Files.xhtml
- [37] GOKHALE, Nitin, Sanjeev BEDEKAR, Sanjay DESHPANDE a Anand THITE. *Practical Finite Element Analysis*. India: Finite To Infinite, 2008. ISBN 978-81-906195-0-9.
- [38] MSC Nastran 2021.4: Linear Static Analysis User's Guide. U.S.: Hexagon, 2021.
- [39] MSC Nastran 2021: Quick Reference Guide. MSC Software Corporation, 2020.
- [40] BAKER, Alan, Stuart DUTTON a Donald KELLY. *Composite Materials for Aircraft Structures*. Second Edition. American Institute of Aeronautics and Astronautics, 2004. ISBN 1-56347-540-5.
- [41] IRISH, Sandra a Ryan SIMMONS. Finite element model validity checks. *FEMCI* [online]. Greenbelt, Maryland, USA, 2009, November 2006 [cit. 2022-12-03]. Available at: <https://femci.gsfc.nasa.gov/validitychecks/index.html>
- [42] IRISH, Sandra. Unit Gravity Loading in All Three Translational Directions. *FEMCI* [online]. Greenbelt, Maryland, USA [cit. 2022-12-03]. Available at: <https://femci.gsfc.nasa.gov/validitychecks/vc3.html>

- [43] ECSS-E-ST-32-03C. *Space engineering: Structural finite element models*. Noordwijk (The Netherlands): ESA Requirements and Standards Division, 2008.
- [44] BOLOGNESE, Jeff. Free-Free Dynamics with a Stiffness Equilibrium Check. *FEMCI* [online]. Greenbelt, Maryland, USA [cit. 2022-12-03]. Available at: <https://femci.gsfc.nasa.gov/validitychecks/vc2.html>
- [45] BEER, Ferdinand P., E. Russell JOHNSTON, John T. DEWOLF a David F. MAZUREK. *Mechanics of Materials*. 6th edition. New York: McGraw-Hill, 2012. ISBN 978-0-07-338028-5.
- [46] *HexWeb® Honeycomb Selector Guide* [online] [cit. 2022-08-11]. Available at: https://www.hexcel.com/user_area/content_media/raw/HexWeb_SelectorGuide_2017.pdf
- [47] ECSS-E-HB-32-20 Part 3A: *Structural materials handbook - Part 3: Load transfer and design of joints and design of structures*. Noordwijk, The Netherlands: ECSS Secretariat, 2011.
- [48] BRUHN, E. F. *Analysis and Design of Flight Vehicle Structures Analysis and Design of Flight Vehicle Structures*. U.S.A: Tri-State offset company, 1973. ISBN 978-0961523404.
- [49] General Python FAQ. *Python* [online]. Python Software Foundation, 2022 [cit. 2022-10-11]. Available at: <https://docs.python.org/3/faq/general.html#id2>
- [50] Python Success Stories. *Python* [online]. Python Software Foundation, 2022 [cit. 2022-10-11]. Available at: <https://www.python.org/about/success/#simulation>
- [51] What is NumPy. *NumPy documentation* [online]. [cit. 2022-10-28]. Available at: <https://numpy.org/doc/stable/user/whatisnumpy.html>
- [52] OpenPyXL in Python – A Brief Introduction. *AskPython* [online]. 2022 [cit. 2022-10-29]. Available at: <https://www.askpython.com/python-modules/openpyxl-in-python>
- [53] Qt Designer Manual. *Qt Group* [online]. [cit. 2022-10-29]. Available at: <https://doc.qt.io/qt-6/qt designer-manual.html#:~:text=Qt%20Designer%20is%20the%20Qt,using%20different%20styles%20and%20resolutions.>
- [54] JOYNER, David. *Introduction to Computing* [online]. USA: McGraw-Hill Education, 2016 [cit. 2022-10-29]. ISBN 978-1-260-08227-2. Available at: https://www.davidjoyner.net/b/wp-content/uploads/2017/03/Joyner_IntroductiontoComputing_1stEdition.pdf
- [55] Generic ASCII Reader. *Altair HyperWorks* [online]. Altair Engineering, 2021 [cit. 2023-05-14]. Available at: https://2021.help.altair.com/2021/hwdesktop/hwd/topics/reference/hwdref/generic_ascii_reader_r.htm

LIST OF ABBREVIATIONS

CAD	Computer Aided Design
CDR	Critical Design Review
CFRP	Carbon Fibre Reinforced Polymer
CLA	Coupled Load Analysis
CoG	Centre of gravity
CS	Coordinate system
DOF	Degree of freedom
ECSS	European Cooperation for Space Standardization
EID	Element identification number
ESA	European Space Agency
FE	Finite Element
FEA	Finite Element Analysis
FEM	Finite Element Method
FI	Failure index
FoS	Factor of safety
GNP	Gross National Product
GUI	Graphical user interface
HM	High-modulus
HR	High-resistance
ILSS	Interlaminar shear strength
JAXA	Aerospace Exploration Agency
L-QSL	Launcher quasi-static loads
LVA	Launch Vehicle Adapter
L/V	Launch Vehicle
MID	Material identification number
MGSE	Mechanical ground support equipment
MoS	Margin of safety
NASA	National Aeronautics and Space Administration
NSM	Non-structural mass
PDR	Preliminary Design Review
PID	Property identification number
POGO	Propulsion Generated Oscillations
PLM	Payload module

PLATO	Planetary Transits and Oscillations of Stars
PSD	Power Spectral Density
QSL	Quasi-static loads
S/C	Spacecraft
SPC	Single-point constraint
SPL	Sound Pressure Level
SRB	Solid rocket booster
SRS	Shock Response Spectrum
SSMS	Small Spacecraft Mission Service
SVM	Service Module

LIST OF SYMBOLS AND PHYSICAL CONSTANTS

dB	Decibel
E	Young's modulus
E_c	Young's modulus of core in through-thickness direction
E_f	Young's modulus of the face skin
FoS_y, FoS_u	Factor of safety to yield strength, ultimate strength
G	Shear Modulus
G_{LZ}, G_{LW}	Out-of- plane shear modulus of the core in directions L and W
G_{1Z}, G_{2Z}	Out-of- plane shear modulus of the CFRP skin in direction 1 and 2
g	Gravitational acceleration
k	Stiffness
NU	Poisson's ratio (in Nastran's nomenclature)
m	Mass
MoS_y, MoS_u	Margin of safety to yield strength, ultimate strength
S	Allowable stress for in-plane shear (for composites)
S_c	Core cell size
t_c	Thickness of the core
t_f	Thickness of the face skin
W	Work of nodal forces applied on FE model
X_c, X_t	Allowable compressive/tensile stress in the longitudinal direction of fibres
Y_c, Y_t	Allowable compressive/tensile stress in the transverse direction of fibres
δW	Residual work of nodal forces
γ	Shear strain
ε	Normal strain
ε_r	Ratio of residual work and work of applied load in FE model
ν	Poisson's ratio
ν_f	Poisson's ratio of the face skin
ρ	Density
σ	Normal stress
σ_{crit}	Critical shear stress
σ_{Mises}	von Mises stress
σ_y, σ_u	Yield stress, Ultimate stress

σ_1, σ_2	Principal stresses or normal stresses in material CS depending on the context
τ	Shear stress
τ_{crit}	Critical shear stress
τ_{LOL}, τ_{LOW}	Allowable stress for out-of-plane shear strength of the core
τ_{ILSS}	Allowable stress for interlaminar shear strength
ω_0	First eigenfrequency

LIST OF APPENDICES

A Result and summary tables data

- A.1 Isotropic shell element components
- A.2 Quasi-isotropic composite element components
- A.3 Orthotropic composite element components
- A.4 Solid element components

A RESULT AND SUMMARY TABLES DATA

Due to the large dimensions of the result Excel tables, only the headers indicating the evaluated data are presented here. Although the data in these Excel sheets are organized with components in rows and corresponding data in columns, the headers are shown in a transposed format as columns, due to limited space. The summary tables are displayed in their original form for each component type. For composite components, two summary tables are provided, as skin and core/ILSS are typically reported separately.

A.1 Isotropic shell element components

- Component Name
- Component ID
- Material Name
- Material ID
- Thickness [m]
- Yield Strength [Pa]
- Ultimate Strength [Pa]
- Max. Normal x stress [Pa]
- EID generating Max. Normal x stress
- LC generating Max. Normal x stress
- Max. Normal y stress [Pa]
- EID generating Max. Normal y stress
- LC generating Max. Normal y stress
- Max. Shear xy stress [Pa]
- EID generating Max. Shear xy stress
- LC generating Max. Shear xy stress
- Min. Normal x stress [Pa]
- EID generating Min. Normal x stress
- LC generating Min. Normal x stress
- Min. Normal y stress [Pa]
- EID generating Min. Normal y stress
- LC generating Min. Normal y stress
- Min. Shear xy stress [Pa]
- EID generating Min. Shear xy stress
- LC generating Min. Shear xy stress
- Max. Major Principal stress [Pa]
- EID generating Max. Major Principal stress
- LC generating Max. Major Principal stress

A.2 Quasi-isotropic composite element components

- Comp Name
- Comp ID
- Material Name (of the material gener. min MoS)
- Material ID
- Yield Strength
- Ultimate Strength
- Max Normal-1 stress
- El ID gener. Max Normal-1 stress
- LC gener. Max Normal-1 stress
- Max Normal-2 stress
- El ID gener. Max Normal-2 stress
- LC gener. Max Normal-2 stress
- Max Shear-12 stress
- El ID gener. Max Shear-12 stress
- LC gener. Max Shear-12 stress
- Max Shear-Z stress (resultant of 1Z and 2Z)
- El ID gener. Max Shear-Z stress
- LC gener. Max Shear-Z stress
- Min Normal-1 stress
- El ID gener. Min Normal-1 stress
- LC gener. Min Normal-1 stress
- Min Normal-2 stress
- El ID gener. Min Normal-2 stress
- LC gener. Min Normal-2 stress
- Min Shear-12 stress
- El ID gener. Min Shear-12 stress
- LC gener. Min Shear-12 stress
- Max Major Principal stress
- El ID gener. Max Major Principal stress
- LC gener. Max Major Principal stress
- Min Minor Principal stress
- El ID gener. Min Minor Principal stress
- LC gener. Min Minor Principal stress
- Max Principal (absolute max betw. Major and Minor) stress
- El ID gener. Max Principal (absolute max betw. Major and Minor) stress
- LC gener. Max Principal (absolute max betw. Major and Minor) stress
- Max Von Mises stress
- El ID gener. Max Von Mises stress (betw. Major and Minor) stress
- LC gener. Max Von Mises stress (betw. Major and Minor) stress
- SF_y
- SF_u
- Min MoS (principal)
- El ID gener. min MoS (principal)
- Ply n° gener. Min MoS (principal)

- LC gener. min MoS (principal)
- Min MoS (Von Mises)
- El ID gener. min MoS (Von Mises)
- ply n° gener. Min MoS (Von Mises)
- LC gener. min MoS (Von Mises)
- CORE
- Material Name
- Material ID
- τ_L Strength
- τ_W Strength
- Max Shear-1Z stress
- El ID gener. Max Shear-1Z stress
- LC gener. Max Shear-1Z stress
- Max Shear-2Z stress
- El ID gener. Max Shear-2Z stress
- LC gener. Max Shear-2Z stress
- Min Shear-1Z stress
- El ID gener. Min Shear-1Z stress
- LC gener. Min Shear-1Z stress
- Min Shear-2Z stress
- El ID gener. Min Shear-2Z stress
- LC gener. Min Shear-2Z stress
- SF_core
- Shear-1Z stress gener. min MoS
- Shear-2Z stress gener. min MoS
- Min MoS
- El ID gener. Min MoS
- LC gener. min MoS
- ILSS
- ILSS allowable
- Shear-1Z stress gener. min MoS ILSS
- Shear-2Z stress gener. min MoS ILSS
- SF_ILSS
- Min Mos ILSS
- El ID gener. min Mos ILSS
- LC gener. min MoS ILSS
- Core Instabilities
- Skin Material Name
- Skin E (Youngs modulus)
- Skin thickness
- Core Material Name
- Core thickness
- Core compressive modulus
- Core cell size
- Core GL
- Core GW

- SF_instabilities
- Sigma crit. IB
- Min MoS Compre IB
- Min MoS Shear IB
- Min MoS Comb IB
- Princ. gener. min MoS Comb. IB
- Shear-12 gener. min MoS Comb. IB
- El ID gener. Min MoS Comb. IB
- LC gener. min MoS Comb. IB
- Sigma crit. W
- Min MoS Compre W
- Min MoS Shear W
- Min MoS Comb W
- Princ. gener. min MoS Comb. W
- Shear-12 gener. min MoS Comb. W
- El ID gener. Min MoS Comb. W
- LC gener. min MoS Comb. W
- Sigma crit. SC
- Min MoS SC
- Princ. gener. min MoS SC
- El ID generating Min MoS SC
- LC generating min MoS SC

A.3 Orthotropic composite element components

- Comp Name
- Comp ID
- Material Name (of the material generating max FI)
- Material ID
- Tensile ultimate strength (at 0°)
- Compression ultimate strength (at 0°)
- Tensile ultimate strength (at 90°)
- Compression ultimate strength (at 90°)
- In-Plane Shear Strength
- Interlaminar Shear Strength
- Max Normal-1 stress
- El ID generating Max Normal-1 stress
- LC generating Max Normal-1 stress
- Max Normal-2 stress
- El ID generating Max Normal-2 stress
- LC generating Max Normal-2 stress
- Max Shear-12 stress
- El ID generating Max Shear-12 stress
- LC generating Max Shear-12 stress
- Max Shear-Z stress (resultant of 1Z and 2Z)
- El ID generating Max Shear-Z stress
- LC generating Max Shear-Z stress
- Min Normal-1 stress
- El ID generating Min Normal-1 stress
- LC generating Min Normal-1 stress
- Min Normal-2 stress
- El ID generating Min Normal-2 stress
- LC generating Min Normal-2 stress
- Min Shear-12 stress
- El ID generating Min Shear-12 stress
- LC generating Min Shear-12 stress
- Max Major Principal stress
- El ID generating Max Major Principal stress
- LC generating Max Major Principal stress
- Min Minor Principal stress
- El ID generating Min Minor Principal stress
- LC generating Min Minor Principal stress
- Max Principal (absolute max between Major and Minor) stress
- El ID generating Max Principal (absolute max between Major and Minor) stress
- LC generating Max Principal (absolute max between Major and Minor) stress
- Max FI (Hill)
- FoS skin
- Max FI (Hill) after FoS
- El ID generating Max FI (Hill)

- ply n° generating Max FI (Hill)
- LC generating Max FI (Hill)
- CORE
- Material Name
- Material ID
- τ_L Strength
- τ_W Strength
- Max Shear-1Z stress
- El ID generating Max Shear-1Z stress
- LC generating Max Shear-1Z stress
- Max Shear-2Z stress
- El ID generating Max Shear-2Z stress
- LC generating Max Shear-2Z stress
- Min Shear-1Z stress
- El ID generating Min Shear-1Z stress
- LC generating Min Shear-1Z stress
- Min Shear-2Z stress
- El ID generating Min Shear-2Z stress
- LC generating Min Shear-2Z stress
- SF_core
- Shear-1Z stress generating min MoS
- Shear-2Z stress generating min MoS
- Min MoS
- El ID generating Min MoS
- LC generating min MoS
- ILSS
- Shear-1Z stress generating min MoS ILSS
- Shear-2Z stress generating min MoS ILSS
- SF_ILSS
- Min Mos ILSS
- El ID generating min Mos ILSS
- LC generating min MoS ILSS

A.4 Solid element components

- Component Name
- Component ID
- Material Name
- Material ID
- Thickness [m]
- Yield Strength [Pa]
- Ultimate Strength [Pa]
- Max. Normal x stress [Pa]
- EID generating Max. Normal x stress
- LC generating Max. Normal x stress
- Max. Normal y stress [Pa]
- EID generating Max. Normal y stress
- LC generating Max. Normal y stress
- Max. Shear xy stress [Pa]
- EID generating Max. Shear xy stress
- LC generating Max. Shear xy stress
- Min. Normal x stress [Pa]
- EID generating Min. Normal x stress
- LC generating Min. Normal x stress
- Min. Normal y stress [Pa]
- EID generating Min. Normal y stress
- LC generating Min. Normal y stress
- Min. Shear xy stress [Pa]
- EID generating Min. Shear xy stress
- LC generating Min. Shear xy stress
- Max. Major Principal stress [Pa]
- EID generating Max. Major Principal stress
- LC generating Max. Major Principal stress

